THE UNIVERSITY OF MICHIGAN

INDUSTRY PROGRAM OF THE COLLEGE OF ENGINEERING

AN EXPERIMENTAL STUDY OF THE STRESSES IN RING STIFFENERS IN LONG THIN-WALLED CYLINDERS SUBJECTED TO BENDING

Wadi Saliba Rumman

A dissertation submitted in partial fulfillment
of the requirements for the degree of
Doctor of Philosophy in the
University of Michigan
1959

June, 1959

IP-373

Doctoral Committee:

Professor Lawrence C. Maugh, Chairman
Associate Professor Samuel K. Clark
Professor Bruce G. Johnston
Professor Leo M. Legatski
Professor Erich H. Rothe

ACKNOWLEDGMENTS

The writer wishes to express his appreciation to the members of his committee for their guidance during the preparation of this dissertation. He is especially grateful to Professor L. C. Maugh, the chairman of his committee, for suggesting the subject of the dissertation and for his untiring and continuing help.

The writer is indebted to the American Electric Power Service Corporation for their financial grant which was used to obtain materials and certain specialized operations required for the building of the model. The help of Mr. George Geisendorfer of the Structural Laboratories of the Civil Engineering Department in the actual building of the model is greatly appreciated.

The rough draft of the dissertation was typed by Mrs. Charles Barrett and Miss Reta Teachout, both of the Civil Engineering Department. The final copy of the dissertation was typed and reproduced by the College of Engineering Industry Program at the University of Michigan. To all persons involved in the typing and preparation of the thesis, the writer is sincerely grateful.

TABLE OF CONTENTS

TABLE OF CONTENTS CONT'D

LIST OF TABLES

LIST OF TABLES CONT'D

LIST OF ILLUSTRATIONS

LIST OF ILLUSTRATIONS CONT'D

LIST OF PHOTOGRAPHS

NOTATIONS

A_r	Cross-sectional area of the ring stiffener
ϵ	Strain
E	Modulus of Elasticity
I_r	Moment of Inertia of the ring stiffener
M	Applied moment on the cylinder
M_{cr}	Critical bending moment on the cylinder
M_r	Bending moment in the ring stiffener
N	Applied longitudinal normal force on the cylinder
N_r	Normal force in the ring stiffener
r	Mean radius of the cylinder
S,s	Spacing of the ring stiffeners
t	Wall thickness of the cylinder
W	Weight on each loading basket of Figure 6
μ	Poisson's ratio
ρ	Radius of curvature of the cylinder
σ	Stress

Other symbols are defined throughout the text.

INTRODUCTION

Statement of the Problem

The problem under investigation is primarily concerned with establishing the nature of the forces acting on ring stiffeners in long thin-walled cylinders subjected to bending. The study of the problem is basically experimental as indicated by the title of the dissertation. Although the need for a rational method of designing the circular stiffeners in steel stacks was the major incentive for the study, nevertheless, the results can be applied to many other similar problems. Many pipe and conduit structures must be designed with ring stiffeners.

Two types of bending of a cylinder are considered: (1) Pure bending as shown in Figure 1a, and (2) Bending caused by transverse local loading shown in Figure 1b.

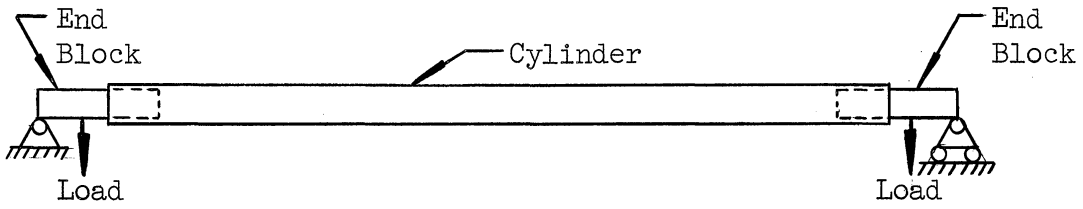

(a) Pure bending of the cylinder.

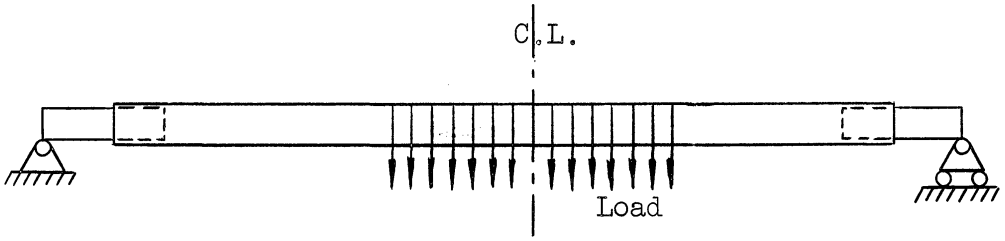

(b) Local loading on the cylinder.

Figure 1. Loading Conditions.

The experimental results are interpreted in terms of three types of action:

(1) Flattening of the cylinder.

(2) The increase of the radii of the cylinder on the compression side and their decrease on the tension side, which will be referred to hereafter as the bulging of the cylinder.

(3) The separate effect of the local loading.

The pure bending of the cylinder produces the first two of the three actions listed above, while bending of the cylinder by the application of local transverse loading involves a combination of all three types.

Analytical procedures are developed to determine the basic parameters upon which the magnitude of the forces acting on the stiffeners depend. The relation of these parameters to all three types of action is discussed in considerable detail.

The experimental data and the analytical methods are both used to establish the formulas which govern the magnitude and distribution of the forces in the ring stiffeners due to the three types of action. The use of these formulas is then illustrated by the design of ring stiffeners in a steel stack.

Historical Outline

Theoretical and experimental studies of the structural behavior of both stiffened and unstiffened thin-walled cylinders have been undertaken by many investigators. These studies, however, were primarily concerned with the strength of the cylinder as a whole with respect to both local and general instability failures.

Brazier[2]* investigated theoretically the ultimate strength of unstiffened thin-walled long cylinders. He showed that under pure bending, a progressive flattening of the cylinder takes place. His results express the applied bending moment on the cylinder as a non-linear function of the curvature in the form:

$$M = \frac{E}{2} \pi r^3 t \left[\frac{2}{\rho} - \frac{3r^4(1 - \mu^2)}{\rho^3 t^2} \right] \qquad (1)$$

Equation (1) differs from the St. Venant equation which expresses the moment as a linear function of the curvature in the form:

$$M = \frac{E\pi r^3 t}{\rho} \qquad (2)$$

A comparative plotting of Equations (1) and (2) is given in Figure 2.

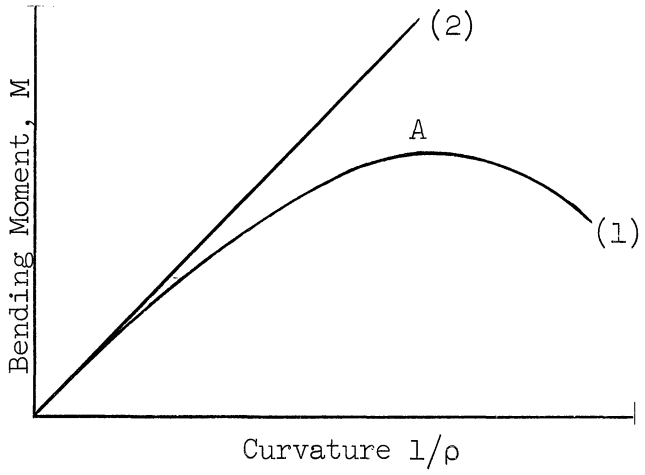

Figure 2. Moment vs. Curvature - Long Unstiffened Cylinder.

The point of instability according to Brazier is reached at point A (see Figure 2) where the bending moment is maximum and is given by

* Numbers in parenthesis refer to the reference at the end of the dissertation.

$$M_{cr} = \frac{2\sqrt{2}\ E\pi rt^2}{9\sqrt{1-\mu^2}} \qquad (3)$$

Although the theoretical work of Brazier gives a quasi-elliptical shape for the originally circular section, yet his experimental work has shown that failure in some cases occurred with a lobed form distortion of the section. His experimental ultimate moments, however, agreed very well with the predicted moments as given by Equation (3). Brazier explained the lobed forms of distortion by pointing out that the compression half of the cylinder is similar to a cylindrical shell subjected to end compression and hydraulic pressure, a problem which was treated by Southwell*, who indicated that the cylinder thus loaded may collapse into lobed forms of distortion.

Lundquist[8] investigated experimentally the strength of thin-walled duralumin cylinders in pure bending. The tests which were made on 58 cylinders showed that the length/radius ratio had no consistent effect upon the bending strength. The test specimens were right circular cylinders of 7.5 or 15.0 inches in radius and were made from sheets with nominal thicknesses of 0.011, 0.016 and 0.022 inches. Lundquist observed that "except for the few cylinders in which preliminary wrinkling occurred, there was no visible deformation of the cylinder prior to failure (collapse of the compression half of the cylinder)."

It is interesting to note, however, that the ultimate bending moments obtained experimentally by Lundquist agree very well with the bending moments according to Equation (3) derived by Brazier.

---

* On the General Theory of Elastic Stability, Phil. Trans. Roy. Soc. A. Vol. 213, pp. 178-244.

Lundquist incorporated in his report the results of tests by Mossman and Robinson[9], and also those obtained by Imperial and Bergstrom which are reported in Reference 15. The Brazier equation agrees very well with practically all results reported by Lundquist except for the region where r/t is below 80. These experimental results as reported by Lundquist are given in the appendix in Figure 36.

Peterson[11] investigated experimentally the strength of the ring-stiffened circular cylinder under bending. The rings were heavy to eliminate the general-instability type failures which involve simultaneous failure of the cylinder wall and the rings. One conclusion which is of interest here is that the gain in strength as the ring spacing "S" is decreased is negligible until a value of S/r of 1/2 has been reached.

Peterson's tests were made on cylinders with r/t varying from 120-750 and s/r of 1/4, 1/2 and 1 for most tests. For one value of r/t(180) additional cylinders were tested with s/r of 2 and 4. The material used was aluminum alloy 7075-T6. Peterson's experimental results for cylinders with s/r greater than about 1/2 are given in the appendix in Figure 37.

Hoff[6], by the use of the energy method, made a theoretical investigation of the deflections in ring and stringer stiffened cylinders subjected to pure bending. The deflections in the rings were assumed according to the results obtained by Brazier[2]. The same equation was used for the distorted shape between rings but with a different coefficient that varies with the distance between rings. In the derivation it was assumed that there is an infinitely large number of longitudinal

stringers distributed continuously around the circumference of the cylinder. Once the distorted shape is known, then the moments in the ring stiffeners can be readily computed. Using Hoff's results, the moments in the ring can be expressed in this form:

$$M_r = \frac{1}{4\pi^2 r^3 t_L} \frac{M^2}{E} S \cos \varphi \qquad (4)$$

where t_L = thickness of an equivalent sheet which is chosen so that the moment of inertia of the sheet is equal to the moment of inertia of the stringers with respect to the horizontal axis of the sections of the cylinder.

Hoff, Bruno and Nardo[7] made an experimental investigation of the ring and stringer stiffened cylinder subjected to bending. One of the purposes of the investigation was to establish the critical value of a parameter above which failure would occur by general instability and below which panel instability would take place. This problem is considerably different from the one under investigation here.

EXPERIMENTAL INVESTIGATION

Tensile Tests

Several tensile tests were made to determine the value of the modulus of elasticity E for the aluminum alloy 6061-T6 that was used in the model.

Four test coupons were tested, two of which were cut from one of the 0.025" thick sheets from which the shell was made, and the other two were cut from the 0.25" thick plate from which the stiffeners were cut and milled. The test specimens were made according to the recommendations of the American Society for Testing Materials.

The average values of the tensile tests are plotted in Figure 3 from which the modulus of elasticity, E, was found to be equal to 10×10^6 psi.

No attempt was made to check the Poisson's ratio of the material. A value of 1/3 will be used as given by the manufacturer.

Description of the Model and Testing Procedures

The model as shown in Figure 4 is essentially a thin-walled long cylinder of constant thickness and radius, and reinforced by equidistant circular rings. The material used in the fabrication of the model as stated above is aluminum alloy 6061-T6.

The circular cylinder is composed of three segments each equal to four feet in length. Each segment was rolled into its circular shape from a 0.025 in. thick sheet to a mean diameter of about 11.28 inches. The radius/thickness ratio of the model is therefore equal to 225.

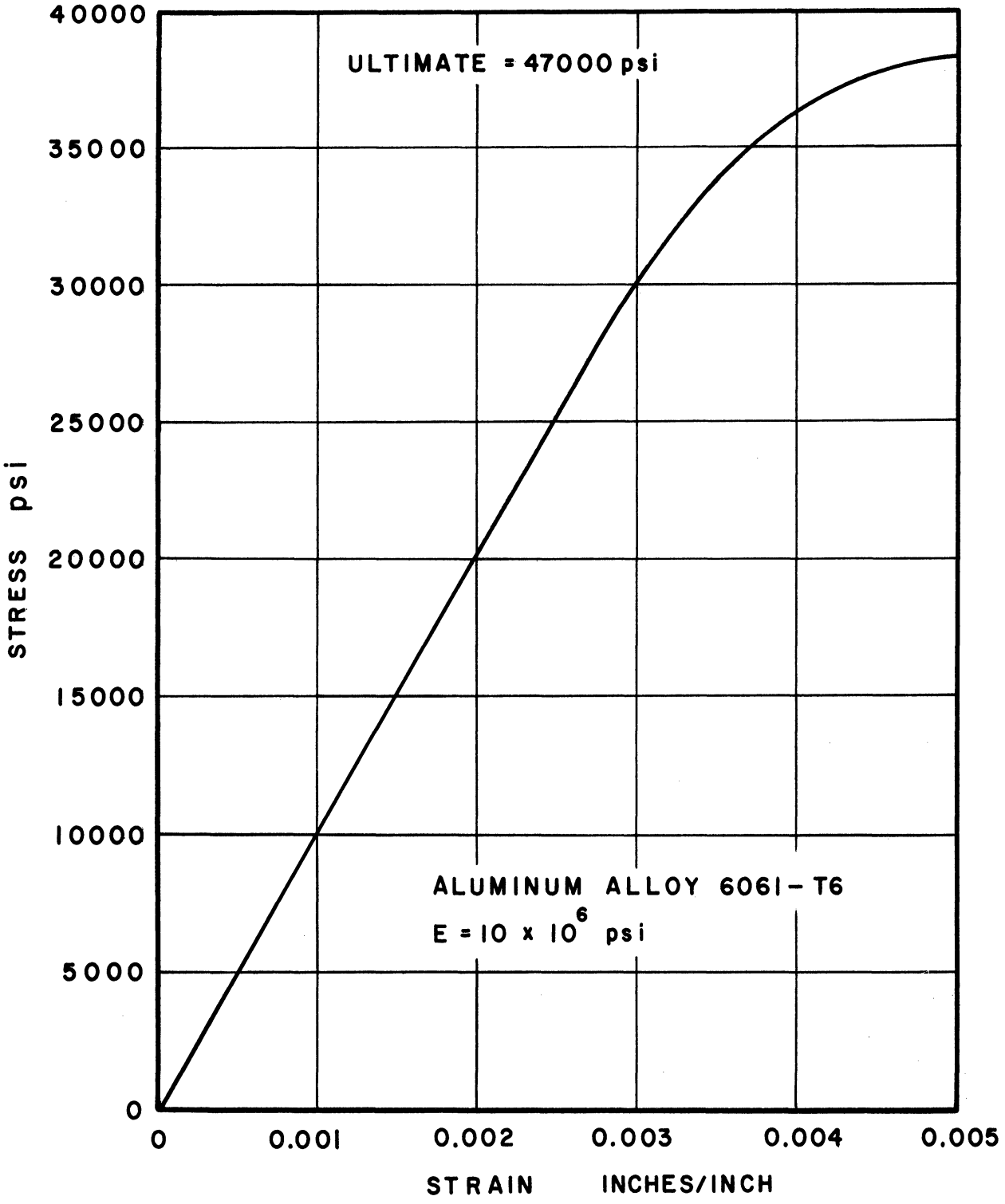

Figure 3. Stress-Strain Diagram.

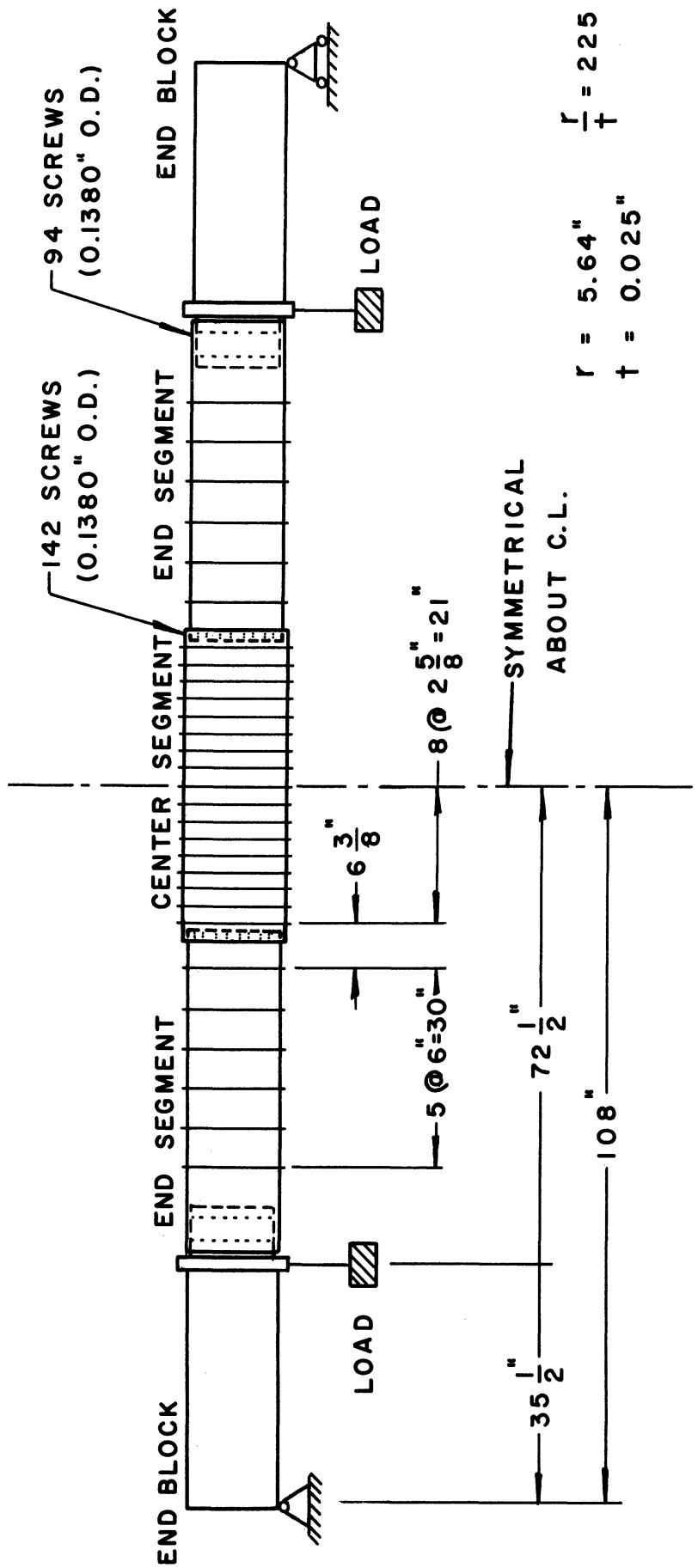

Figure 4. General Arrangement of the Model.

The stiffeners were rolled from bars that were cut from a 0.25 in. thick plate. The bars were machined to the specified thickness of the stiffeners and were rolled to the right diameter. In each stiffener an allowance was made for a splice.

The end segments of the model were reinforced by 1/4" x 1/4" stiffeners spaced equally at 6 inches center to center. No strain gages were mounted on the end segments and no change in the size or spacing of their stiffeners was made during the test.

On the center segment, which is the actual test specimen of the model, two different size stiffeners were used during the test, 1/4" x 3/16" (width x thickness) and 1/4" x 1/8". For each of the two sizes, the stiffeners were originally spaced at 2-5/8" with provisions to remove some of the stiffeners during the test so that their spacing could be increased to 5-1/4", 10-1/2" and 21".

All the connections in the model were made by steel machine screws and nuts. The screws used in the splicing of the shell were 0.138" in outside diameter and those used to connect the stiffeners to the shell were 0.112" in outside diameter.

Two wooden end blocks were connected to the model for the purpose of end supports and application of the load.

Electrical strain gages, type SR4, manufactured by the Baldwin Lima-Hamilton Corp., were mounted on both the inside and the outside of the shell of the center segment as shown in Figure 5. Most of these gages were AR-1 rectangular rosettes, but some were single A-7 gages located at certain check points.

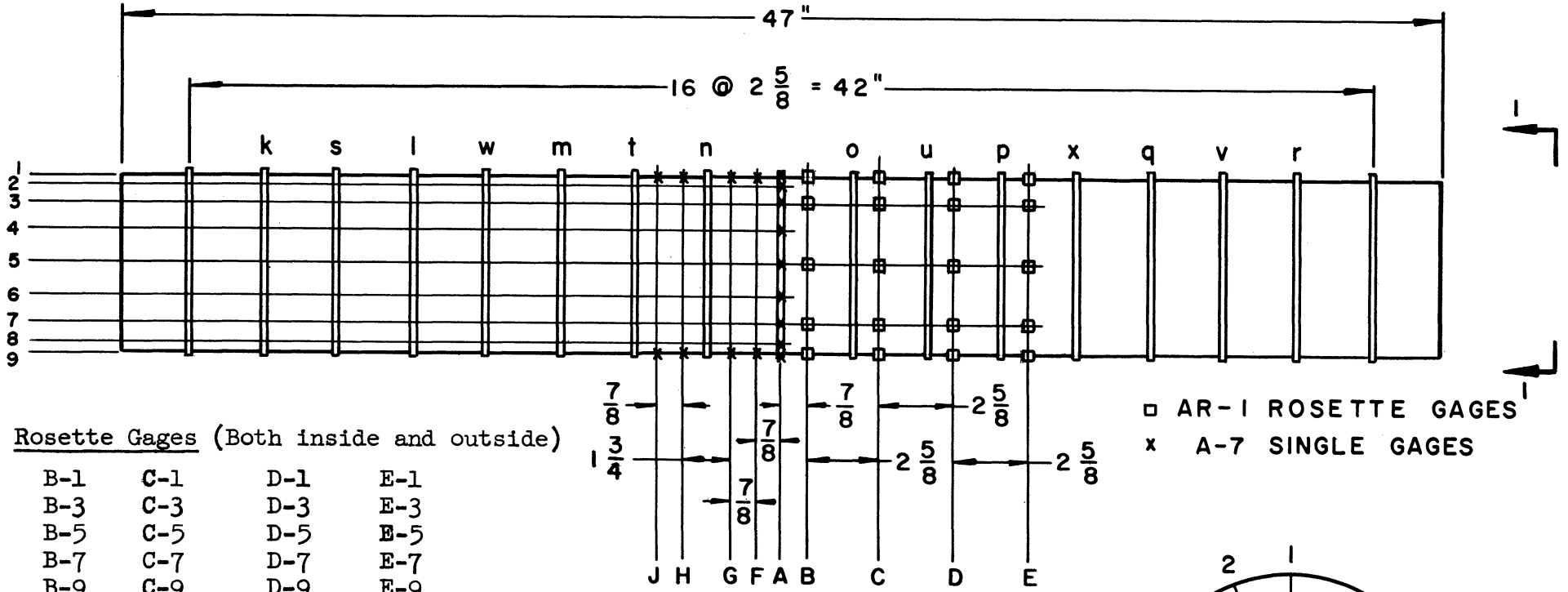

Rosette Gages (Both inside and outside)

B-1	C-1	D-1	E-1
B-3	C-3	D-3	E-3
B-5	C-5	D-5	E-5
B-7	C-7	D-7	E-7
B-9	C-9	D-9	E-9

Single Gages (Both inside and outside)

A-1
A-2
A-3
A-4
A-5
A-6
A-7
A-8
A-9
F-1
F-9
G-1
G-9
H-1
H-9
J-1
J-9
} Check Gages

A-10
A-11
} Check Gages

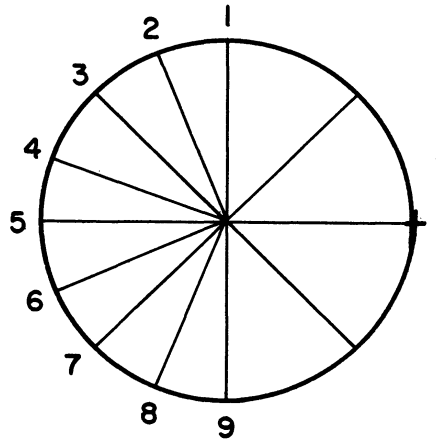

Figure 5. Center Segment of the Model.

The stiffener located at the center of the center segment was gaged with A-7 gages. Also A-7 gages were mounted on the inside of the shell opposite to those on the stiffener.

Dummy gages were mounted on both the inside and the outside of a circular cylinder, four feet long, rolled from a 0.025 in. aluminum sheet (alluminum alloy 6061-T6) to a diameter equal to that of the model. For any one group of active gages, a dummy gage was used with the same gage factor and lot number. The gage factor was 2.03 for all rosette gages and 1.95 for all single A-7 gages except for those single gages placed on the outside face of the 1/4" x 1/8" stiffener whose gage factor was 1.94.

The center segment with its stiffeners spaced at 2-5/8" is shown in Figure 5. The location of the gages and their designation is also included. It is to be noted that the spacing was increased to 5-1/4" by removing stiffeners k, l, m, n, o, p, q and r. Similarly the 10-1/2" spacing was achieved by the additional removal of stiffeners s, t, u, and v, while the 21" spacing was accomplished by finally removing the stiffeners w and x.

A constant bending moment in the shell was obtained by loading both loading baskets simultaneously with equal increments of the load (Figure 4). The local loading on the model was achieved by using loading baskets at the 14 locations shown in Figure 6 in which the load from the weights in the basket was applied to the model by bands passed over the upper half of the shell or stiffeners.

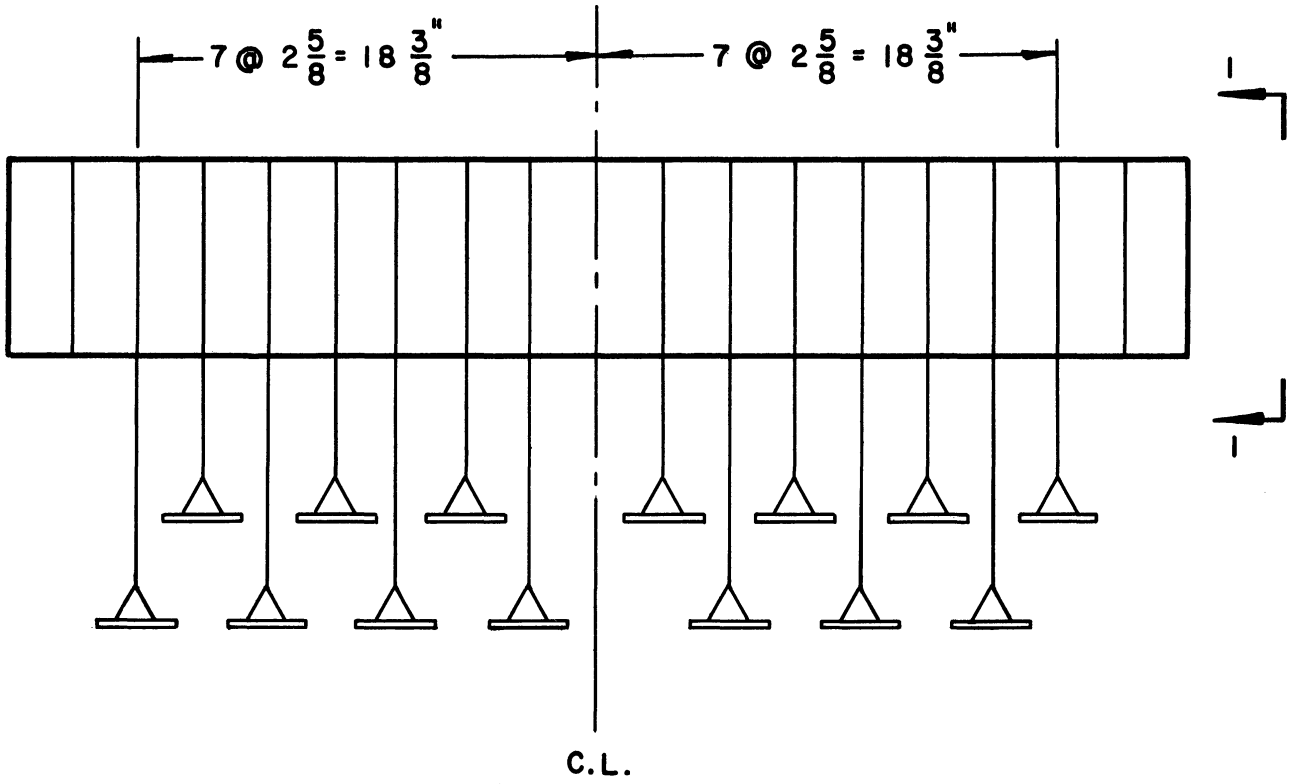

CENTER SEGMENT OF THE MODEL

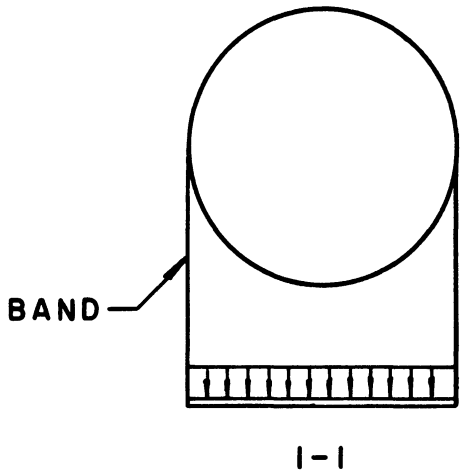

Figure 6. Local Loading of the Model.

Tabulation of Data

The strains at the gage locations shown in Figure 5 were recorded for the two types of loading and for the two different size stiffeners. The spacing of the stiffeners was changed during the test.

As the main interest in this study is to determine the character and distribution of the forces acting on the stiffeners, the major emphasis is placed on the strains recorded on the outside face of the stiffener located at the center of the test segment of the model (stiffener A in Figure 5). The strains of the gages on the inside of the shell and opposite to those on the outside face of the stiffeners are affected appreciably by any local longitudinal bending and other local conditions. Due to the fact that these local conditions are difficult to evaluate, it is felt that the recorded strains of these gages can not be used to advantage in the evaluation of the data.

The strains recorded on the outside face of the stiffener are converted into stresses and are tabulated in Tables 1, 2, 3, and 4. Tables 1 and 2 give the stresses on the outside face of the stiffener for different stiffener spacing and for different values of the applied pure bending moment on the cylinder. The values of Table 1 are for the 1/4" x 1/8" (width x thickness) stiffeners and those of Table 2 are for the 1/4" x 3/16" stiffeners.

Tables 3 and 4 give the stresses on the outside face of the stiffeners when the model is subjected to the local loading illustrated in Figure 6. The separate effect of the local loading is given in Tables 5 and 6 which are obtained by subtracting the stresses of Tables

1 and 2 from those of Tables 3 and 4 respectively. The stresses of Tables 5 and 6 are tabulated as a function of the load W on each of the 14 baskets of Figure 6.

It should be noted that the moment of 3218 in-lbs. in Tables 1, 2, 3 and 4 is the moment at the center of the model due to the weight of the cylinder, the end blocks and the end loading baskets (see Figure 7). This moment is computed on the basis that the total weight of the shell and stiffeners is equal to 25 lbs., the weight of each end loading basket is equal to 27 lbs., and the weight of each wooden end block is equal to 58.5 lbs. with the center of gravity at a distance of 23 inches from the end supports.

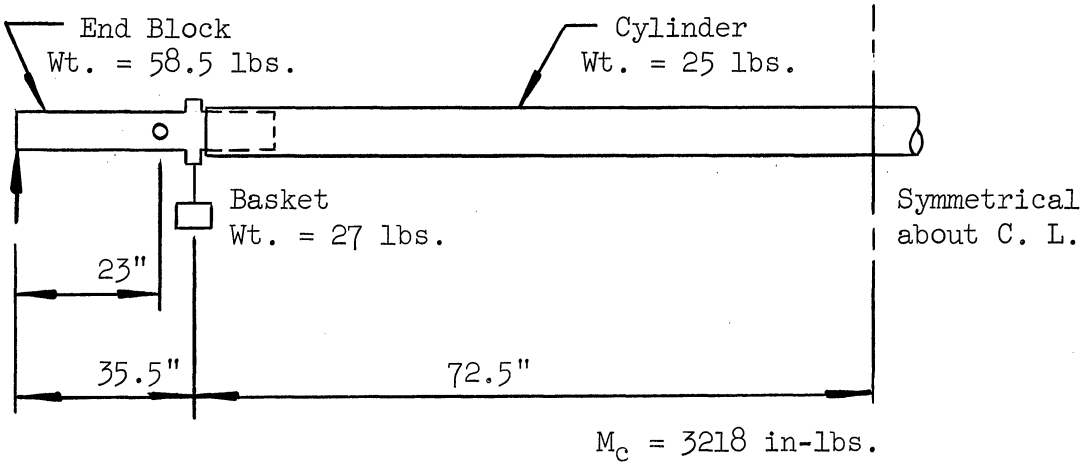

Figure 7. Dead Load of the Model

In Tables 3 and 4 the moments of 6744, 11522, 16299 and 21077 are obtained when the total load of each of the 14 baskets of Figure 6 (including the weight of each basket of 1/2 lbs.) is 5-1/6 lbs., 12-1/6 lbs., 19-1/6 lbs., and 26-1/6 lbs. respectively. (See loading condition of Table 3.)

Some of the transverse stresses on the shell are given in Table 7 when the model is subjected to pure bending. As an example for the designation of the location, consider I-7B-T, where 7B refers to the location as given in Figure 5, I refers to the inside of the shell and T designates the transverse direction. The letter O will refer to the outside of the shell.

The transverse stresses as given in Table 7 were computed directly from the recorded longitudinal and transverse strains by the following equation:

$$\sigma_T = \frac{E}{1 - \mu^2} \quad (\epsilon_T + \mu\epsilon_L) \qquad (5)$$

the subscripts T and L refer to the transverse and longitudinal direction on the shell respectively.

The variation in the stress on the outside face of the 1/4" x 1/8" stiffeners as a function of the applied pure bending moment on the cylinder, is given graphically in Figure 8. The stresses are plotted for five locations on the stiffeners and for a spacing of 10-1/2 inches. The data for Figure 8 is tabulated in Table 8 which is partially taken from Table 1 and is completed by adding to it the results of another test with larger values of M.

Table 1

STRESSES ON THE OUTSIDE FACE OF THE STIFFENER, PSI.

(Pure bending)

Spacing →	S = 2-5/8"					S = 5-1/4"				
Gage	Moments in-lbs.					Moments in-lbs.				
	3218	6744	11522	16299	21077	3218	6744	11522	16299	21077
0-1A	+150	+275	+ 410	+ 475	+ 490	+150	+280	+ 397	+ 450	+ 435
2A	+110	+205	+ 305	+ 363	+ 390	+ 85	+150	+ 210	+ 218	+ 163
3A	+ 88	+180	+ 310	+ 440	+ 570	+ 55	+120	+ 230	+ 350	+ 485
4A	+ 35	+105	+ 220	+ 355	+ 505	+ 20	+ 65	+ 190	+ 380	+ 615
5A	+ 10	+ 35	+ 110	+ 235	+ 395	+ 15	+ 65	+ 185	+ 375	+ 620
6A	- 15	- 18	- 5	+ 35	+ 95	+ 3	+ 25	+ 75	+ 165	+ 300
7A	- 95	-190	- 325	- 465	- 600	- 45	-105	- 205	- 330	- 465
8A	-105	-230	- 430	- 655	- 945	-110	-250	- 480	- 760	-1080
9A	-155	-345	- 665	-1025	-1435	-180	-400	- 770	-1160	-1615

Spacing →	S = 10-1/2"					S = 21"				
Gage	Moments in-lbs.					Moments in-lbs.				
	3218	6744	11522	16299	21077	3218	6744	11522	16299	21077
0-1A	+135	+250	+ 345	+ 325	+ 215	+140	+250	+ 300	+ 300	+ 200
2A	+ 80	+130	+ 150	+ 115	+ 5	- 10	- 20	- 50	- 210	- 780
3A	+ 65	+130	+ 220	+ 315	+ 400	+ 40	+ 90	+ 160	+ 260	+ 200
4A	+ 50	+135	+ 305	+ 555	+ 840	+ 40	+110	+ 270	+ 580	+1180
5A	+ 35	+ 90	+ 240	+ 475	+ 765	+ 40	+120	+ 260	+ 540	+1020
6A	- 8	0	+ 45	+ 135	+ 310	+ 20	+ 40	+ 100	+ 190	+ 350
7A	- 55	-120	- 215	- 320	- 460	- 80	-130	- 210	- 300	- 540
8A	-120	-270	- 515	- 820	-1170	- 70	-200	- 440	- 720	-1150
9A	-200	-435	- 820	-1285	-1805	-180	-400	- 780	-1240	-1820

$\frac{1}{4}$" x $\frac{1}{8}$"

Stiffeners

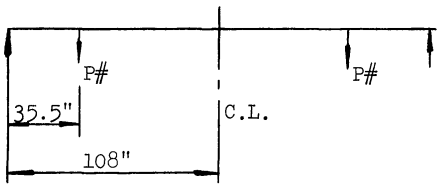

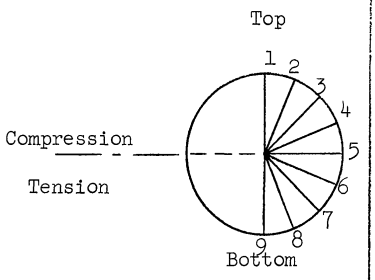

$M_c = 3218 + 35.5P$

where P = Load on each basket

Loading Condition

Table 2

STRESSES ON THE OUTSIDE FACE OF THE STIFFENER, PSI

(Pure bending)

Spacing →	S = 2-5/8"				S = 5-1/4"			
Gage	Moment in-lbs.				Moment in-lbs.			
	3218	6744	11522	16299	3218	6744	11522	16299
0-1A	+100	+215	+ 370	+ 515	+120	+235	+ 377	+ 498
2A	+ 70	+150	+ 245	+ 340	+ 70	+120	+ 170	+ 200
3A	+ 25	+ 77	+ 170	+ 287	+ 10	+ 25	+ 65	+ 125
4A	+ 25	+ 70	+ 147	+ 257	+ 20	+ 60	+ 163	+ 310
5A	+ 10	+ 35	+ 77	+ 145	+ 15	+ 40	+ 118	+ 248
6A	- 35	- 65	- 63	- 30	+ 5	+ 20	+ 65	+ 145
7A	- 40	- 80	- 135	- 190	- 30	- 55	- 98	- 140
8A	- 85	-195	- 355	- 535	- 80	-175	- 340	- 530
9A	-110	-240	- 425	- 650	-140	-305	- 570	- 855

Spacing →	S = 10-1/2"			
Gage	Moment in.-lbs.			
	3218	6744	11522	16299
0-1A	+130	+280	+443	+535
2A	+ 50	+ 90	+115	+ 95
3A	+ 10	+ 25	+ 52	+ 90
4A	+ 20	+ 70	+190	+350
5A	+ 20	+ 70	+205	+395
6A	+ 20	+ 60	+155	+275
7A	+ 15	+ 25	+ 45	+ 40
8A	- 70	-140	-260	-440
9A	-160	-330	-635	-975

$\frac{1}{4}$" x $\frac{3}{16}$"

Stiffeners

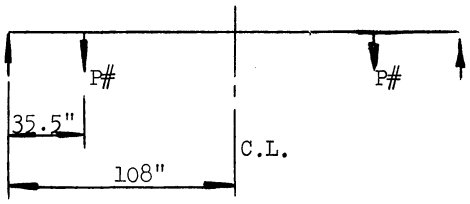

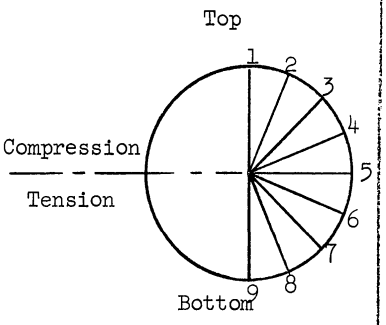

$M_c = 3218 + 35.5P$

where P = Load on each basket

Loading Condition

Table 3

STRESSES ON THE OUTSIDE FACE OF THE STIFFENER, PSI.

(Local loading)

Spacing →	S = 2-5/8"					S = 5-1/4"				
Gage	Moment in-lbs.					Moment in-lbs.				
	3218	6744	11522	16299	21077	3218	6744	11522	16299	21077
0-1A	+150	+510	+ 990	+1460	+1880	+150	+730	+1490	+2210	+2850
2A	+110	+320	+ 590	+ 820	+1020	+ 85	+345	+ 685	+1015	+1255
3A	+ 88	+ 63	- 7	- 127	- 267	+ 55	-165	- 475	- 785	-1105
4A	+ 35	-165	- 445	- 745	-1035	+ 20	-460	-1110	-1750	-2340
5A	+ 10	+ 30	+ 100	+ 200	+ 340	+ 15	+ 45	+ 165	+ 315	+ 525
6A	- 15	+315	+ 765	+1225	+1715	+ 3	+623	+1503	+2413	+3323
7A	- 95	- 15	+ 105	+ 205	+ 295	- 45	+165	+ 455	+ 715	+ 965
8A	-105	-325	- 645	-1025	-1425	-110	-420	- 940	-1500	-2080
9A	-155	-575	-1185	-1855	-2545	-180	-800	-1710	-2690	-3680

Spacing →	S = 10-1/2"					S = 21"				
Gage	Moment in-lbs.					Moment in-lbs.				
	3218	6744	11522	16299	21077	3218	6744	11522	16299	21077
0-1A	+135	+995	+2115	+3165	+4135	+140	+1460	+3000	+4540	+6010
2A	+ 80	+460	+ 960	+1400	+1810	- 10	+ 640	+1260	+1850	+2310
3A	+ 65	-355	- 915	-1525	-2105	+ 40	- 600	-1560	-2500	-3470
4A	+ 50	-780	-1910	-3030	-4080	+ 40	-1540	-3360	-5080	-6710
5A	+ 35	+ 95	+ 265	+ 475	+ 725	+ 40	+ 290	+ 460	+ 720	+1080
6A	- 8	+1032	+2442	+3932	+5382	+ 20	+1680	+3750	+5850	+7990
7A	- 55	+255	+ 745	+1195	+1615	- 80	+ 520	+1210	+1860	+2450
8A	-120	-590	-1290	-2030	-2820	- 70	- 720	-1680	-2720	-3780
9A	-200	-1120	-2380	-3680	-5010	-180	-1380	-3040	-4730	-6430

$\frac{1}{4}$" x $\frac{1}{8}$" Stiffeners

W lbs.	M_c in.-lbs.
0	3218
5-1/6	6744
12-1/6	11522
19-1/6	16299
26-1/6	21077

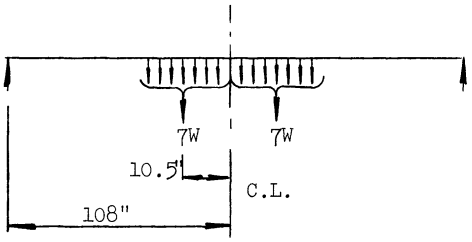

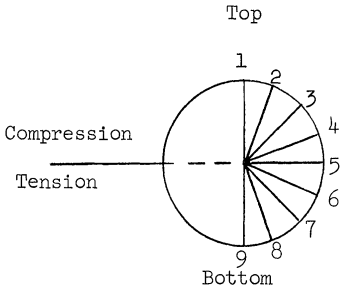

$M_c = 3218 + 682.5W$

where W = Load on each basket in lbs.

Loading Condition

Table 4

STRESSES ON THE OUTSIDE FACE OF THE STIFFENER, PSI.

(Local loading)

Gage	Moment in-lbs.			
	3218	6744	11522	16299
0-1A	+130	+760	+1430	+2100
2A	+ 50	+310	+ 590	+ 840
3A	+ 10	-210	- 530	- 840
4A	+ 20	-480	-1140	-1780
5A	+ 20	+ 90	+ 180	+ 290
6A	+ 20	+660	+1480	+2310
7A	+ 15	+305	+ 635	+ 935
8A	- 70	-310	- 710	-1170
9A	-160	-730	-1520	-2410

$\frac{1}{4}$" x $\frac{3}{16}$" Stiffeners

Spacing = $10\frac{1}{2}$"

NOTE: See loading condition of Table 3.

Table 5

STRESSES ON THE OUTSIDE FACE OF THE STIFFENER
DUE TO THE SEPARATE EFFECT OF THE LOCAL LOADING, PSI

(Local loading minus bending)

Spacing →	S = 2-5/8"				S = 5-1/4"			
Gage	Load W lbs.				Load W lbs.			
	5-1/6	12-1/6	19-1/6	26-1/6	5-1/6	12-1/6	19-1/6	26-1/6
0-1A	+ 235	+ 580	+ 985	+1390	+ 450	+1093	+1760	+2415
2A	+ 115	+ 285	+ 457	+ 630	+ 195	+ 475	+ 797	+1092
3A	- 117	- 317	- 567	- 837	- 285	- 705	-1135	-1590
4A	- 270	- 665	-1100	-1540	- 525	-1300	-2130	-2955
5A	- 5	- 10	- 35	- 55	- 20	- 20	- 60	- 95
6A	+ 333	+ 770	+1190	+1620	+ 598	+1428	+2248	+3023
7A	+ 175	+ 430	+ 670	+ 895	+ 270	+ 660	+1045	+1430
8A	- 95	- 215	- 370	- 480	- 170	- 460	- 740	-1000
9A	- 230	- 520	- 830	-1110	- 400	- 940	-1530	-2065

Spacing →	S = 10-1/2"				S = 21"			
Gage	Load W lbs.				Load W lbs.			
	5-1/6	12-1/6	19-1/6	26-1/6	5-1/6	12-1/6	19-1/6	26-1/6
0-1A	+ 745	+1770	+2840	+3920	+1210	+2700	+4240	+5810
2A	+ 330	+ 810	+1285	+1805	+ 660	+1310	+2060	+3090
3A	- 485	-1135	-1840	-2505	- 690	-1720	-2760	-3670
4A	- 915	-2215	-3585	-4920	-1650	-3630	-5660	-5530
5A	+ 5	+ 25	0	- 40	+ 170	+ 200	+ 180	+ 60
6A	+1032	+2397	+3797	+5072	+1640	+3650	+5660	+7640
7A	+ 375	+ 960	+1515	+2075	+ 650	+1420	+2160	+2990
8A	- 320	- 775	-1210	-1650	- 520	-1240	-2000	-2630
9A	- 685	-1560	-2395	-3205	- 980	-2260	-3490	-4610

$\frac{1}{4}$" x $\frac{1}{8}$"

Stiffeners

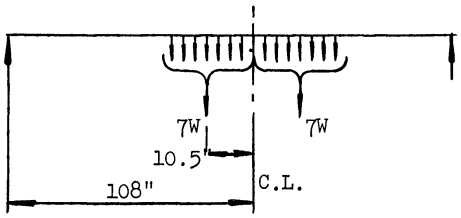

Loading Condition

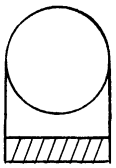

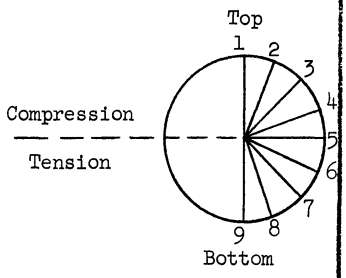

Table 6

STRESSES ON THE OUTSIDE FACE OF THE STIFFENER
DUE TO THE SEPARATE EFFECT OF THE LOCAL LOADING, PSI

(Local loading minus bending)

Gage	Load W lbs.		
	$5\frac{1}{6}$	$12\frac{1}{6}$	$19\frac{1}{6}$
0-1A	+ 480	+ 987	+1565
2A	+ 220	+ 475	+ 745
3A	- 235	- 582	- 930
4A	- 550	-1330	-2130
5A	+ 20	- 25	- 105
6A	+ 600	+1325	+2035
7A	+ 280	+ 590	+ 895
8A	- 170	- 450	- 730
9A	- 400	- 885	-1435

$\frac{1}{4}$" x $\frac{3}{16}$" Stiffeners

Spacing = $10\frac{1}{2}$"

NOTE: See loading condition of Table 5.

Table 7

TRANSVERSE STRESSES ON THE SHELL, PSI.

(Pure bending)

Location	Moment in-lbs.			
	4993	10460	16025	21350
I-1B-T	+ 34	+ 34	+ 56	+101
I-3B-T	+ 11	- 34	- 11	- 11
I-5B-T	- 11	- 45	- 79	-146
I-7B-T	+ 79	+180	+248	+349
I-9B-T	+169	+383	+574	+799
0-1B-T	+ 45	+ 56	+ 68	+ 90
0-3B-T	0	- 45	- 68	- 68
0-5B-T	+ 23	+ 68	+146	+270
0-7B-T	- 23	- 23	- 11	+ 34
0-9B-T	- 34	- 23	- 56	- 56
I-1D-T	+ 11	+ 11	+ 23	+ 45
I-3D-T	- 34	- 45	- 45	- 34
I-5D-T	- 11	- 45	- 68	-135
I-7D-T	+ 34	+ 90	+113	+135
I-9D-T	+ 45	+101	+180	+349
0-1D-T	- 45	- 90	-158	-225
0-3D-T	- 45	- 79	-124	-169
0-5D-T	+ 11	+ 45	+ 90	+214
0-7D-T	+ 68	+158	+203	+281
0-9D-T	0	+ 11	+ 11	0

$\frac{1}{8}$" x $\frac{1}{4}$" Stiffeners

S = $10\frac{1}{2}$ Inches

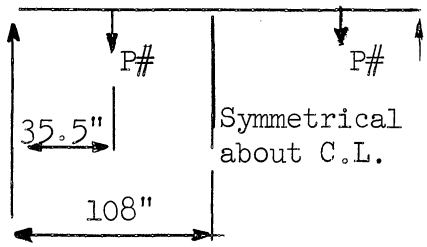

$$M_c = 3218 + 35.5P$$

where P = Load on each basket

Loading Condition

Table 8

STRESSES ON THE OUTSIDE FACE OF THE STIFFENER, PSI.

(Pure bending)

Gage	Moment in-lbs.							
	3218	6744	11522	16299	21077	26959	30491	34218
0-1A	+135	+250	+345	+325	+215	+ 85	- 65	- 265
2A	+ 80	+130	+150	+115	+ 5	- 720	- 880	-1330
3A	+ 65	+130	+220	+315	+400	+ 265	+ 215	+ 115
4A	+ 50	+135	+305	+555	+840	+1370	+1820	+2380
5A	+ 35	+ 90	+240	+475	+765	+1465	+1955	+2575
6A	- 8	0	+ 45	+135	+310	+ 572	+ 772	+ 992
7A	- 55	-120	-215	-320	-460	- 715	- 885	-1075
8A	-120	-270	-515	-820	-1170	-1720	-2270	-2770
9A	-200	-435	-820	-1285	-1805	-2600	-3140	-3800

NOTE:

See loading diagram of Table 1.

S = 10 $\frac{1}{2}$"

$\frac{1}{4}$" x $\frac{1}{8}$" Stiffeners

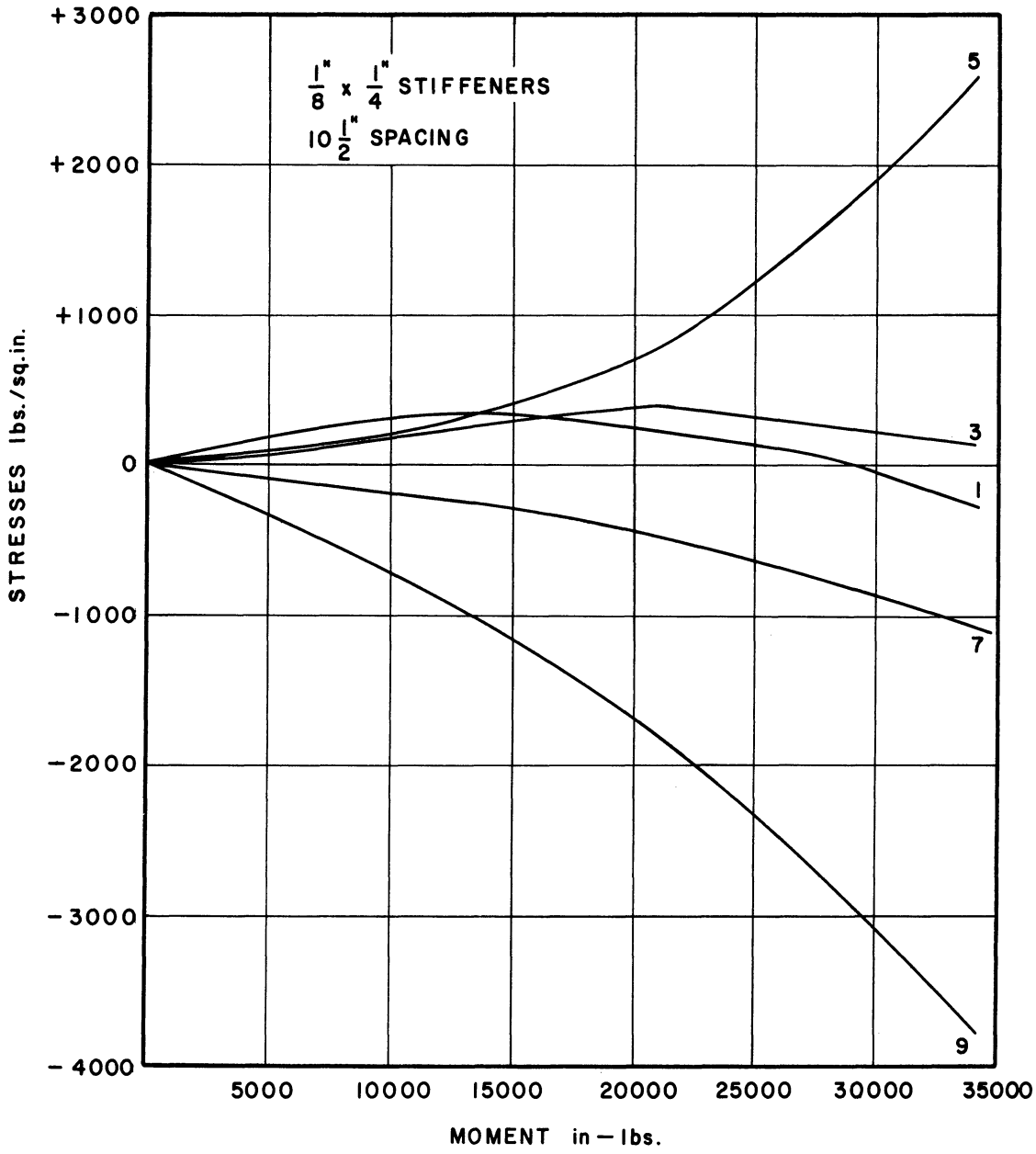

Figure 8. Stresses on the Outside Face of the Stiffener Vs. Pure Applied Bending Moment.

ANALYTICAL INVESTIGATION

Interpretation of the Data

A study of the curves in Figure 8 shows that the variation of the stress in the stiffener is a nonlinear function of the applied pure bending moment on the cylinder, especially at points 1, 5 and 9 (top, center and bottom of the stiffener). One also observes that the tensile stress on the outside face of the stiffener at point 1, increases nonlinearly until the applied bending moment reaches a certain value, after which the tensile stress begins to decrease with the increase of the moment.

The above behavior suggests that the stresses on the stiffener, due to an applied pure bending moment on the cylinder, are caused by more than one type of action. Two types of action can be given to explain the above stress variation in the stiffener as a function of the applied pure bending moment. These types of action are:

(1) the flattening of the cylinder, i.e., an increase in the horizontal diameter and a decrease in the vertical diameter of the cylinder. This is caused by the curvature of the cylinder when subjected to bending, whereby the longitudinal stresses at both the top and bottom halves of the cylinder will have resultant forces acting towards the center of the cylinder, thus causing it to flatten. (See Figure 10.)

(2) The bulging of the cylinder. This is caused by the tendency of the cylinder to change its circular shape when subjected to bending, as the radii of the cylinder in the compression half tend to increase and those in the tension half tend to decrease due to Poisson's ratio. (See Figure 15.)

The stiffeners can be visualized as tending to retain the original circular shape of the cylinder when subjected to pure bending, against both its tendency to flatten and its tendency to bulge.

The bulging of the cylinder will subject the stiffeners to normal stresses which are tension on the compression half of the cylinder and compression on the tension half of the cylinder. All forces and stresses due to this type of action will be shown later to be linear with the applied moment on the cylinder.

The flattening of the cylinder tends to create bending moments in the stiffeners with compression on the outside face of the stiffener at both the top and bottom (points 1 and 9) and tension on the outside face of the stiffener at the center (point 5). The stresses due to the flattening action will be shown later to vary nonlinearly with the applied moment on the cylinder.

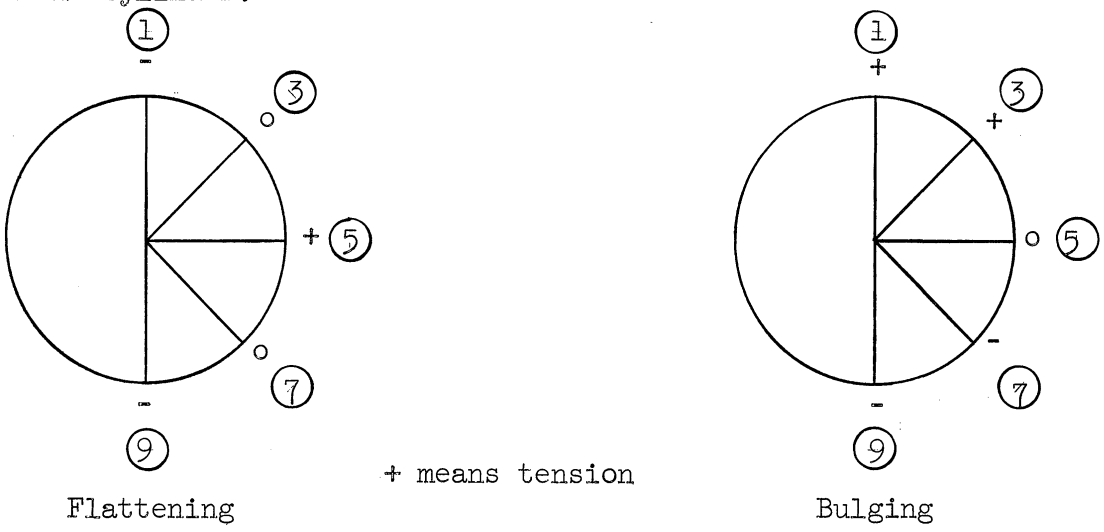

Figure 9. Types of Stress on the Outside Face of the Stiffener.

Figure 9 shows the types of stresses on the outside face of the stiffener due to the two types of action, the flattening and the bulging.

It is seen from Figure 9 that the flattening and the bulging cause the same type of stress on the outside face of the stiffener at point 9 and opposite stresses on the outside face of the stiffener at point 1. At point 5 flattening will be the main contributing factor to the stresses, while bulging will be the main contributing factor to the stress at points 3 and 7.

The transverse stresses on the shell (Table 7) are very sensitive to any imperfections in the shell and to any variations in the cross-section of the cylinder. For this reason no consistent pattern of variation is obtained by studying the stresses of Table 7 except at point 5 where the flattening of the cylinder is clearly indicated by the tensile stresses on the outside and the compressive stresses on the inside of the shell. Furthermore, these stresses at point 5 vary nonlinearly with the applied bending moment on the cylinder according to approximately the same rule as the variation of the stresses on the stiffener.

The Effect of the Flattening of the Cylinder

The flattening of the cylinder is illustrated in Figure 10, where both the compressive and tensile longitudinal stresses at the top and bottom halves of the cylinder respectively, have resultant forces, R, parallel to the plane of bending (vertical forces) and acting toward the inside of the cylinder. The longitudinal stress σ_x at any angle φ measured from the vertical as shown in Figure 10b is equal to:

$$\sigma_x = -\frac{Er}{\rho} \cos \varphi \qquad (6)$$

The resultant of the longitudinal stresses acting toward the inside of the cylinder can be computed at any angle φ by considering a unit length

both transversely and longitudinally. The value of R per unit of surface (see Figure 10c) will be equal to:

$$R = \frac{Ert}{\rho^2} \cos \varphi \qquad (7)$$

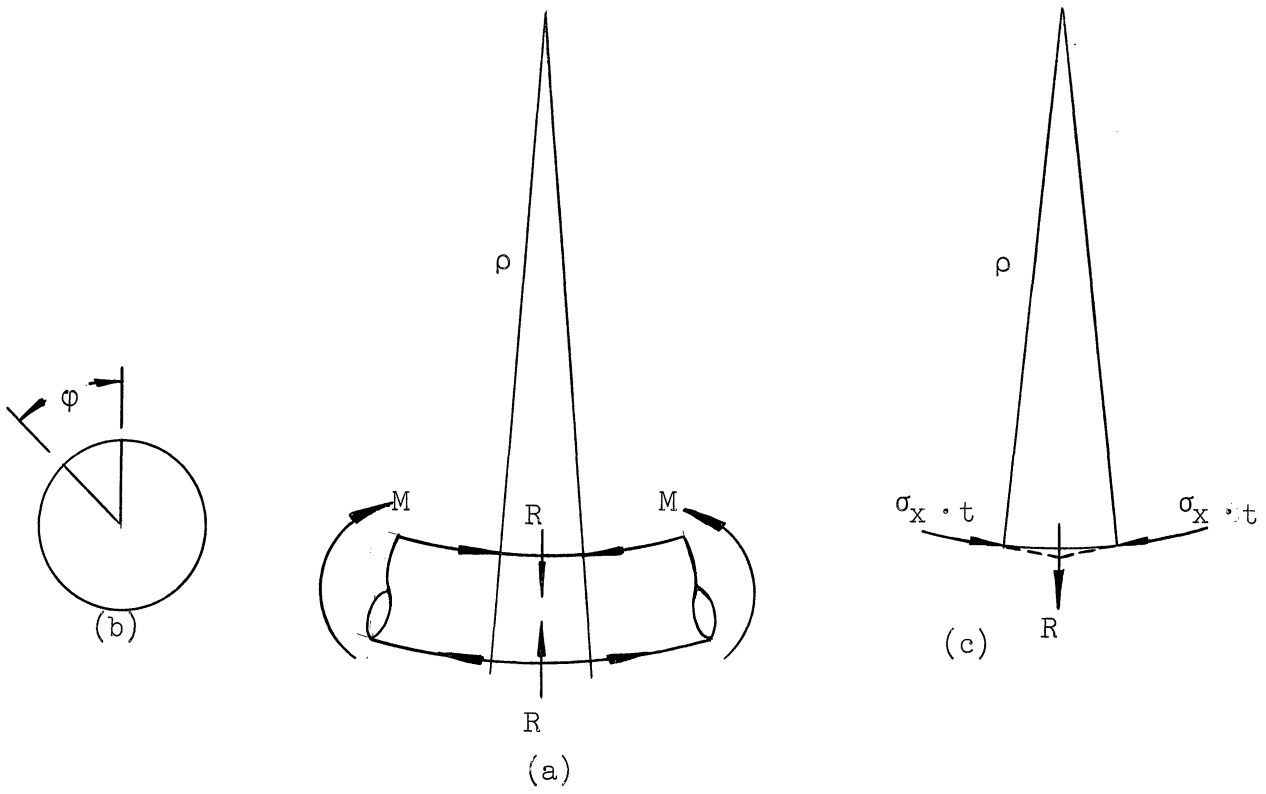

Figure 10. Illustration of the Flattening of the Cylinder.

The flattening of the cylinder is, therefore, equivalent to subjecting it to vertical pressure whose magnitude is $\frac{Ert}{\rho^2} \cos \varphi$ per unit circumferential area as was noted by Brazier[2].

The distribution of the forces on any stiffener, due to the flattening of the cylinder, can be assumed to vary according to the variation of the pressure on the cylinder. Figure 11 shows the assumed loading

on a stiffener due to the flattening of the cylinder. It should be mentioned that a vertical force of p cos φ/circumferential unit length is equal to p/horizontal unit length.

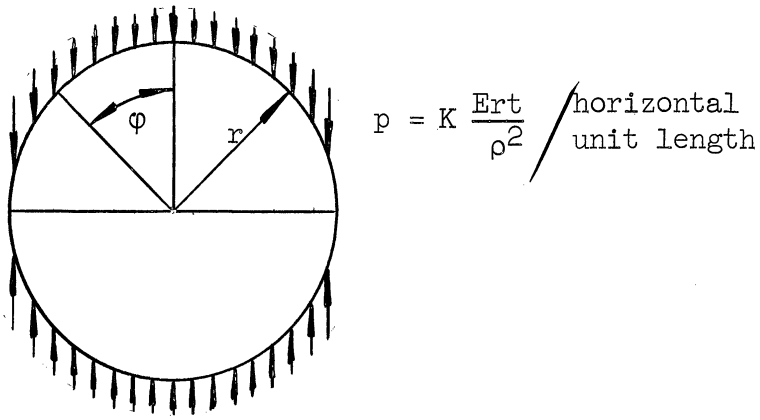

Figure 11. Distribution of the Forces Acting on a Ring Stiffener Due to the Flattening of the Cylinder.

Due to the flattening of the cylinder the stiffener is acted on by the vertical pressure shown in Figure 11 whose magnitude is $K \frac{Ert}{\rho^2}$/horizontal unit length. K which has the unit of length is a function of very complex nature and varies with the spacing "s" of the stiffeners and with the other parameters of the problem. The value of K will be discussed later.

The bending moments and the normal forces in the stiffener, subjected to the flattening forces of Figure 11, are given by the following equations:

$$M_r = -\frac{pr^2}{4} \cos 2\varphi \qquad (8)$$

$$N_r = -p\, r \sin^2 \varphi \qquad (9)$$

where $p = K \frac{Ert}{\rho^2}$

\+ moment in the ring will designate tension on the outside

\+ normal force in the ring will designate tension.

The maximum possible value for K is the magnitude of the spacing "S" of the stiffeners assuming that the shell is completely ineffective in resisting the vertical pressures resulting from the flattening of the cylinder.

If one assumes that K = S, then:

$$M_r = - S \frac{Ert}{\rho^2} \frac{r^2}{4} \cos 2\varphi$$

If $1/\rho^2$ is taken to be equal to $\frac{M^2}{E^2I^2} = \frac{M^2}{E^2\pi^2r^6t^2}$, then M_r will reduce to the following form:

$$M_r = - \frac{1}{4\pi^2r^3t} \frac{M^2}{E} S \cos 2\varphi \qquad (10)$$

Equation (10) is identical with Equation (4) which was obtained by using Hoff's results (Reference 6). It should be noted that t_L in Equation (4) becomes t in Equation (10).

It is important to note that the value of K varies primarily with the spacing "S" of the rings and with the stiffness of the rings relative to the shell. Also that K will approach the value of S in case of closely spaced rigid rings. Hoff[6] pointed out that his analysis was based on assumptions for the deflections which will represent the true shape of the structure in case of rigid stringers or a great number of very closely spaced rings. This, of course, is not the case in the present problem.

The Value of K

The vertical pressure acting on the cylinder as a result of its flattening will be resisted in both the transverse and the longitudinal directions. This resistance can be closely approximated by assuming that

it is similar to a beam subjected to a uniform transverse load and supported on an elastic foundation. The parameters of K can therefore be obtained by studying the analogous problem of an infinitely long beam (Figure 12) loaded by a uniformly distributed load q, and uniformly supported by an elastic support whose spring constant is K_1(lbs./in.^{2}). The continuous beam is also supported at different points by concentrated elastic supports whose spacing is equal to "S" and whose spring constant is K_2(lbs./in.).

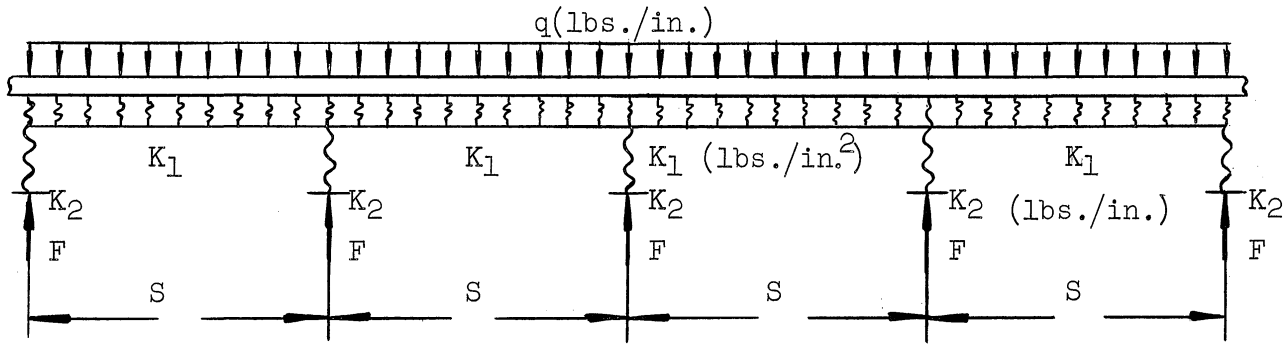

Figure 12. Infinitely Long Beam on Elastic Supports.

The magnitude of the force, F, in any one of the concentrated elastic supports can be obtained by the method of superposition as illustrated in Figure 13. Figure 13a shows the elastically supported beam acted on by the uniformly distributed load q and Figure 13b shows the elastically supported beam acted on by the concentrated loads (F forces).

The deflection Δ_1 of Figure 13a is simply equal to

$$\Delta_1 = \frac{q}{k_1} .$$

The deflection Δ_F (Figure 13b) due to the system of concentrated supports should be equal to Δ_1 minus the deformation in the elastic concentrated support. This relationship can be written in the following form:

$$\Delta_F = \frac{q}{k_1} - \frac{F}{k_2} \tag{11}$$

The deflection Δ_F will be obtained by the use of the reciprocal theorem.

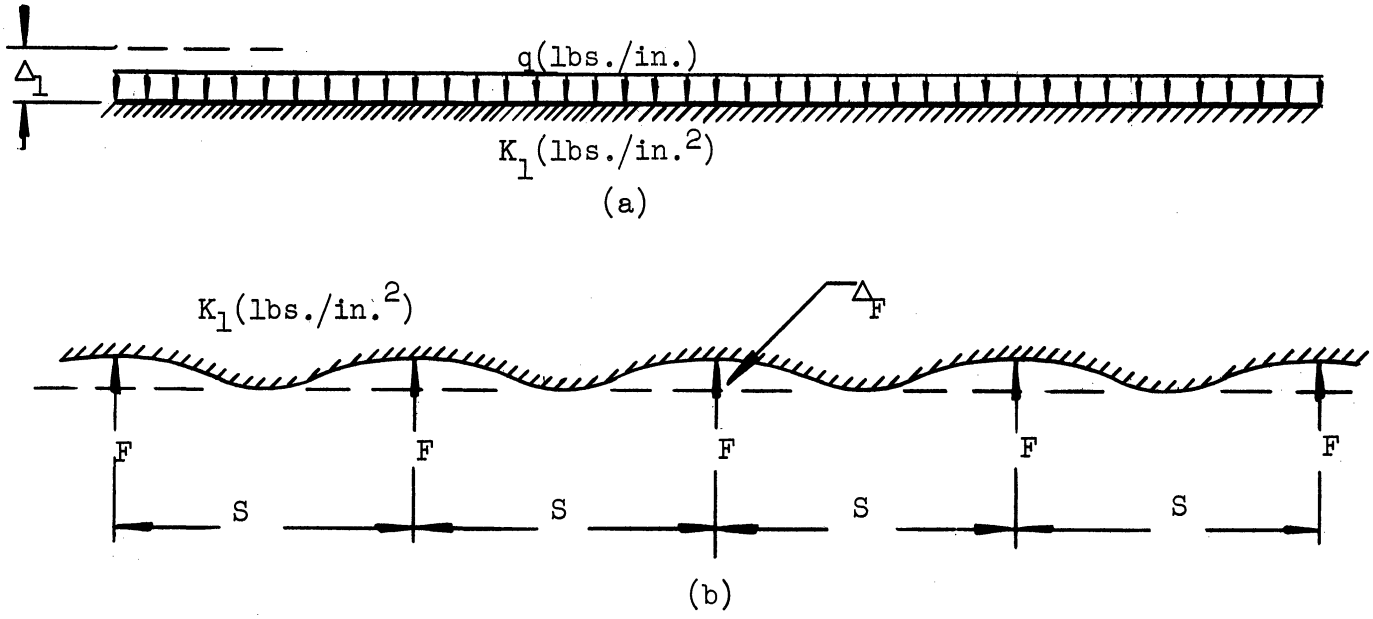

Figure 13. Infinitely Long Beam on Elastic Supports.

The displacement curve (Figure 14) of an infinitely long beam, elastically supported, and acted on by a unit concentrated load, is given by the following equation: (See page 11 of Reference 5.)

$$y = \frac{\lambda}{2k_1}\left[e^{-\lambda x}(\cos \lambda x + \sin \lambda x)\right] \tag{12}$$

where

$$\lambda = \sqrt[4]{\frac{k_1}{4EI}}$$

E = the modulus of Elasticity of the beam

I = the moment of Inertia of the beam.

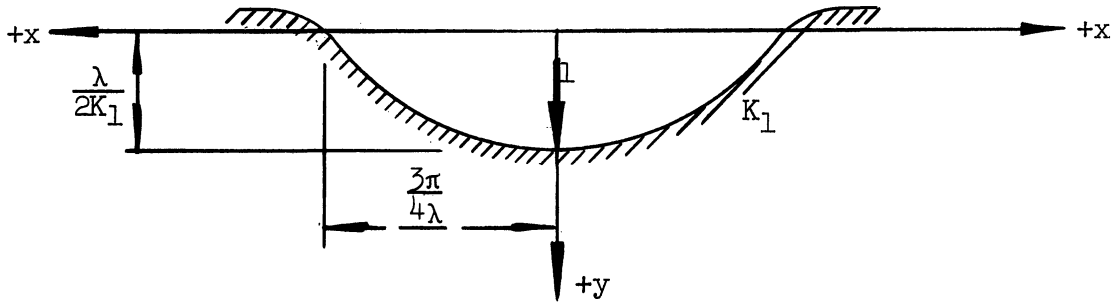

Figure 14. Infinitely Long Beam on an Elastic Support Loaded by a Unit Concentrated Load.

Using the reciprocal theorem the deflection Δ_F of Figure 13b will therefore be equal to:

$$\Delta_F = F \frac{\lambda}{2k_1} \left[1 + 2 \sum_{n=1}^{\infty} e^{-n\lambda s} (\cos n\lambda s + \sin n\lambda s) \right] \qquad (13)$$

If the value of Δ_F as given by Equation (13) is substituted in Equation (11), then F can be written in the following form:

$$F = \frac{q}{\frac{\lambda}{2} \left[1 + 2 \sum_{n=1}^{\infty} e^{-n\lambda s} (\cos n\lambda s + \sin n\lambda s) \right] + \frac{k_1}{k_2}} \qquad (14)$$

It should be mentioned that $\frac{k_1}{k_2}$ will be equal to zero for the case of rigid supports ($k_2 = \infty$).

If we let

$$\left[1 + 2 \sum_{n=1}^{\infty} e^{-nx} (\cos nx + \sin nx)\right] = \psi(x) \tag{15}$$

Then the force F of Equation (14) will be written in the form:

$$F = \frac{q}{\frac{\lambda}{2}\left[\psi(\lambda s)\right] + \frac{k_1}{k_2}} \tag{16}$$

The resistance of the stiffeners when subjected to the flattening action will be analogous to the resistance of the concentrated elastic supports, while the resistance of the shell will be analogous to the resistance of the uniformly distributed elastic supports (Figure 12). Therefore the forces on the stiffeners $K \frac{Ert}{\rho^2}$ (Figure 11) will be assumed to have the same parameters as the force F of Equation (16), in which case $\frac{Ert}{\rho^2}$ will be equivalent to q. The parameters of K can therefore be obtained in the following manner:

$$K_1 \sim \frac{Et^3}{r^4} \qquad K_2 \sim \frac{EI_r}{r_r^4}$$

$$\therefore \frac{K_1}{K_2} \sim \frac{t^3}{I_r} \cdot \left(\frac{r_r}{r}\right)^4$$

or

$$\frac{K_1}{K_2} = C_1 \frac{t^3}{I_r} \left(\frac{r_r}{r}\right)^4 = C_1 \frac{t^3}{I_r} \tag{17}$$

where: t = thickness of the cylinder

r = mean radius of the cylinder

r_r = mean radius of the stiffener

I_r = moment of inertia of the ring stiffener

C_1 = constant

$$\lambda \sim \sqrt[4]{\frac{Et^3}{r^4 Et^3}} \sim \frac{1}{r}$$

or
$$\lambda = \frac{C_2}{r} \tag{18}$$

where C_2 = constant.

Note that r_r is taken equal to r.

The function K will therefore take the form:

$$K = \frac{1}{\frac{\lambda}{2}\left[\psi(\lambda s)\right] + C_1 \frac{t^3}{I_r}} \tag{19}$$

where $\lambda = \frac{C_2}{r}$.

The numerical values of the constants C_1 and C_2 will be evaluated later by the use of the experimental data.

The Effect of the Bulging of the Cylinder

The bulging of the cylinder is caused by the increase of the radii in the compression half and a decrease in the tension half of the cylinder due to Poisson's ratio. The longitudinal stresses in the cylinder due to an applied pure bending moment will be equal to:

$$\sigma_x = -\frac{M}{\pi r^2 t} \cos \varphi \tag{20}$$

where φ is measured as shown in Figure 15.

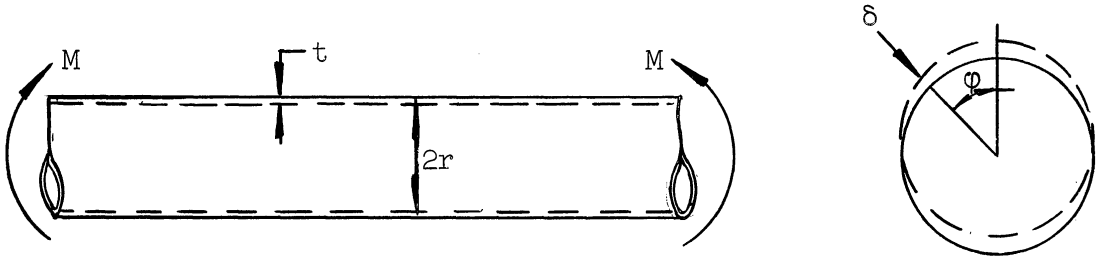

Figure 15. Illustration of the Bulging of the Cylinder.

The radial displacements in the cylinder due to the bulging will be equal to:

$$\delta = \frac{\mu M}{\pi r t E} \cos \varphi \qquad (21)$$

The distribution of the radial forces acting on the stiffeners will be assumed proportional to the radial displacement δ (Equation 21) or equal to Z cos φ. The tangential forces Z sin φ will satisfy the equilibrium conditions. This distribution of the forces on the stiffeners due to bulging is given in Figure 16.

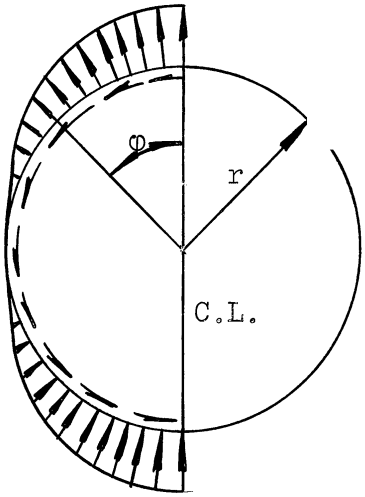

Radial Forces = Z cos φ
Tangential Forces = Z sin φ

Symmetrical about C.L.

Figure 16. Distribution of the Forces Acting on a Ring Stiffener Due to the Bulging of the Cylinder.

If the shear and normal deformations are ignored, then the loading of Figure 16 produces no bending moments in the ring, a condition which indicates that the total strain energy in the ring is approaching a minimum. For this condition of no bending moments, the normal forces in the ring will be given by the following equation:

$$N_r = Zr \cos \varphi \qquad (22)$$

The stiffeners, due to bulging of the cylinder, are therefore mainly subjected to normal forces. For this reason the parameters of Z of Figure 16 can be obtained by utilizing the solution of the following similar problem. Consider an infinitely long cylinder subjected to uniformly distributed line loads, acting along different circular sections and spaced at a distance "s" (Figure 17).

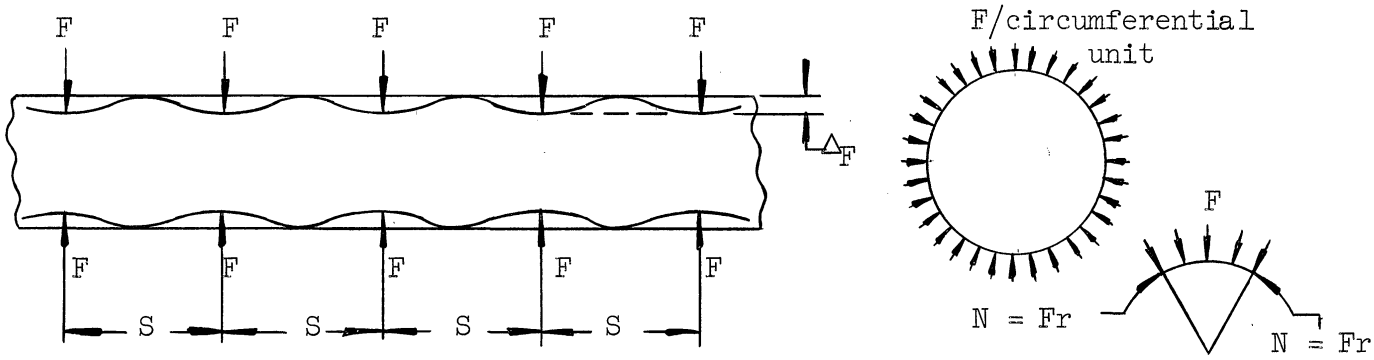

Figure 17. Infinitely Long Cylinder Subjected to Equally Spaced Radial Loads.

The radial displacement of the cylinder under any one of the "F" loads can be obtained by the reciprocal theorem if one uses the solution of an infinitely long cylinder loaded uniformly along one circular section as shown in Figure 18.

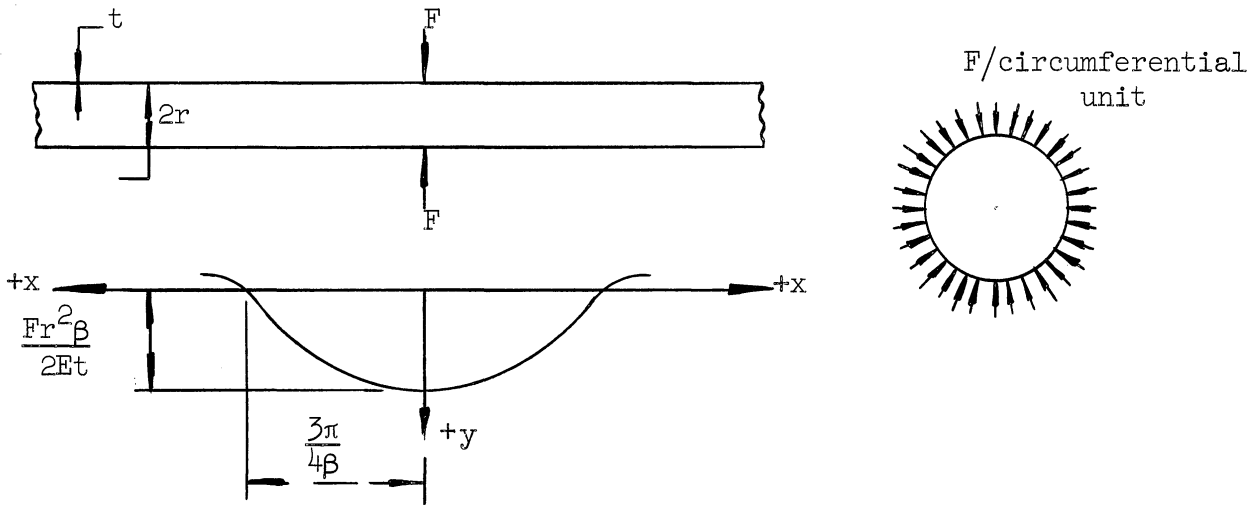

Figure 18. Infinitely Long Cylinder Subjected to Uniformly Distributed Radial Loading Along a Circular Section.

The radial displacements of the cylinder of Figure 18 are given by the equation:*

$$y = \frac{Fr^2\beta}{2Et} e^{-\beta x} (\sin \beta x + \cos \beta x) \qquad (23)$$

where $\beta^4 = \frac{3(1 - \mu^2)}{r^2t^2}$

Using the reciprocal theorem the radial displacement, Δ_F, of Figure 17 can therefore be written in the form:

$$\Delta_F = \frac{Fr^2\beta}{2Et} \left[1 + 2 \sum_{n=1}^{\infty} e^{-n\beta s} (\sin n\beta s + \cos n\beta s)\right]$$

But $\left[1 + 2 \sum_{n=1}^{\infty} e^{-n\beta s} (\sin n\beta s + \cos n\beta s)\right] = \psi(\beta s)$ as has been defined by Equation (15).

$$\therefore \Delta_F = \frac{Fr^2\beta}{2Et} \left[\psi(\beta s)\right] \qquad (24)$$

The tangential components of the forces "F" (Figure 17) can be written as:

$$N = Fr \quad \text{or} \quad F = \frac{N}{r}$$

The normal forces in the stiffener due to the bulging of the cylinder are given in Equation (22). Therefore, the parameters governing the radial displacements in the cylinder at any stiffener location, due to the action of the stiffeners on the cylinder can be established by substituting N_r of Equation (22) for Fr of Equation (24). These radial displacements should be equal to the displacements in the cylinder due to

* See page 396, Reference 14.

bulging (given by Equation 21), minus the radial displacement in the stiffener itself. This strain condition can be expressed by the following equation:

$$\frac{Zr \cos \varphi \, r\beta}{2Et}\left[\psi\,(\beta s)\right] = \frac{\mu}{\pi r t}\frac{M}{E}\cos\varphi - \frac{Zr^2}{AE}\cos\varphi \qquad (25)$$

(Note that $N_r = Zr \cos \varphi$ of Equation (22) was substituted for (Fr) of Equation (24). Also that r_r is taken equal to r.) Solving for Z of Equation (25), one obtains:

$$Z = \frac{\frac{\mu M}{\pi r^3}}{\frac{\beta}{2}\left[\psi(\beta s)\right] + \frac{t}{A_r}} \qquad (26)$$

It should be noted here that the purpose of using the results of another problem was to establish the major parameters relative to the magnitude of the forces acting on the stiffeners due to the bulging of the cylinder. Z as given by Equation (26) should only be used to establish the parameters rather than the magnitude of the forces acting on the stiffener. Two constants can be introduced to define the magnitude of Z which will make it possible to express the value of Z in the form:

$$Z = \frac{\frac{\mu M}{\pi r^3}}{\frac{\beta_1}{2}\left[\psi(\beta_1 s)\right] + C_3\frac{t}{A_r}} \qquad (27)$$

where $\beta_1 = \frac{C_4}{\sqrt{rt}}$.

If the value of Z as given by Equation (27) is substituted in Equation (22), then the following expression for N_r will result:

$$N_r = \frac{\frac{\mu M}{\pi r^2} \cos \varphi}{\frac{\beta_1}{2}\left[\psi(\beta_1 s)\right] + C_3 \frac{t}{A_r}} \qquad (28)$$

where N_r = normal forces in the ring,

t = thickness of the cylinder wall,

A_r = cross-sectional area of the stiffener,

$\beta_1 = \frac{C_4}{\sqrt{rt}}$

Equation (28) gives the normal forces in the ring stiffeners due to bulging of the cylinder when subjected to pure bending. The constants C_3 and C_4 will be determined later on by the use of the experimental results.

The Separate Effect of the Local Loading

The bending moments in the cylinder resulting from the application of any local loading will cause the cylinder to flatten and to bulge. In addition to the flattening and the bulging of the cylinder, the local loading will have a separate effect on the ring stiffeners.

Two types of local loading on the cylinder will be considered:

a. Uniformly distributed radial loading acting on the top half of the cylinder,

b. Vertical loading uniformly distributed with respect to the horizontal diameter and acting on the top half of the cylinder.

If the cylinder is loaded by uniformly distributed radial loading on the top half, then the forces on the stiffeners, due to the separate effect of this loading, can be assumed to follow the distribution shown

in Figure 19, where w is the magnitude of the radial pressure on the cylinder. The tangential forces of $\frac{2}{\pi}$ w'sin φ will satisfy the equilibrium condition. This distribution will be shown later to be justified by the experimental stresses.

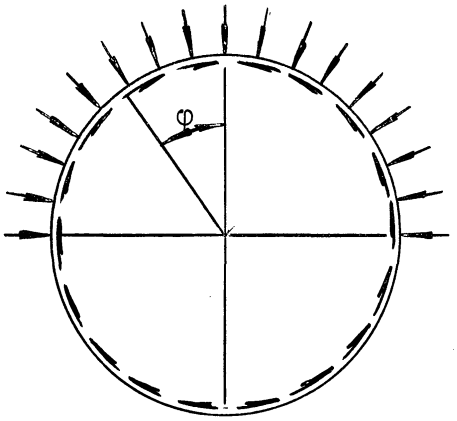

Figure 19. Forces on the Stiffener Due to the Separate Effect of Local Radial Loading.

K' (Figure 19), which has the unit of length, is a function varying with the spacing of the stiffeners and with the other parameters of the problem.

The bending moments and the normal forces in the ring loaded as shown in Figure 19 are given by the following equations:

$$\left.\begin{aligned} M_r &= \left(\frac{1}{2} - \frac{3}{2\pi}\cos\varphi - \frac{1}{\pi}\varphi\sin\varphi\right) w'r^2 \\ &\left[\text{For } 0 \leq \varphi \leq \frac{\pi}{2}\right] \\ M_r &= \left(\sin\varphi - \frac{1}{2} - \frac{3}{2\pi}\cos\varphi - \frac{1}{\pi}\varphi\sin\varphi\right) w'r^2 \\ &\left[\text{For } \frac{\pi}{2} \leq \varphi \leq \pi\right] \end{aligned}\right\} \quad (29)$$

$$N_r = \left(-\frac{1}{2\pi}\cos\varphi - 1 + \frac{1}{\pi}\varphi\sin\varphi\right) w'r \qquad \left[\text{For } 0 \leq \varphi \leq \frac{\pi}{2}\right]$$

$$N_r = \left(-\frac{1}{2\pi}\cos\varphi - \sin\varphi + \frac{1}{\pi}\varphi\sin\varphi\right) w'r \qquad \left[\text{For } \frac{\pi}{2} \leq \varphi \leq \pi\right] \qquad (30)$$

In the above equations

$+M_r$ designates tension on the outside,

$+N_r$ designates tension

If the cylinder is subjected to uniformly distributed vertical pressure acting on one half of the cylinder, then the forces on the stiffeners, due to the separate effect of this loading, can be assumed to follow the distribution shown in Figure 20, where Q is the magnitude of the vertical pressure on the cylinder per horizontal unit area. The tangential forces of $\frac{2}{\pi}$ Q'sin φ/circumferential unit, will satisfy the equilibrium condition.

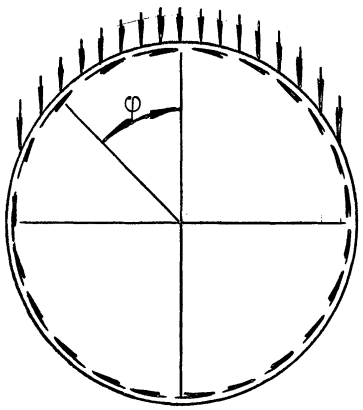

Vertical load =
K'Q = Q'/horizontal unit

Tangential loading =
$\frac{2}{\pi}$ Q' sin φ/circumferential unit

Figure 20. Forces on the Stiffener Due to The Separate Effect of Local Vertical Pressure.

The bending moments and the normal forces in the ring subjected to the forces of Figure 20 are given by the following equations:

$$M_r = \left(\frac{1}{8} - \frac{5}{6\pi}\cos\varphi + \frac{1}{2}\sin^2\varphi - \frac{1}{\pi}\varphi\sin\varphi\right) Q'r^2 \quad \left[\text{For } 0 \leq \varphi \leq \frac{\pi}{2}\right]$$

$$M_r = \left(-\frac{3}{8} - \frac{5}{6\pi}\cos\varphi + \sin\varphi - \frac{1}{\pi}\varphi\sin\varphi\right) Q'r^2 \quad \left[\text{For } \frac{\pi}{2} \leq \varphi \leq \pi\right] \qquad (31)$$

$$N_r = \left(\frac{7}{6\pi}\cos\varphi - \sin^2\varphi + \frac{1}{\pi}\varphi\sin\varphi\right) Q'r \quad \left[\text{For } 0 \leq \varphi \leq \frac{\pi}{2}\right]$$

$$N_r = \left(-\frac{7}{6\pi}\cos\varphi - \sin\varphi + \frac{1}{\pi}\varphi\sin\varphi\right) Q'r \quad \left[\text{For } \frac{\pi}{2} \leq \varphi \leq \pi\right] \qquad (32)$$

In the above equations:

$+M_r$ designates tension on the outside

$+N_r$ designates tension.

The Value of K'

The maximum value that K' can assume is s (spacing of the stiffeners) if the shell is assumed to be completely ineffective in resisting the local forces. This assumption, however, can be completely inaccurate, especially as the spacing of the stiffeners increases.

A more accurate approach to the magnitude of K' can be obtained by assuming that K' varies according to the same rule as K of Equation (19),

or:

$$K' = \frac{1}{\frac{\lambda'}{2}\left[\psi(\lambda's)\right] + C_5\frac{t^3}{I_r}} \tag{33}$$

where $\lambda' = \frac{C_6}{r}$.

The numerical values of the constants C_5 and C_6 will be determined later by the use of the experimental results.

The values of the function $\psi(x)$ as defined in Equation (15) are given in Table 9.

Table 9

VALUES OF THE FUNCTION $\psi(x)$

x	$\psi(x)$	x	$\psi(x)$	x	$\psi(x)$
0.10	20.000	1.40	1.459	3.40	0.921
0.20	10.000	1.50	1.370	3.60	0.929
0.30	6.667	1.60	1.295	3.80	0.938
0.40	5.001	1.70	1.230	4.00	0.949
0.50	4.002	1.80	1.174	4.50	0.973
0.60	3.335	1.90	1.127	5.00	0.991
0.70	2.861	2.00	1.086	5.50	1.000
0.80	2.506	2.20	1.021	6.00	1.003
0.90	2.230	2.40	0.976	6.50	1.004
1.00	2.011	2.60	0.945	7.00	1.003
1.10	1.833	2.80	0.927	7.50	1.001
1.20	1.686	3.00	0.919	8.00	1.001
1.30	1.563	3.20	0.917		

$$\psi(x) = 1 + 2\sum_{n=1}^{\infty} e^{-nx}(\cos nx + \sin nx)$$

CORRELATION OF THE ANALYTICAL INVESTIGATION TO THE EXPERIMENTAL RESULTS

Tabulation of the stresses in the stiffener in terms of:

(a) Flattening of the cylinder.

The experimental stresses on the outside face of the stiffener due to the flattening of the cylinder are tabulated in Tables 10 and 11 for the two different size stiffeners. The values in Tables 10 and 11 are obtained by means of the following assumptions:

(1) The experimental stresses at the center of the stiffener (point 5) as recorded in Tables 1 and 2 are only due to the flattening of the cylinder. Therefore the stress at point 5 provides the basis for determining the magnitudes of the experimental stresses due to flattening.

(2) The distribution of the stresses around the stiffener due to flattening is governed by Equations (8) and (9) which were based on an assumed distribution for the flattening forces (see Figure 11). As shown by Equation (8) the magnitude of the stresses, due to the bending moments caused by flattening, varies according to cos 2φ. The effect of the normal forces as given by Equation (9) is small.

(3) The effective width of the shell acting as an integral part of the stiffener is equal to 24 times the thickness of the shell.

(b) Bulging of the cylinder.

The experimental stresses on the outside face of the stiffener due to the bulging of the cylinder are tabulated in Tables 12 and 13 for the two size stiffeners. Table 12 is obtained by subtracting the values of Table 10 from the corresponding values of Table 1, while Table 13 is obtained by subtracting the values of Table 11 from those of Table 2. In other workds, in a cylinder subjected to pure bending, the stresses in the stiffener due to bulging are equal to the total measured stresses minus the stresses due to flattening.

(c) Separate effect of the local loading.

The experimental stresses on the outside face of the stiffener due to the separate effect of the local radial loading have already been tabulated in Tables 5 and 6. The values of Table 5 are obtained by subtracting the values of Table 1 from the corresponding values of Table 3, while the values of Table 6 are obtained by subtracting the values of Table 2 from the corresponding values of Table 4. In other words, the stresses in the stiffener due to the separate effect of the local loading are taken to be equal to the total measured stresses minus the stresses which are only caused by the bending of the cylinder.

Experimental stresses for the local loading are only available for S = 10-1/2 inches in case of the 1/4" x 3/16" stiffener.

Variation of the Stresses in the Stiffener with Respect to the Load due to:

(a) Flattening of the cylinder.

The theoretical stresses in the stiffener due to the flattening of the cylinder vary proportional to $1/\rho^2$ (see Figure 11). Thus to

Table 10

STRESSES ON THE OUTSIDE FACE OF THE STIFFENER
DUE TO THE FLATTENING OF THE CYLINDER, PSI

(Pure bending)

Spacing →	S = 2-5/8"					S = 5-1/4"				
Gage ↓	Moment in-lbs.					Moment in-lbs.				
	3218	6744	11522	16299	21077	3218	6744	11522	16299	21077
0-1A	- 10	- 35	- 112	- 239	- 402	- 15	- 65	- 194	- 387	- 626
2A	- 7	- 25	- 79	- 170	- 285	- 11	- 46	- 138	- 275	- 445
3A	0	0	- 1	- 2	- 4	0	0	- 2	- 4	- 6
4A	+ 7	+ 25	+ 77	+ 166	+ 278	+ 11	+ 46	+ 134	+ 268	+ 434
5A	+ 10	+ 35	+ 110	+ 235	+ 395	+ 15	+ 65	+ 190	+ 380	+ 615
6A	+ 7	+ 25	+ 77	+ 166	+ 278	+ 11	+ 46	+ 134	+ 268	+ 434
7A	0	0	- 1	- 2	- 4	0	0	- 2	- 4	- 6
8A	- 7	- 25	- 79	- 170	- 285	- 11	- 46	- 138	- 275	- 445
9A	- 10	- 35	- 112	- 239	- 402	- 15	- 65	- 194	- 387	- 626

Spacing →	S = 10-1/2"					S = 21"				
Gage ↓	Moment in-lbs.					Moment in-lbs.				
	3218	6744	11522	16299	21077	3218	6744	11522	16299	21077
0-1A	- 35	- 90	- 245	- 485	- 780	- 40	-122	- 265	- 550	-1040
2A	- 25	- 64	- 174	- 345	- 554	- 28	- 86	- 188	- 391	- 738
3A	0	0	- 2	- 5	- 7	0	- 1	- 2	- 5	- 10
4A	+ 25	+ 64	+ 169	+ 334	+ 539	+ 28	+ 84	+ 183	+ 381	+ 718
5A	+ 35	+ 90	+ 240	+ 475	+ 765	+ 40	+120	+ 260	+ 540	+1020
6A	+ 25	+ 64	+ 169	+ 334	+ 539	+ 28	+ 84	+ 183	+ 381	+ 718
7A	0	0	- 2	- 5	- 7	0	- 1	- 2	- 5	- 10
8A	- 25	- 64	- 174	- 345	- 554	- 28	- 86	- 188	- 391	- 738
9A	- 35	- 90	- 245	- 485	- 780	- 40	-122	- 265	- 550	-1040

$\frac{1}{4}$" x $\frac{1}{8}$"

Stiffeners

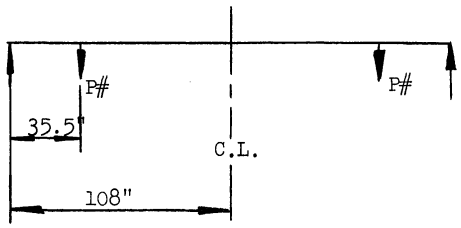

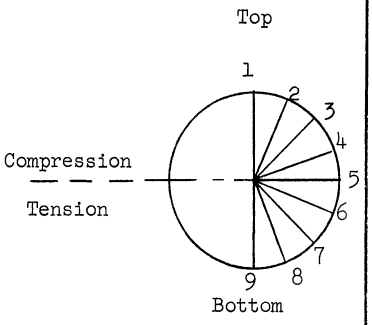

$M_c = 3218 + 35.5P$

where P = Load on each basket

Loading Condition

Table 11

STRESSES ON THE OUTSIDE FACE OF THE STIFFENER
DUE TO THE FLATTENING OF THE CYLINDER, PSI

(Pure bending)

Spacing →	S = 2-5/8"				S = 5-1/4"				S = 10-1/2"			
Gage ↓	Moment in-lbs				Moment in-lbs				Moment in-lbs			
	3218	6744	11522	16299	3218	6744	11522	16299	3218	6744	11522	16299
0-1A	- 10	- 35	- 77	- 149	- 15	- 40	- 121	- 254	- 20	- 70	- 210	- 405
2A	- 7	- 25	- 55	- 106	- 11	- 28	- 87	- 181	- 14	- 50	- 150	- 288
3A	0	0	0	- 2	0	0	- 2	- 3	0	0	- 3	- 5
4A	+ 7	+ 25	+ 55	+ 102	+ 11	+ 28	+ 83	+ 175	+ 14	+ 50	+ 145	+ 277
5A	+ 10	+ 35	+ 77	+ 145	+ 15	+ 40	+ 118	+ 248	+ 20	+ 70	+ 205	+ 395
6A	+ 7	+ 25	+ 55	+ 102	+ 11	+ 28	+ 83	+ 175	+ 14	+ 50	+ 145	+ 277
7A	0	0	0	- 2	0	0	- 2	- 3	0	0	- 3	- 5
8A	- 7	- 25	- 55	- 106	- 11	- 28	- 87	- 181	- 14	- 50	- 150	- 288
9A	- 10	- 35	- 77	- 149	- 15	- 40	- 121	- 254	- 20	- 70	- 210	- 405

$\frac{1"}{4}$ x $\frac{3"}{16}$

Stiffeners

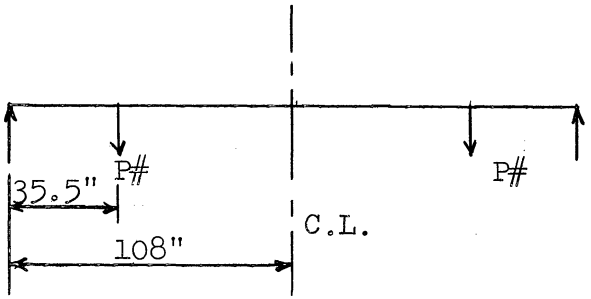

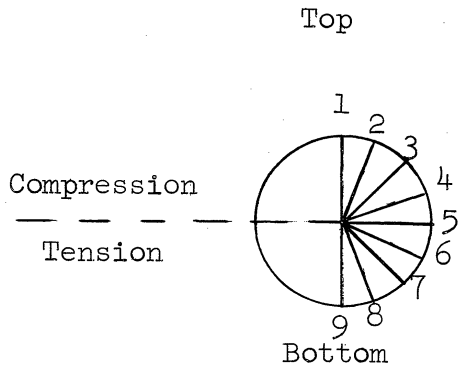

$M_c = 3218 + 35.5P$

where P = Load on each basket

Loading Condition

Table 12

STRESSES ON THE OUTSIDE FACE OF THE STIFFENER
DUE TO THE BULGING OF THE CYLINDER

(Pure bending)

Spacing →	S = 2-5/8"					S = 5-1/4"				
Gage	Moment in-lbs.					Moment in-lbs.				
	3218	6744	11522	16299	21077	3218	6744	11522	16299	21077
0-1A	+160	+310	+ 522	+ 714	+ 892	+165	+345	+ 591	+ 837	+1061
2A	+117	+230	+ 384	+ 533	+ 675	+ 96	+196	+ 348	+ 493	+ 608
3A	+ 88	+180	+ 311	+ 442	+ 574	+ 55	+120	+ 232	+ 354	+ 491
4A	+ 28	+ 80	+ 143	+ 189	+ 227	+ 9	+ 19	+ 56	+ 112	+ 181
5A	0	0	0	0	0	0	0	0	0	0
6A	- 22	- 43	- 82	- 131	- 183	- 8	- 21	- 59	- 103	- 134
7A	- 95	-190	- 324	- 463	- 594	- 45	-105	- 203	- 326	- 459
8A	- 98	-205	- 351	- 485	- 660	- 99	-204	- 342	- 485	- 635
9A	-145	-310	- 553	- 786	-1033	-165	-335	- 576	- 773	- 989

Spacing →	S = 10-1/2"					S = 21"				
Gage	Moment in-lbs.					Moment in-lbs.				
	3218	6744	11522	16299	21077	3218	6744	11522	16299	21077
0-1A	+170	+340	+ 590	+ 810	+ 995	+180	+372	+ 565	+ 850	+1240
2A	+105	+194	+ 324	+ 460	+ 559	+ 18	+ 66	+ 135	+ 181	- 42
3A	+ 65	+130	+ 222	+ 320	+ 407	+ 40	+ 91	+ 162	+ 271	+ 210
4A	+ 25	+ 71	+ 136	+ 221	+ 301	+ 12	+ 26	+ 87	+ 199	+ 462
5A	0	0	0	0	0	0	0	0	0	0
6A	- 17	- 64	- 124	- 199	- 229	- 8	- 44	- 83	- 191	- 368
7A	- 55	-120	- 213	- 315	- 453	- 80	-129	- 208	- 295	- 530
8A	- 95	-206	- 341	- 475	- 616	- 42	-114	- 252	- 329	- 412
9A	-165	-345	- 575	- 800	-1025	-140	-278	- 515	- 690	- 780

$\frac{1}{4}$" x $\frac{1}{8}$"

Stiffeners

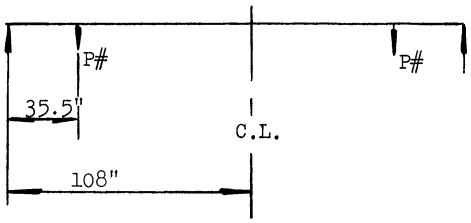

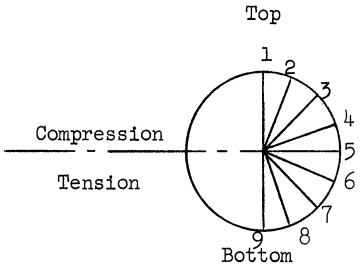

$M_c = 3218 + 35.5P$

where P = Load on each basket

Loading Condition

Table 13

STRESSES ON THE OUTSIDE FACE OF THE STIFFENER
DUE TO THE BULGING OF THE CYLINDER
PSI
(Pure bending)

Spacing →	S = 2-5/8"				S = 5-1/4"				S = 10-1/2"			
Gage ↓	Moment in-lbs				Moment in-lbs				Moment in-lbs			
	3218	6744	11522	16299	3218	6744	11522	16299	3218	6744	11522	16299
0-1A	+110	+250	+ 447	+ 664	+135	+275	+ 498	+ 752	+150	+350	+ 653	+ 940
2A	+ 77	+175	+ 300	+ 446	+ 81	+148	+ 257	+ 381	+ 64	+140	+ 265	+ 383
3A	+ 25	+ 77	+ 170	+ 289	+ 10	+ 25	+ 67	+ 128	+ 10	+ 25	+ 55	+ 95
4A	+ 18	- 45	+ 92	+ 155	+ 9	+ 32	+ 80	+ 135	+ 6	+ 20	+ 45	+ 73
5A	0	0	0	0	0	0	0	0	0	0	0	0
6A	- 42	- 90	- 118	- 132	- 6	- 8	- 18	- 30	+ 6	+ 10	+ 10	- 2
7A	- 40	- 80	- 135	- 188	- 30	- 55	- 96	- 137	+ 15	+ 25	+ 48	+ 45
8A	- 78	-170	- 300	- 429	- 69	-147	- 253	- 349	- 56	- 90	- 110	- 153
9A	-100	-205	- 348	- 501	-125	-265	- 449	- 601	-140	-260	- 425	- 570

$\frac{1}{4}$" x $\frac{3}{16}$"

Stiffeners

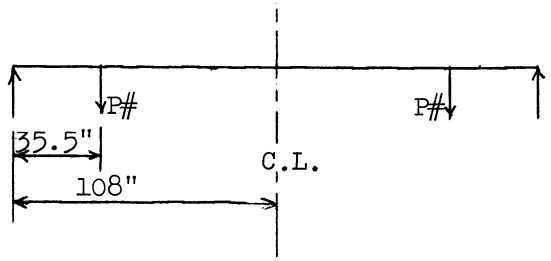

$M_c = 3218 + 35.5P$

where P = Load on each basket

Loading Condition

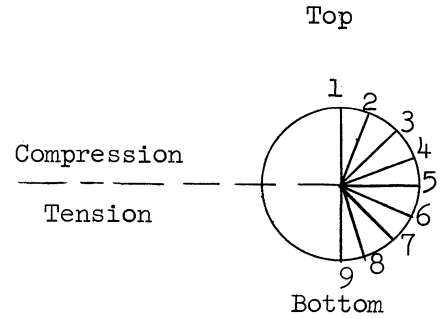

establish the variation of the stresses on the stiffener with respect to the applied bending moment, one has to study the variation of the curvature, $1/\rho$, with respect to M.

The curvature of the cylinder, $1/\rho$, of the long unstiffened cylinder subjected to pure bending varies nonlinearly with the moment (see Reference 2) due to the progressive flattening of the cylinder. The relationship between the moment and the curvature is given by Equation (1). Equation (2) relates the moment to the curvature if no progressive flattening is assumed. Both Equations(1) and (2) are plotted in Figure 21 for the model considered in this thesis.

It should be stated that the vertical divergence between curves (1) and (2) in Figure 21 will change with variations in the r and t values of the cylinder and that the curves shown are drawn for a long unstiffened cylinder whose r = 5.64 inches and t = 0.025 inches.

For a stiffened cylinder the true curve, expressing the relationship between the applied bending moment and the curvature, although not quantitatively determinable, should fall between curves (1) and (2). Therefore, for a stiffened cylinder, it will be reasonable to assume that the curvature, $1/\rho$, varies linearly with the moment as given by curve (2) especially for the lower values of M where the divergence between curves (1) and (2) is negligible. On the other hand the use of an assumed curve falling between curves (1) and (2) is more justifiable for the higher values of the applied pure bending moment.

If the variation in the curvature, $1/\rho$, is linear with the moment, (curve 2) then the theoretical stresses in the stiffener due to the flattening of the cylinder will be proportional to the square of the moment.

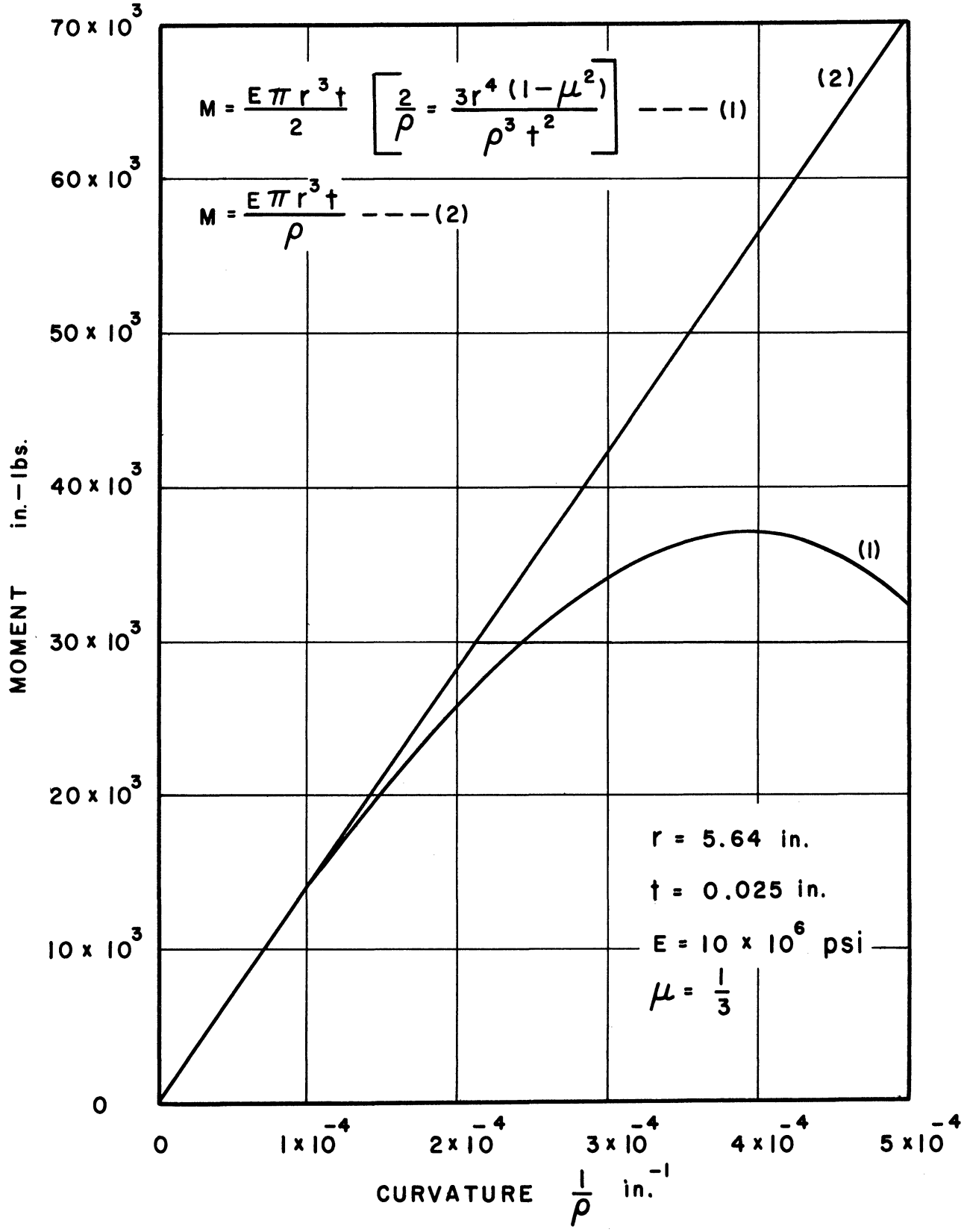

Figure 21. Moment Vs. Curvature - Long Unstiffened Cylinder (Model).

Figure 22 shows a comparative plotting of the stresses on the outside face of the stiffener at point 5, due to flattening, as a function of the applied bending moment on the cylinder. Both the theoretical and experimental stresses are plotted relative to the stress when M = 11522 in-lbs. This stress when M = 11522 in-lbs. is taken to be equal to unity. The good agreement between the experimental and theoretical values justifies the assumption that the experimental stresses at the center of the stiffener (point 5) are only due to the flattening of the cylinder, when subjected to pure bending.

(b) Bulging of the cylinder.

The theoretical stresses in the stiffener, due to the bulging of the cylinder, vary linearly with the applied bending moment (see Equation 28).

The comparison with the experimental results is given in Figure 23 where both the experimental and theoretical stresses at the top of the stiffener (point 1) are plotted relative to the stress when M = 11522 in-lbs. The stress at point 1 when M = 11522 is taken to be equal to unity for both the theoretical and experimental values.

(c) Separate effect of the local loading (flattening and bulging effects are removed).

The theoretical stresses in the stiffener, due to the separate effect of the local loading, vary linearly with the intensity of the load (see Equations 29 and 30). The comparison with the experimental results is given in Figure 24 where both the theoretical and experimental stresses at the top of the stiffener (point 1) are plotted relative to the stress when W = 12-1/6 lbs. (See Tables 5 and 6). Both the theoretical and experimental stresses are taken to be equal to unity when W = 12-1/6 lbs.

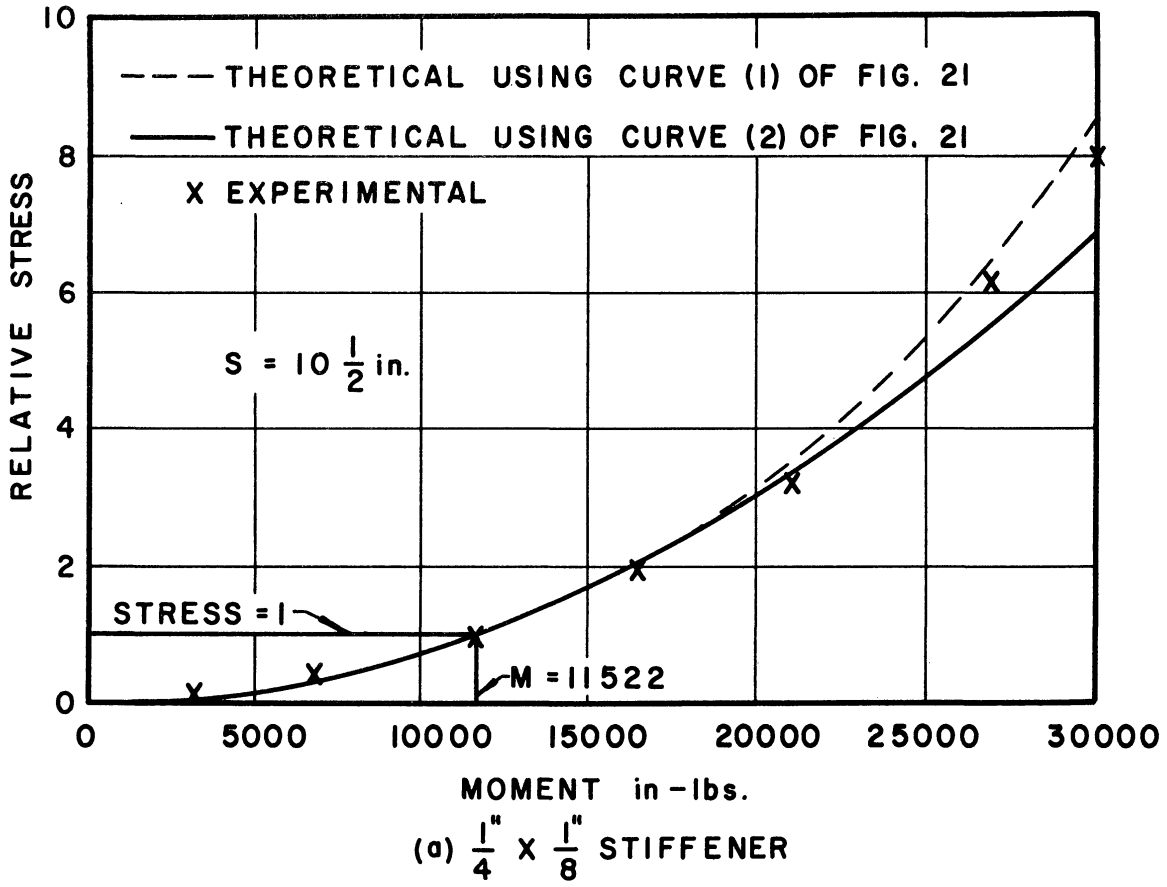

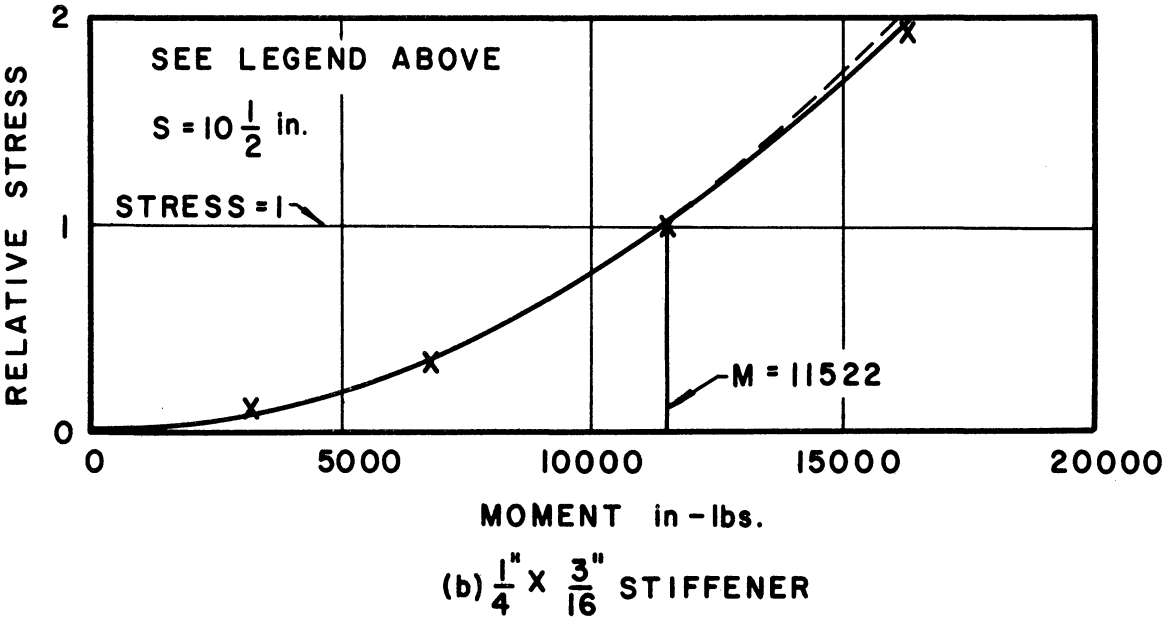

Figure 22. Relative Stress Vs. Moment
(Flattening)

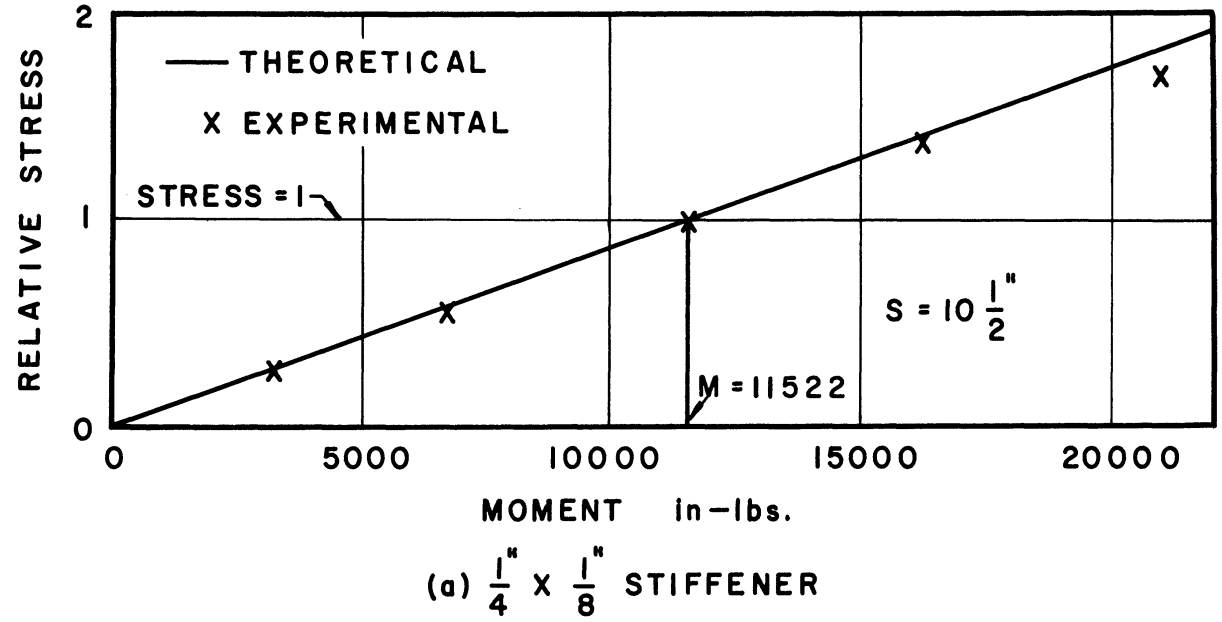

(a) $\frac{1}{4}$" X $\frac{1}{8}$" STIFFENER

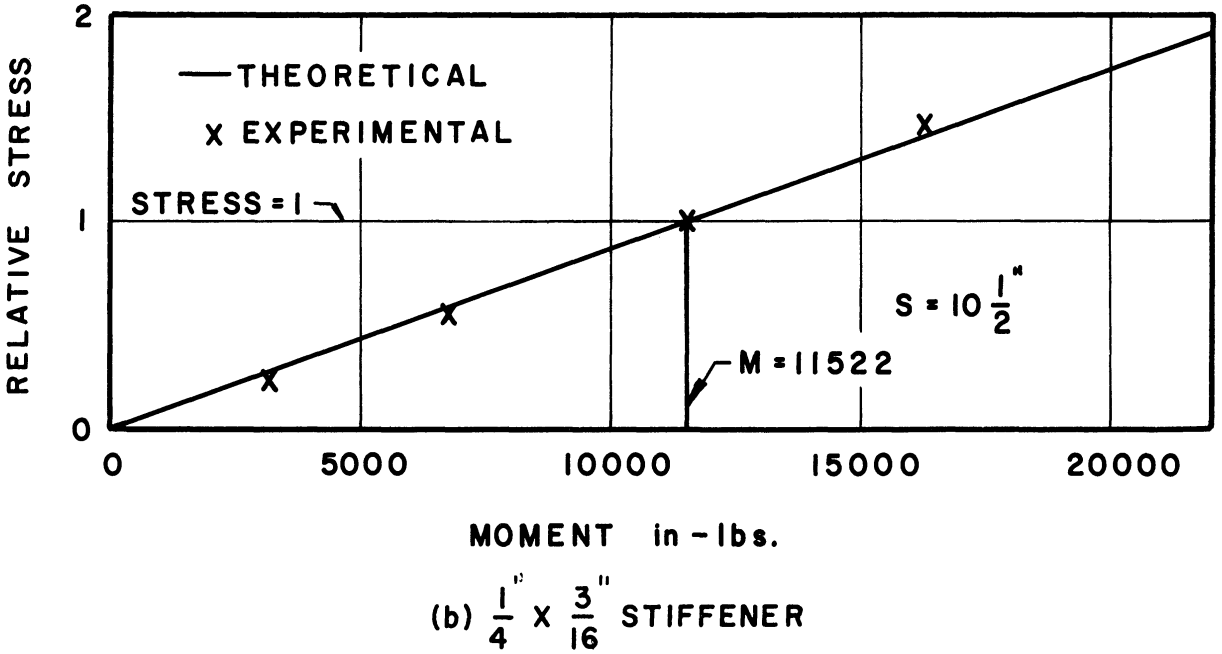

(b) $\frac{1}{4}$" X $\frac{3}{16}$" STIFFENER

Figure 23. Relative Stress Vs. Moment (Bulging)

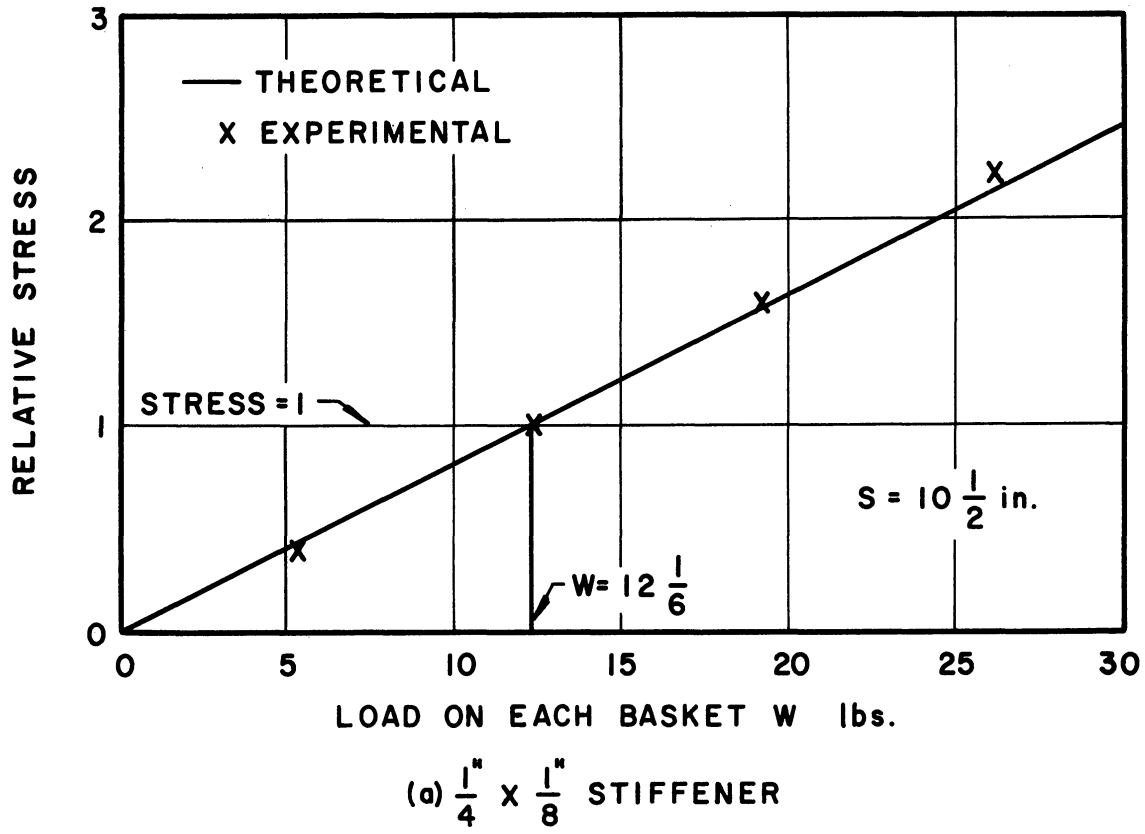

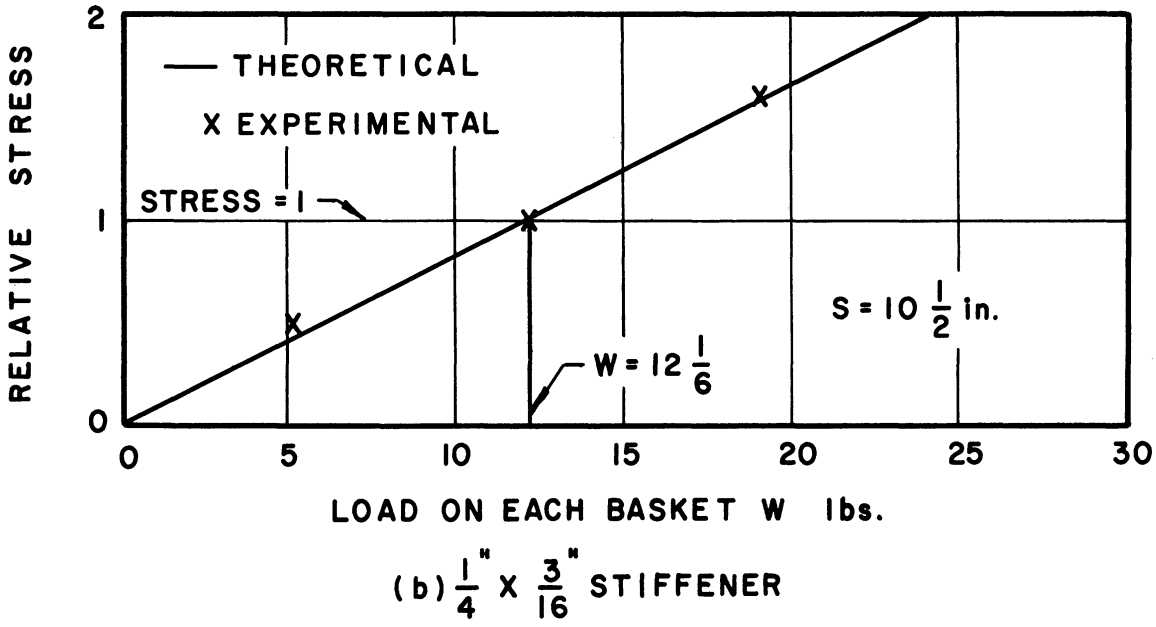

Figure 24. Relative Stress Vs. Load
(Separate effect of the local loading)

Variation of the Stresses in the Stiffener with Respect to the Spacing and Size of the Stiffeners - Evaluation of the Analytical Constants by the Use of the Experimental Data.

(a) Flattening of the cylinder.

The analytical constants C_1 and C_2 (Equation 19) which are associated with the size and spacing of the stiffeners will be determined by the use of the experimental data. The dimensions and properties for the two size stiffeners, which will be needed for the evaluation of all the analytical constants, are given in Table 14.

The experimental value of K (Equation 19) which is associated with the flattening of the cylinder is evaluated in Table 15 by the use of the experimental results. Table 15 gives the value of K for both the 1/4" x 1/8" and the 1/4" x 3/16" stiffeners when S = 10-1/2 inches and M = 11522 in-lbs. To explain Table 15, consider the 1/4" x 1/8" stiffener. The computed stress at point 5 using Equation (8) and (9) is expressed in terms of K and is found to be equal to 65.05 K. Equating this

Table 14

PROPERTIES AND DIMENSIONS OF THE STIFFENERS

	1/4" x 1/8" (width x thickness) stiff.	1/4" x 3/16" (width x thickness) stiff.
A_r (in.^{2})	0.04625	0.06188
I_r (in.^{4})	0.00009838	0.0002664
C (in.)	0.08682	0.11951
$\frac{I_r}{C}$ (in.^{3})	0.001133	0.002229
r (in.)	5.640	5.640
t (in.)	0.025	0.025

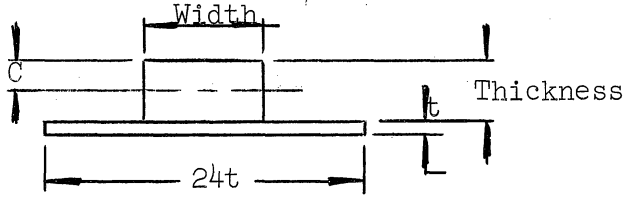

Cross-Section of the Stiffener

value of the computed stress to the experimental stress of 240 psi, one obtains the value of K to be equal to 3.69 inches as shown in Table 15.

Table 15

EXPERIMENTAL VALUES OF K DUE TO THE FLATTENING OF THE CYLINDER

(S = 10-1/2 in. M = 11522 in-lbs)

	$\frac{1}{4}$" x $\frac{1}{8}$" stiffener	$\frac{1}{4}$" x $\frac{3}{16}$" stiffener
M (in-lbs.)	11522	11522
$K\frac{Ert}{\rho^2}$ (lbs./in.)	0.00945K	0.00945K
M_r at $\varphi = 90°$ (in-lbs.)	+0.075K	+0.075K
N_r at $\varphi = 90°$ (lbs.)	-0.0533K	-0.0533K
Computed Stress (lbs./sq.in.)	+65.05K	+32.79K
Experimental Stress (lbs./sq.in.)	+240	+205
Experimental K (in.)	3.69	6.25

$$\frac{1}{\rho} = \frac{M}{EI} = \frac{M}{E\pi r^3 t}$$

M_r and N_r are given in Equations (8) and (9)

If the values of K as obtained in Table 15 are substituted in Equation (19), then the following two equations will result:

$$3.69 = \frac{1}{\frac{\lambda}{2}[\psi(\lambda s)] + 0.159C_1} \tag{34}$$

$$6.25 = \frac{1}{\frac{\lambda}{2}[\psi(\lambda s)] + 0.0586C_1} \tag{35}$$

Note that t^3/I_r of Equation (19) is equal to 0.159 for the 1/4" x 1/8" stiffener and is equal to 0.0586 for the 1/4" x 3/16" stiffener. Solving Equations (34) and (35) simultaneously, one obtains

$$C_1 = 1.1$$

The same procedure can be used to determine the value of C_1 when S = 5-1/4" or S = 2-5/8", in which case

$$C_1 = 0.74 \quad (S = 5\text{-}1/4")$$

$$C_1 = 1.65 \quad (S = 2\text{-}5/8")$$

It should be mentioned that the recorded experimental strains that were used to evaluate C_1 are small and that any small error in their measurement effects the value of C_1 appreciably. This can be illustrated by assuming that the recorded experimental stress at point 5 of the 1/4" x 1/8" stiffener is 270 instead of 240 (a difference of only 3 micro-inches in the measured strain). On this basis, the value of the experimental K of Table 15 will be equal to 4.15 instead of 3.69. If this change of 4.15 instead of 3.69 is made in Equation (34), then the simultaneous solution of Equations (34) and (35) will give a value for C_1 of 0.805 instead of 1.1. A value of unity for C_1 will be used on the basis that unity represents approximately the average of the C_1 values computed above and also that this value, as will be shown later, results in computed stresses that agree very well with all experimental data available (see Figure 25).

By similar algebraic calculations the value of λ which will best satisfy the experimental data is found to be equal to 0.195 $in.^{-1}$.

$$\therefore C_2 = \lambda r = 1.1$$

The constants C_1 and C_2 of Equation (19) which are associated with the flattening of the cylinder and which are related to the size and spacing of the stiffeners will be taken to be equal to 1.0 and 1.1 respectively. After C_1 and C_2 are selected the stresses in the stiffener due to the flattening of the cylinder can be computed using Equations (19), (8) and (9). Equation (19) can now be written in the following form:

$$K = \frac{1}{\frac{\lambda}{2}\left[\psi(\lambda s)\right] + 1.0\,\frac{t^3}{I_r}} \qquad (19a)$$

where $\lambda = \frac{1.1}{r}$.

Figure 25 gives the variation of both calculated and experimental stresses in the stiffener, due to flattening, at points 1 and 9 (top and bottom of the stiffener) as a function of the spacing of the stiffeners. Both the calculated stresses as obtained from Equations (19a), (8) and (9) in which the above values of C_1 and C_2 are used, and the experimental stresses are shown for the 1/4" x 1/8" (Figure 25a) and the 1/4" x 3/16" (Figure 25b) stiffeners. The good agreement between the calculated and experimental stresses justifies the selected values of C_1 and C_2.

(b) Bulging of the cylinder.

The analytical constants C_3 and C_4 of Equation (28) which were obtained in connection with the bulging of the cylinder and which are related to the size and spacing of the stiffeners, will be evaluated by the use of the experimental data.

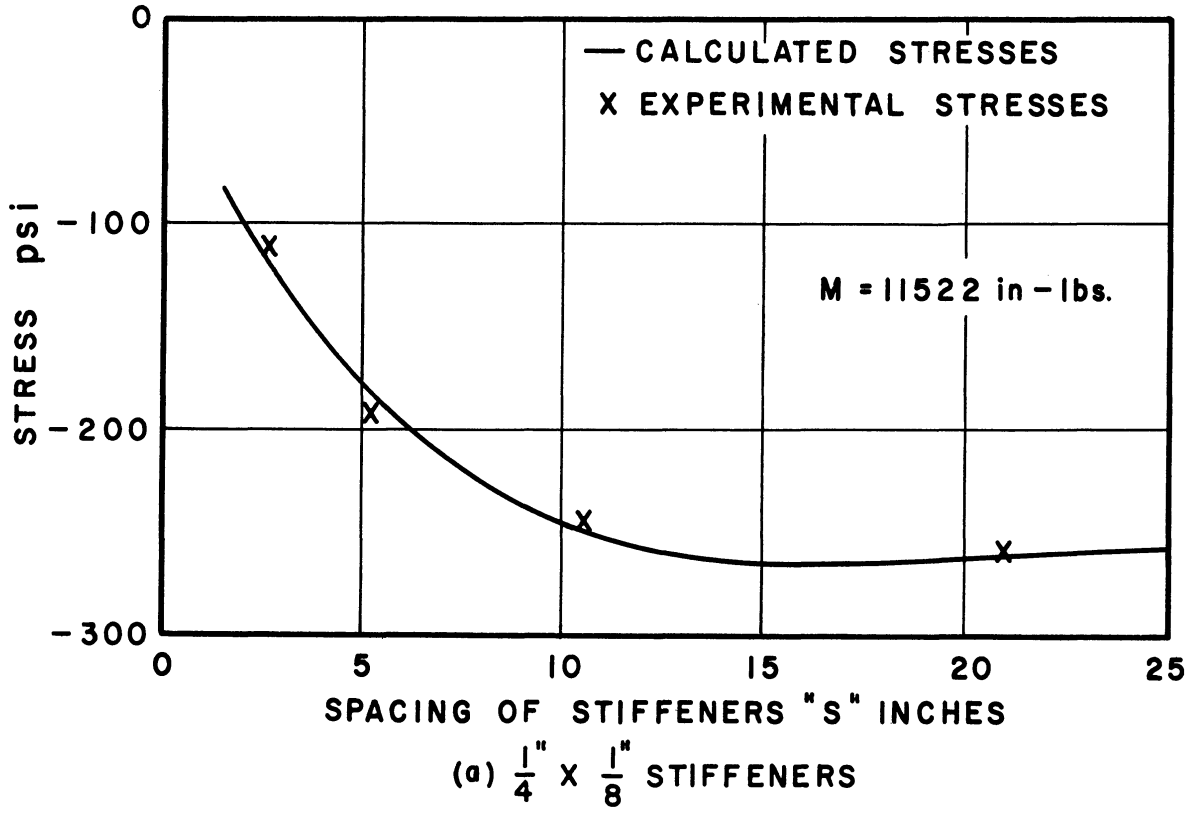

(a) $\frac{1}{4}$" X $\frac{1}{8}$" STIFFENERS

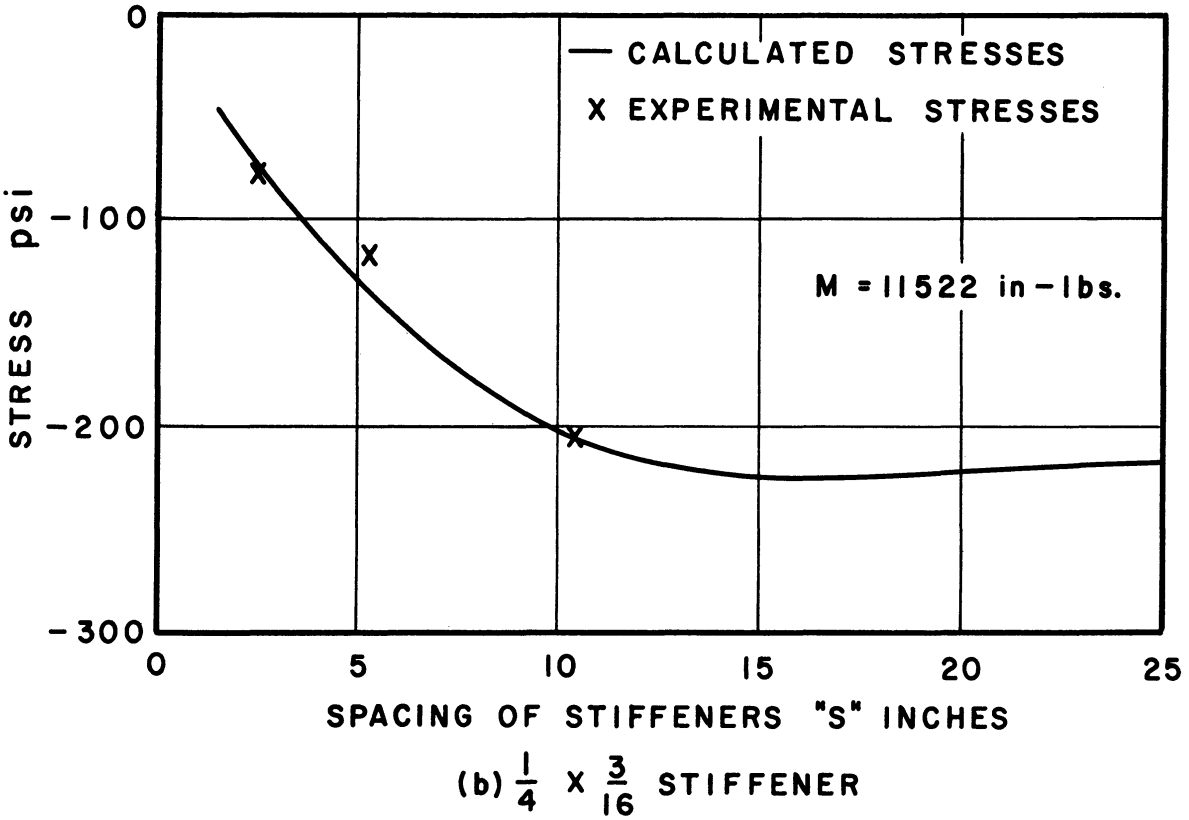

(b) $\frac{1}{4}$ X $\frac{3}{16}$ STIFFENER

Figure 25. Stresses on the Outside Face of the Stiffener at Top or Bottom Vs. The Spacing of the Stiffeners (Flattening).

For M = 11522 in-lbs., the expression $\frac{\mu M}{\pi r^2}$ of Equation (28) will be equal to 38.5 lbs./in. The value of $\frac{t}{A_r}$ of Equation (28) is equal to 0.541 in.$^{-1}$ for the 1/4" x 1/8" stiffeners and is equal to 0.404 in.$^{-1}$ for the 1/4" x 1/8" stiffeners. The average normal force N_r of points 1 and 9 as computed from the experimental stresses (Tables 12 and 13) for S = 10-1/2", will be equal to 27 lbs. for the 1/4" x 1/8" stiffeners and 33 lbs. for the 1/4" x 3/16" stiffeners.

If the above values are substituted in Equation (28), the following two equations will result

$$27 = \frac{38.5}{\frac{\beta_1}{2}\left[\psi(\beta_1 S)\right] + 0.541 C_3} \tag{36}$$

$$33 = \frac{38.5}{\frac{\beta_1}{2}\left[\psi(\beta_1 S)\right] + 0.404 C_3} \tag{37}$$

The value of C_3 as determined from Equations (36) and (37) is equal to 1.9.

The same procedure can be used to determine the value of C_3 when S = 5-1/4" and S = 2-5/8" in which case

$C_3 = 0.7$ (S = 5-1/4")

$C_3 = 0.5$ (S = 2-5/8")

As can be seen from Equations (36) and (37), the value of C_3 is very sensitive to any small variation in N_r. The variations in C_3 can therefore be attributed to experimental errors especially that the strains used in determining C_3 are small. A value of unity for C_3 has been found to represent the best value for correlating with the experimental data.

The value of the constant C_4 of Equation (28) can also be determined by similar algebraic procedures. The value of β_1 that agrees best with the experimental data is found to be equal to 1.8 in.$^{-1}$.

$$\therefore \quad C_4 = \beta_1 \sqrt{rt}$$

$$= 0.677 \quad \text{say} \quad 0.7$$

The values of C_3 and C_4 of Equation 28 will be taken to be equal to 1.0 and 0.7 respectively. After C_3 and C_4 are determined, the stresses in the stiffener due to bulging can be calculated by using Equation (28) which can now be written in the following form:

$$N_r = \frac{\frac{\mu M}{\pi r^2} \cos \varphi}{\frac{\beta_1}{2} [\psi(\beta_1 S)] + 1.0 \frac{t}{A_r}} \qquad (28a)$$

where $\beta_1 = \frac{0.7}{\sqrt{rt}}$

The variations of the stresses in the stiffener due to the bulging of the cylinder are given in Figure 26 as a function of the spacing of the stiffeners. Both the calculated stresses as obtained from Equation (28a) and the experimental stresses are plotted for the 1/4" x 1/8" and the 1/4" x 3/16" stiffeners at points 1 and 9 (top and bottom of the stiffener). The reasonably good agreement between the calculated and experimental stresses justifies the selected values of C_3 and C_4.

(c) Separate effect of the local loading.

The analytical constants C_5 and C_6 of Equation (33) which are assumed to be associated with the separate effect of the local loading on the cylinder can also be determined by the use of the experimental results. The value K' as obtained from the experimental data is evaluated in the tabular form of Table 16.

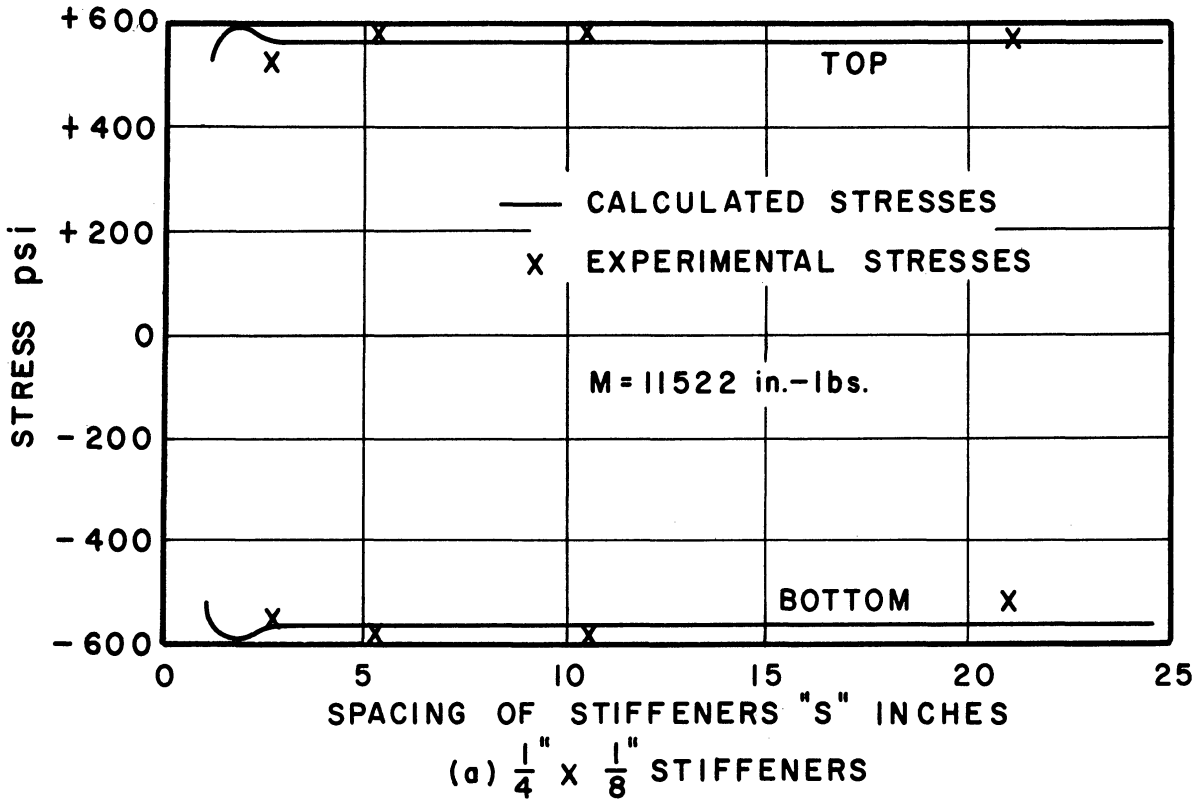

(a) $\frac{1}{4}$" X $\frac{1}{8}$" STIFFENERS

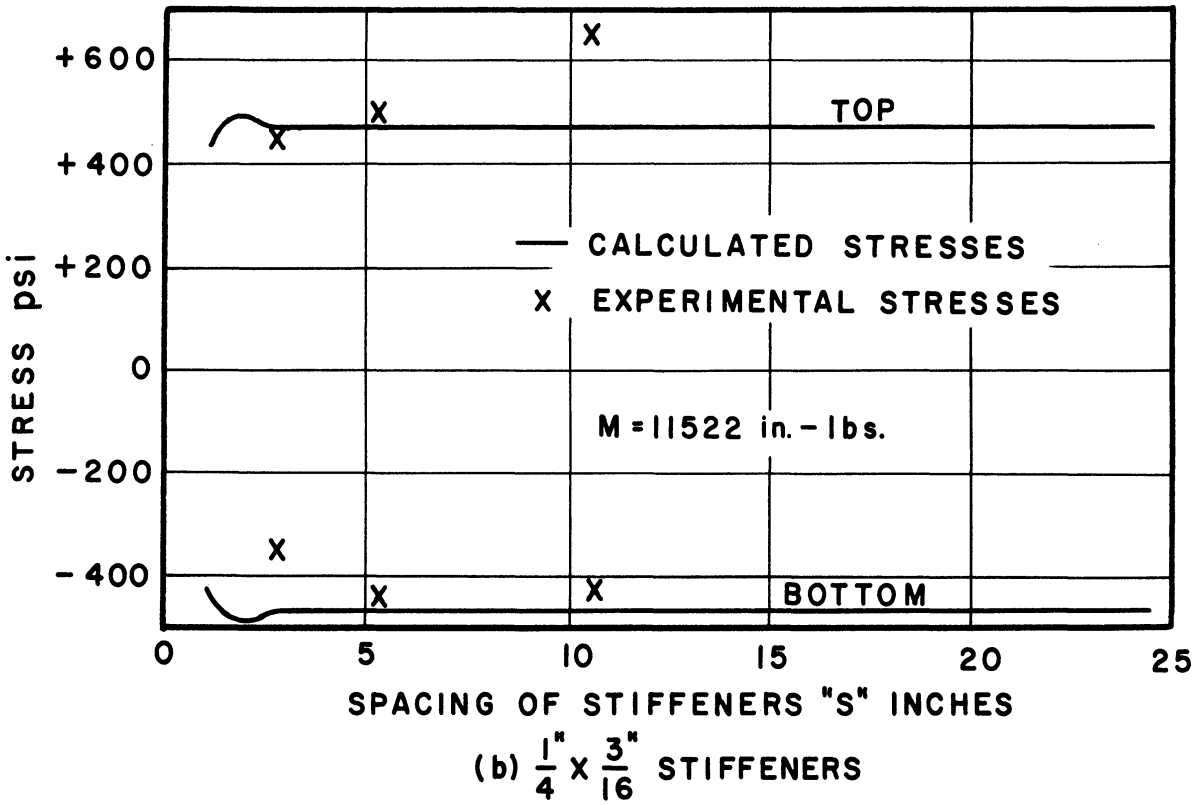

(b) $\frac{1}{4}$" X $\frac{3}{16}$" STIFFENERS

Figure 26. Stresses on the Outside Face of the Stiffener at the Top and Bottom Vs. The Spacing of the Stiffeners (Bulging).

Table 16

EXPERIMENTAL VALUES OF K' DUE TO THE SEPARATE EFFECT OF THE LOCAL RADIAL LOADING ON THE CYLINDER

(S = 10-1/2 in. W = 19-1/6 lbs.)

	$\frac{1}{4}$" x $\frac{1}{8}$" stiffeners	$\frac{1}{4}$" x $\frac{3}{16}$" stiffeners
w' (lbs./in.)	0.6K'	0.6K'
M_r at $\varphi = 0$ (in-lbs.)	+0.43K'	+0.43K'
N_r at $\varphi = 0$ (lbs.)	-3.92K'	-3.92K'
M_r at $\varphi = \pi$ (in-lbs.)	-0.43K'	-0.43K'
N_r at $\varphi = \pi$ (lbs.)	+0.54K'	+0.54K'
Computed Stress at $\varphi = 0$ (psi)	+295K'	+130K'
Computed Stress at $\varphi = \pi$ (psi)	-368K'	-184K'
Average Computed Stress (psi)	332K'	157K'
Average Experimental Stress (psi)	2618	1500
Experimental K' (in.)	7.9	9.5

M_r and N_r are given in Equations (29) and (30).

w' is the radial load on the stiffener (see Figure 19).

The substitution of the K' values as obtained in Table 16 in Equation (33) results in the following two equations:

$$7.9 = \frac{1}{\frac{\lambda'}{2}[\psi(\lambda' S)] + 0.159 C_5} \tag{38}$$

$$9.5 = \frac{1}{\frac{\lambda'}{2}[\psi(\lambda' S)] + 0.0586 C_5} \tag{39}$$

The value of C_5 as obtained by solving Equations (38) and (39) will be equal to 0.21.

Further algebraic calculations result in a value of $\lambda' = 0.08$ from which $C_6 = 0.45$.

The values of the constants C_5 and C_6 of Equation (33) which are assumed to be associated with the separate effect of the local loading of the types shown in Figures 19 and 20 will be taken to be equal to 0.21 and 0.45 respectively. After C_5 and C_6 are determined, the stresses in the stiffener due to the separate effect of the local loading can be calculated by using Equations (33), (29) and (30). Equation (33) can now be written in the following form:

$$K' = \frac{1}{\frac{\lambda'}{2}[\psi(\lambda'S)] + 0.21\frac{t^3}{I_r}} \qquad (33a)$$

where $\lambda' = \frac{0.45}{r}$

Figure 27 shows the variations of the stresses in the stiffener due to the separate effect of the radial local loading, as a function of the spacing of the stiffeners. Both the calculated stresses as obtained from Equations (33a), (29) and (30) in which the above values of C_5 and C_6 are used, and the experimental stresses are shown for the 1/4" x 1/8" stiffener at points 1 and 9 (top and bottom of the stiffener). It should be noted that the values of C_5 and C_6 were chosen so that the best agreement was obtained between experimental and calculated stresses at both the top and bottom of the stiffener. Any attempt to obtain better agreement on the top of the stiffener would have resulted in more discrepany between calculated and experimental stresses at the bottom of the

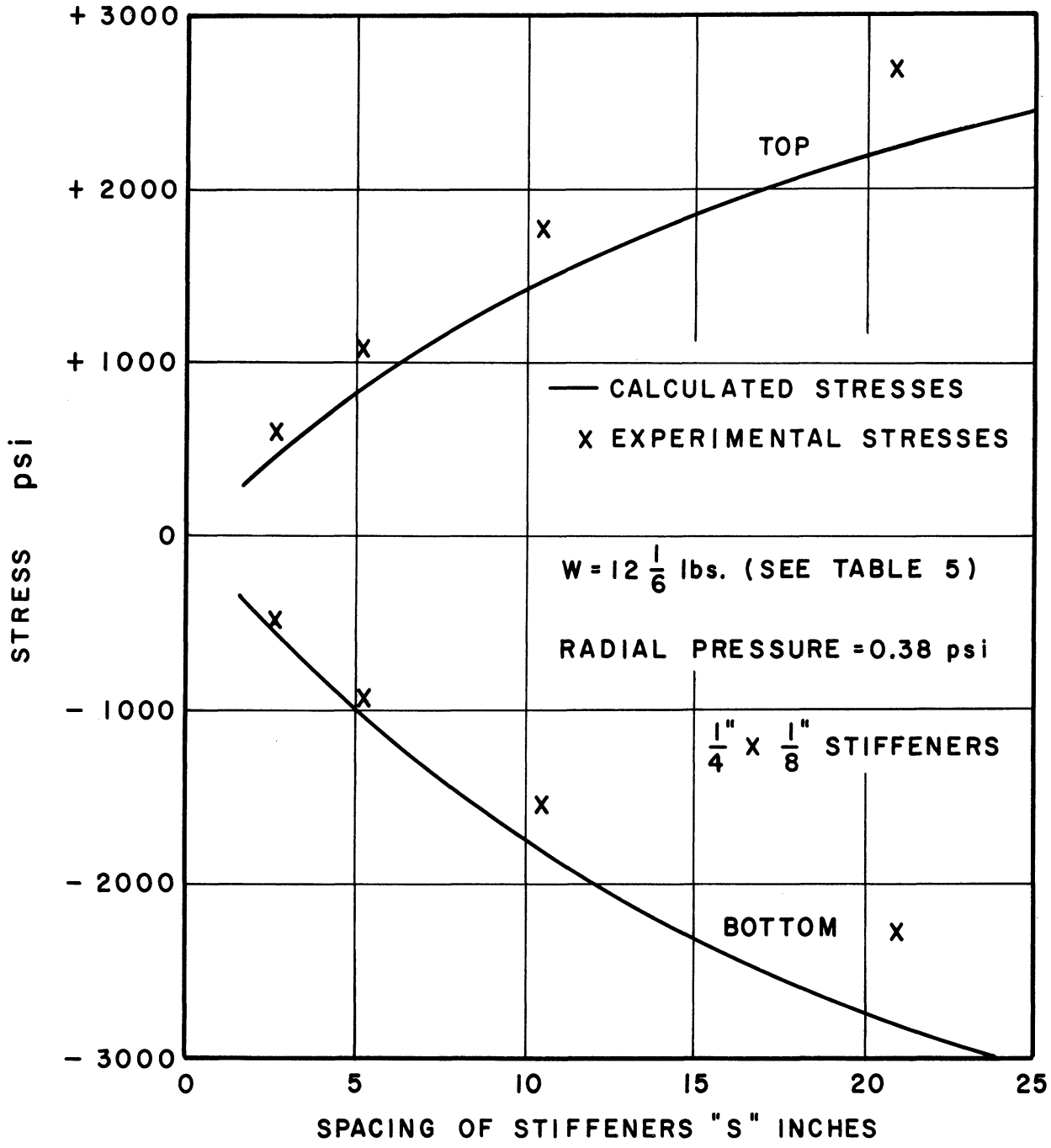

Figure 27. Stresses on the Outside Face of the Stiffener at Top and Bottom Vs. The Spacing of the Stiffeners (Separate effect of the local loading).

stiffener, and vice versa. It is believed that this discrepancy is the result of assuming that the baskets transmitting the local loading on the cylinder produce uniform radial pressure on the top half of the shell. This assumption can be in error due mainly to the frictional forces between the bands and the shell. It is interesting to observe the better agreement between calculated and experimental stresses on the bottom half of the stiffener (see Figure 30).

Variation of the stresses around the stiffener due to:

(a) Flattening of the cylinder.

In the separation of the experimental stresses of Tables 1 and 2 into the effects due to the flattening and the bulging of the cylinder, it was assumed that the distribution of the stresses around the stiffener, due to the flattening effect, is governed by Equations (8) and (9) which were obtained from the analytical investigation. Therefore, due to the flattening of the cylinder, no comparison can be made between calculated and experimental stresses on the stiffener insofar as the distribution of the stresses around the stiffener is concerned. Figure 28 is given only for the purpose of showing the distribution of the stresses around the stiffener, due to flattening, and not for comparison.

(b) Bulging of the cylinder.

Figure 29 gives the variation of the stresses around the stiffener due to the bulging of the cylinder. The stresses are plotted for both the 1/4" x 1/8" and the 1/4" x 3/16" stiffeners, when M = 11522 in-lbs. and S = 10-1/2 in. The discrepancy between the calculated and the experimental stresses can be attributed to the following:

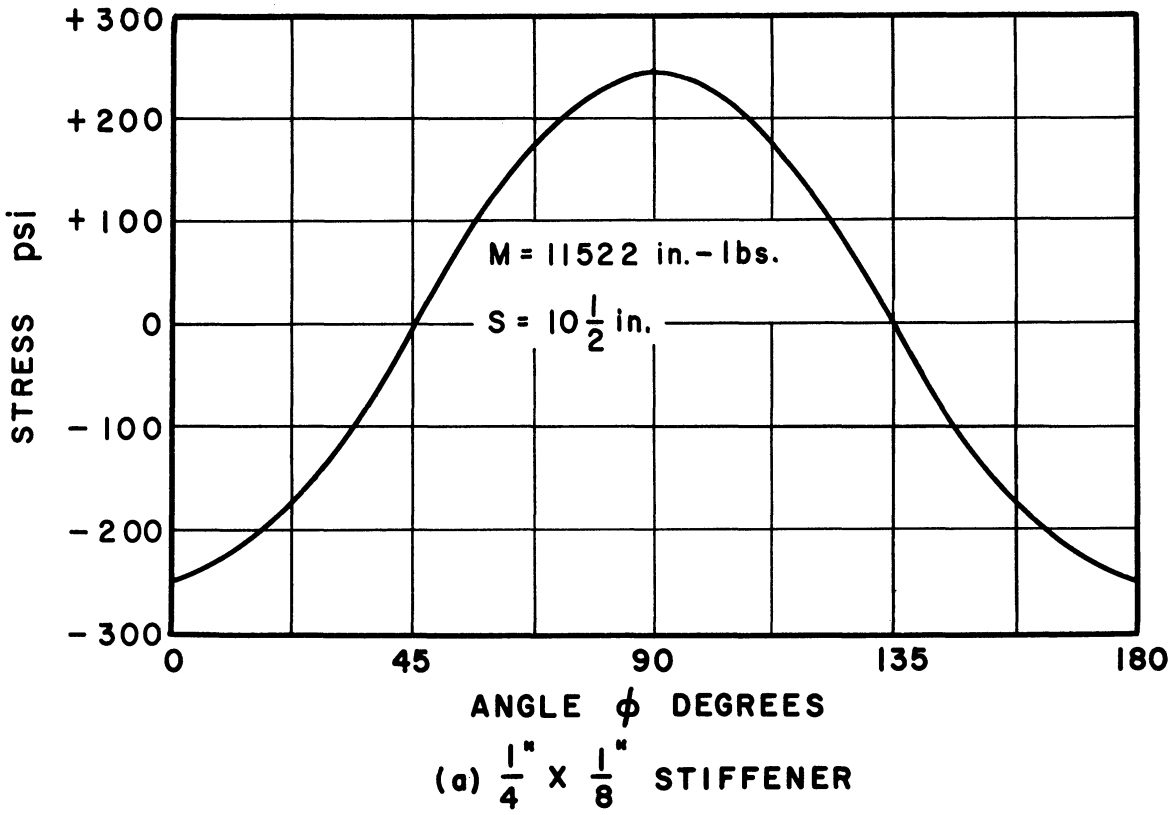

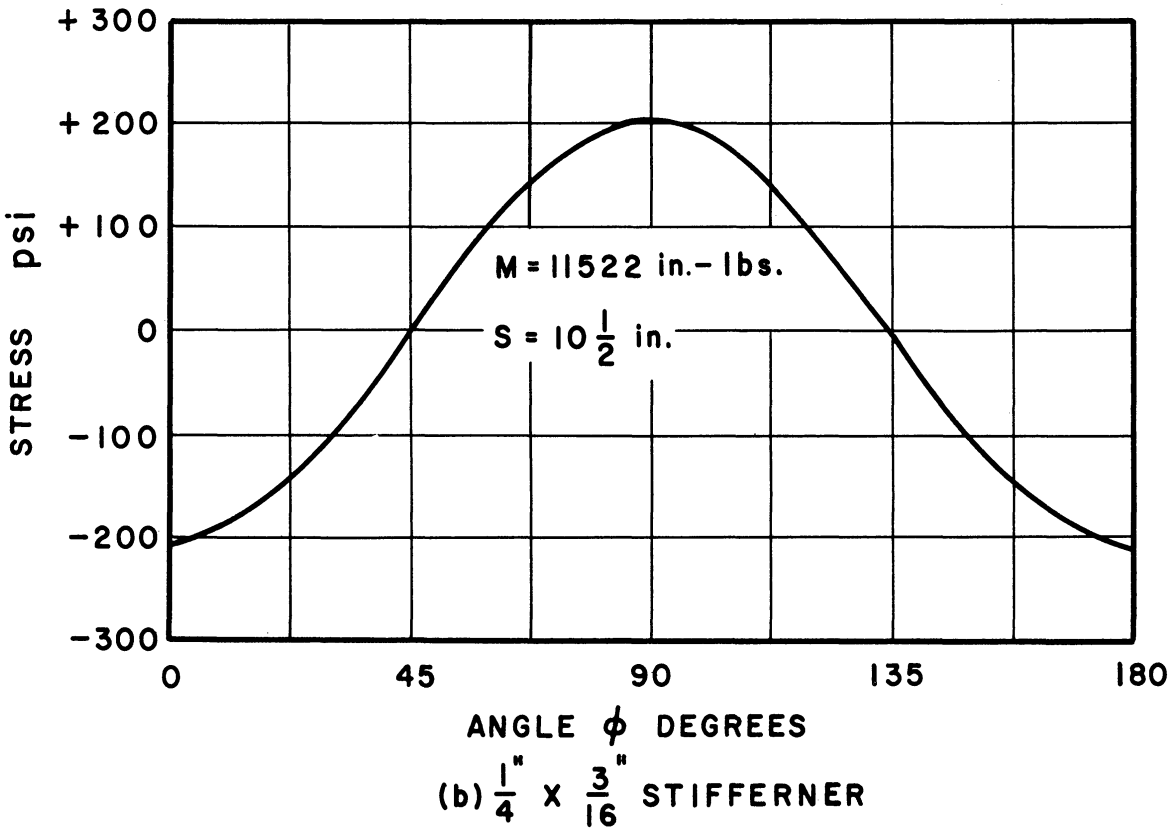

Figure 28. Variation of the Stresses Around the Stiffener (Flattening).

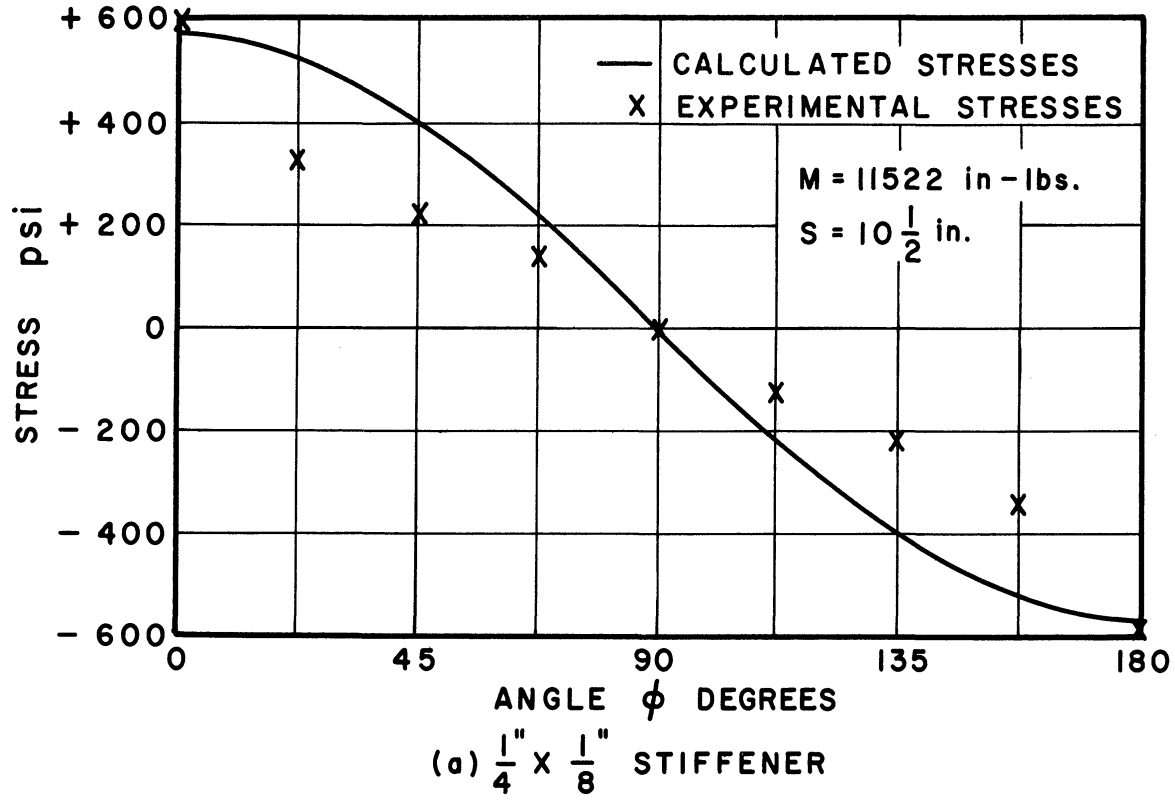

(a) $\frac{1}{4}$" X $\frac{1}{8}$" STIFFENER

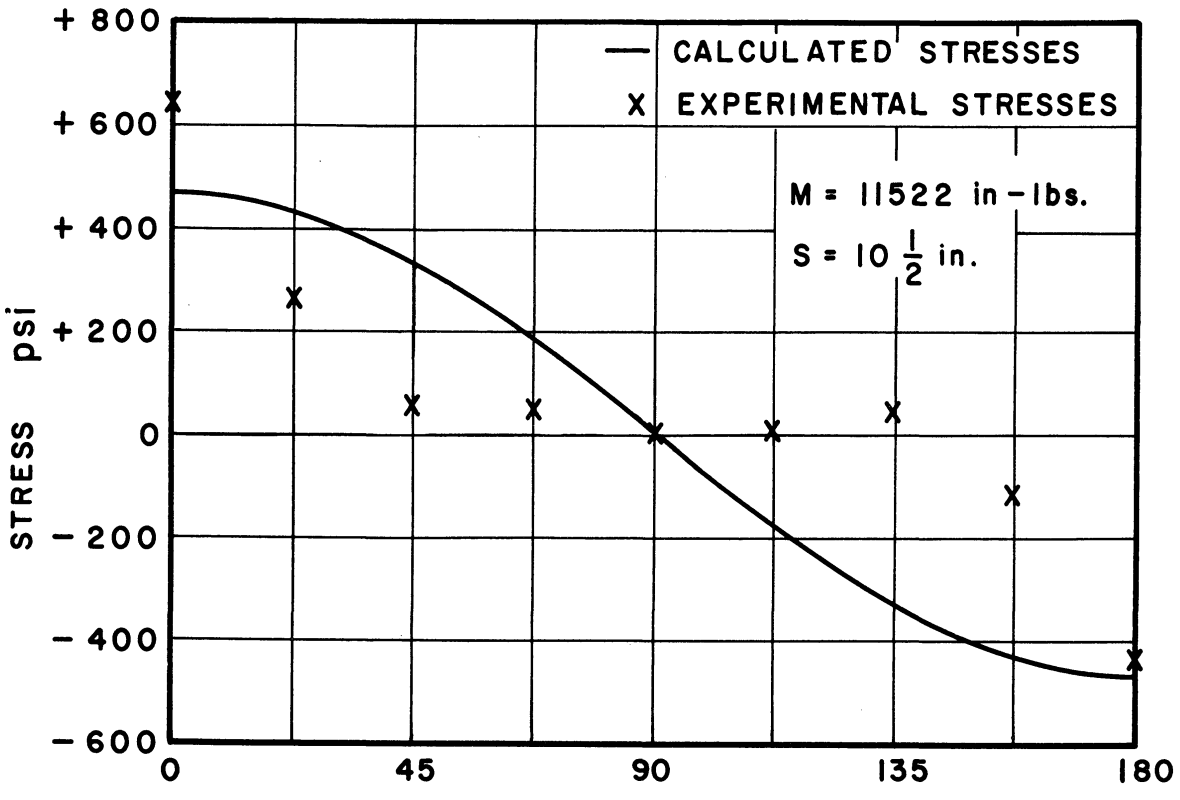

(b) $\frac{1}{4}$" X $\frac{3}{16}$" STIFFENER

Figure 29. Variation of the Stresses Around the Stiffener (Bulging).

(1) The distribution of the experimental stresses around the stiffener, due to the flattening effect, was assumed to be identical with the results of the analytical investigation. This means that all the experimental errors are carried over with the experimental stresses due to the bulging of the cylinder.

(2) The distribution of the forces on the stiffener due to the bulging effect is very sensitive to any variation in the assumed circular section of the cylinder. The stresses in the stiffener due to bulging are computed on the basis of a certain distribution of forces acting on a perfectly circular section thus producing no bending moments in the stiffener. Any slight variations in the circular shape of the stiffener or in the distribution of the forces can produce bending moments in the stiffener which will result in appreciable changes in the stress.

(c) Separate effect of the local loading.

The variation of the stresses around the stiffener as a result of the separate effect of the local radial loading is given in Figure 30. The stresses are plotted for the 1/4" x 1/8" and the 1/4" x 3/16" stiffeners when the radial pressure on the top half of the cylinder is equal to 0.38 lbs./sq.in., [i.e., W = 12-1/6 lbs. (see Tables 5 and 6)] and when S = 10-1/2 in.

It is important to mention that the agreement between the calculated and the experimental stresses, insofar as the distribution of the stresses around the stiffener is concerned, justifies the assumed distribution of the forces of Figure 19.

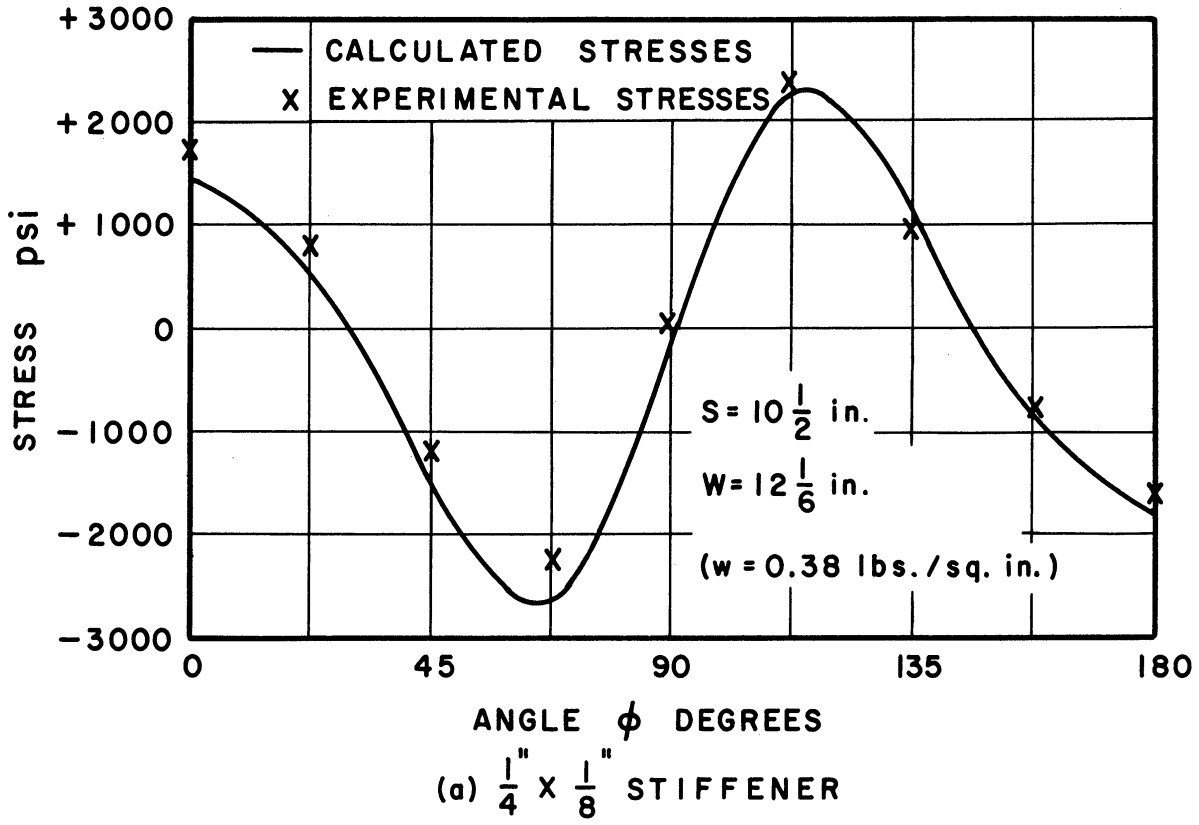

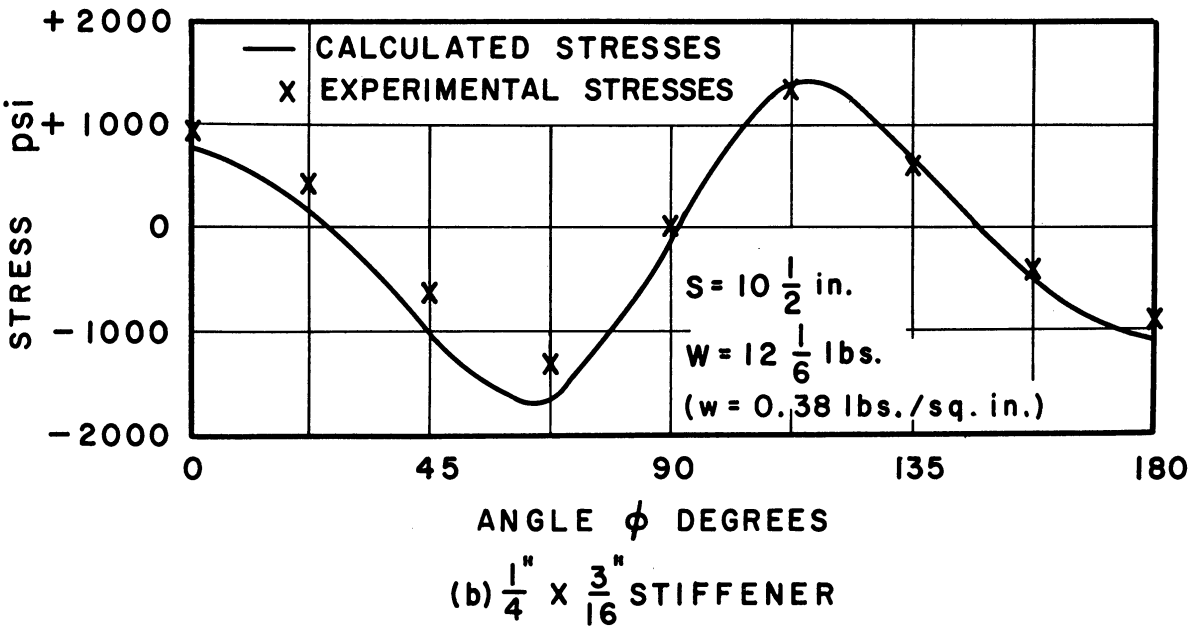

Figure 30. Variation of the Stresses Around the Stiffener (Separate Effect of the Local Loading).

CALCULATION OF THE STRESSES IN THE STIFFENERS OF STEEL STACKS

General Discussion

The formulas that have been developed in this thesis for the determination of the forces acting on the ring stiffeners were based on a cylinder of constant wall-thickness and radius. This is not true in the case of steel stacks where both the radius and the thickness of the shell vary. However, for any one segment of the shell of the stack where the thickness is uniform, the variation in the radius per foot of height is relatively small. For this reason one is justified, for design purposes, to consider any segment of the stack as uniform in both its wall-thickness and radius.

The steel stack will be considered to be subjected to the following forces:

(1) The longitudinal normal forces on the shell, which are caused by the weight of the stack including the insulation and the lining.

(2) The transverse local wind pressure on the shell.

(3) The applied bending moments on the shell which will be caused by the wind forces or any other dynamic action. The applied moments which will be used in the design of the ring stiffeners will be taken as those moments that, when combined with the normal forces, will produce the ultimate longitudinal stress in the shell. The ultimate stress in the shell will be controlled by either the yield of the material or the local buckling of the shell.

Practical Example - Loads and Dimensions of a Steel Stack

The stresses in four different size stiffeners will be computed for the 9/16 in. plate segment of the steel stack shown in Figure 31. The following loading and assumptions will be used:

(1) The static wind pressure on the shell in the region of the 9/16 in. plate is equal to 28 lbs./sq.ft. This is assumed to be caused by a wind velocity of 100 miles/hour.

(2) The longitudinal normal force on the shell is equal to 738 kips, which is the average value for the normal forces at the top and bottom of the 9/16 in. plate segment (see Figure 31).

(3) The spacing of the ring stiffeners, which from a practical point of view is controlled by the standard plate width of 8 feet, is therefore taken as 96 inches.

(4) An average cross-section is used for the segment in which case:

The mean radius of the shell	$r = 173$ in.
The thickness of the shell	$t = 0.5625$ in.
The radius/thickness ratio	$\frac{r}{t} = 307$
The cross-sectional area of the steel shell	$A_s = 612$ sq. in.
The moment of inertia	$I_s = 9.15 \times 10^6$ in.^{4}

(5) The bending moment will be selected so that the total longitudinal stress in the shell (flexural stress plus direct stress caused by the normal force) is equal to either the yield stress of the steel, which will be taken equal to 40 kips/sq.in., or the buckling stress of the shell. The buckling stress will be based on the capacity

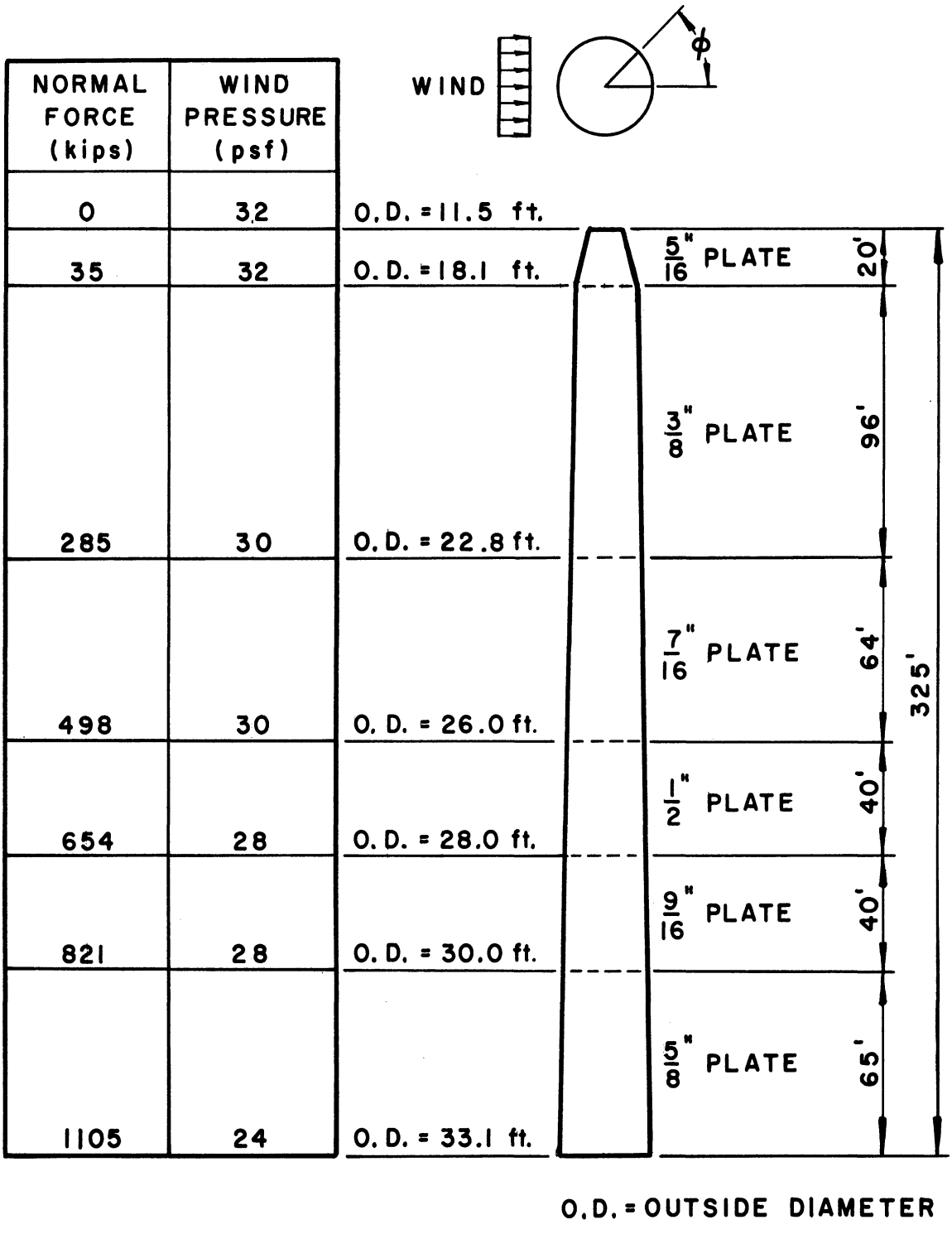

Figure 31. General Dimensions and Loads of Steel Stack.

of the shell in pure bending, due to the fact that the major part of the stress in the shell is caused by bending. The buckling stress is determined from the results of the experimental work of Peterson[11] which are given in the appendix in Figure 37. Using Figure 37, one obtains (for r/t = 307):

$$\sigma_{cr} = 0.0014 = 42 \text{ kips/sq. in.}$$

Therefore, the ultimate longitudinal stress in the shell will be taken as 40 kips/sq. in. which is the assumed yield point of the material.

The ultimate bending moment on the shell can therefore be calculated:

$$\text{Stress due to N} = \frac{N}{A_s} = \frac{738}{612} = 1.2 \text{ k/sq. in.}$$

$$\text{Therefore stress due to M} = 40 - 1.2 = 38.8 \text{ k/sq. in.}$$

$$\text{Therefore M} = \frac{(38.8)(9.15 \times 10^6)}{173} = 2.05 \times 10^6 \text{ in.-kips.}$$

The applied bending moment on the shell which will be used to determine the stresses in the stiffeners, due to both the flattening and the bulging of the shell, will be taken equal to 2.05×10^6 in.-kips.

(6) The cross-sections of the four different size stiffeners are given in Figure 32. An effective width of 24t is used. The shell face of the stiffener will be referred to as the outside face, while the wide flange face will be designated as the inside face of the stiffener.

Stresses in the Stiffener Due to the Longitudinal Normal Force N

The normal forces in the ring stiffeners of a long cylinder, subjected to a longitudinal normal force, can be established in the case of equally spaced stiffeners on a cylinder of uniform radius and thickness.

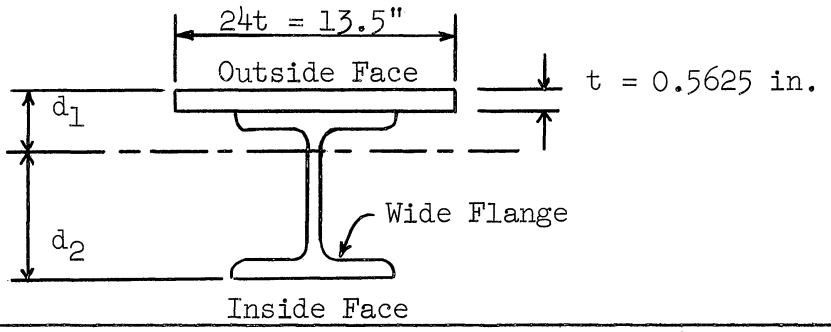

Stiffener	Wide Flange	d_1 (in.)	d_2 (in.)	A ($in.^2$)	I ($in.^4$)
I	4 WF 13	1.07	3.65	11.45	25.5
II	6 WF 20	1.76	5.00	13.50	79.7
III	6 WF 25	1.99	4.94	14.96	98.4
IV	8 WF 31	2.62	5.95	16.71	185.6

Figure 32. Cross-Sections of the Stiffeners of a Steel Stack.

The radial displacement in the cylinder at a stiffener location due to the action of the forces of the stiffeners on the cylinder, should be equal to the radial displacement in the cylinder due to the normal force, N, minus the radial displacement in the stiffener itself. The above strain condition can be expressed by the following equation:

$$\frac{N_r r\beta}{2Et}\,[\psi(\beta s)] = \frac{\mu N}{2\pi tE} - \frac{N_r r}{A_r E} \qquad (40)$$

The left hand side of Equation (40) represents the radial displacement in the cylinder at the stiffener locations due to the action of the stiffeners on the cylinder. This displacement is obtained from Equation (24) where N_r is substituted for Fr. Solving for N_r in Equation (40), one obtains:

$$N_r = \frac{\frac{\mu N}{2\pi r}}{\frac{\beta}{2}[\psi(\beta s)] + \frac{t}{A_r}} \qquad (41)$$

where: $\beta = \sqrt[4]{\frac{3(1-\mu^2)}{r^2 t^2}}$

N = longitudinal normal force on the cylinder,

N_r = the normal forces in the ring stiffeners.

For steel where $\mu = 0.3$, $\beta = \frac{1.285}{\sqrt{rt}}$.

The stresses in the stiffeners of the 9/16 in. plate segment of the steel stack, due to the longitudinal normal force of 738 kips are computed in Table 17, for the four different size stiffeners.

Table 17

STRESSES IN THE STIFFENERS OF A STEEL STACK DUE TO THE LONGITUDINAL NORMAL FORCE ON THE SHELL

Stiffener	$\frac{t}{A_r}$	β	$\psi(\beta s)$	$\frac{\mu N}{2\pi r}$	N_r (kips)	Stress K/sq.in.)
I	0.0493	0.1305	1.0000	0.204	+1.78	+0.156
II	0.0417	0.1305	1.0000	0.204	+1.91	+0.142
III	0.0376	0.1305	1.0000	0.204	+1.98	+0.132
IV	0.0337	0.1305	1.0000	0.204	+2.06	+0.123
$\psi(\beta s)$ is evaluated in Table 9						

Stresses in the Stiffener due to the Flattening of the Shell

The bending moments and the normal forces in the stiffeners due to the flattening of the shell will be computed by the use of Equations (19a)*, (8) and (9). The value of "$\frac{1}{\rho}$" is determined from Figure 33 where an assumed curve for the stiffened shell is used. It should be mentioned

* Page 61

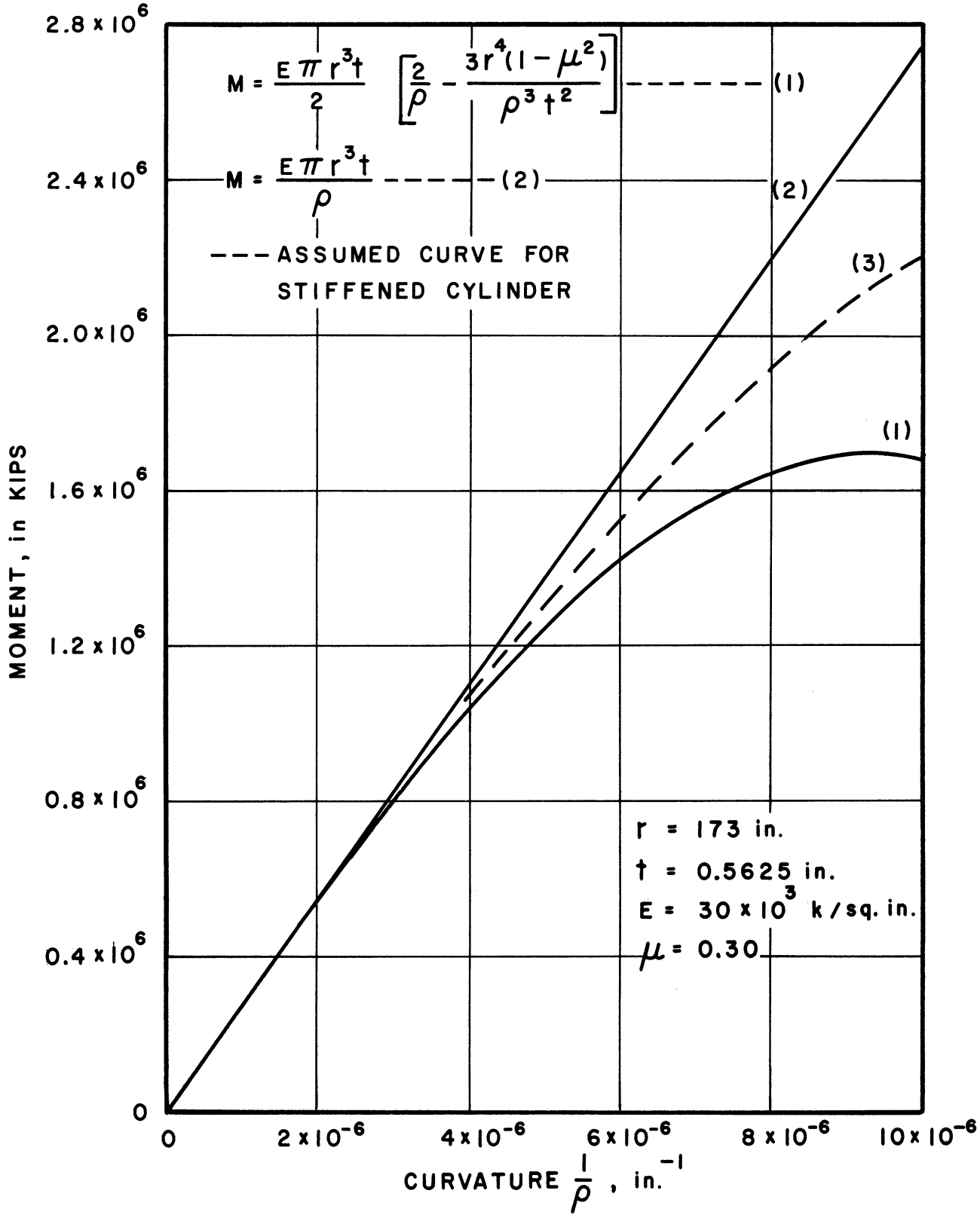

Figure 33. Moment Vs. Curvature-Steel Stack

that curves (1) and (2) in Figure 33 are drawn for the unstiffened shell and that curve (2) assumes no progressive flattening of the shell. The design curve (3) which is assumed to represent the true relationship between the curvature $\frac{1}{\rho}$ and the applied moment on the stiffened shell is taken to be the average between curves (1) and (2). For an applied moment on the shell of 2.05×10^{6} in-kips, the value of $\frac{1}{\rho}$ as determined from curve (3) of Figure 33 is equal to 8.8×10^{-6} in.$^{-1}$.

The bending moments and the normal forces as well as the stresses, due to flattening, are computed in Table 18 at three locations in the stiffeners. The angle φ is defined in Figure 31.

Stresses in the Stiffener Due to the Bulging or the Shell

The normal forces in the stiffeners due to the bulging of the shell will be evaluated by the use of Equation (28a)*. The stresses are evaluated in Table 19 at three locations in the stiffeners.

Stresses in the Stiffener Due to the Separate Effect of the Local Loading

The bending moments and the normal forces in the stiffeners due to the separate effect of the local loading will be evaluated by the use of Equations (33a)**, (31) and (32). It should be mentioned that the separate effect of the local loading on the shell (transverse wind pressure) is assumed to subject the stiffeners to the loading shown in Figure 20***. Equations (31) and (32) which give the values of the bending moments and normal forces for the loading of Figure 20 are evaluated for different values of φ in Table 23 in the appendix. Note that φ in Figure 20 has different orientation from φ of Figure 31.

---

* Page 64

** Page 67

*** The transverse distribution of Figure 20 represents a common but not the actual pressure distribution on a cylinder due to wind. Other pressure distributions can be treated similarly.

Table 18

STRESSES IN THE STIFFENERS OF A STEEL STACK DUE TO FLATTENING

Stiffener →	I	II	III	IV
t^3/I_r (in^{-1})	0.00697	0.00223	0.00181	0.00096
λ (in^{-1})	0.00636	0.00636	0.00636	0.00636
ψ (λS)	3.28	3.28	3.28	3.28
K (in.)	57.5	79.0	81.7	87.8
Ert/ρ^2 (K/sq.in.)	2.26×10^{-4}	2.26×10^{-4}	2.26×10^{-4}	2.26×10^{-4}
$K\ Ert/\rho^2$ (K/in.)	0.0130	0.0179	0.0184	0.0199
M_r at $\varphi = 0$ or $\varphi = \pi$ (in-K)	-97.2	-134.0	-137.6	-148.9
M_r at $\varphi = \pi/2$ (in-K)	+97.2	+134.0	+137.6	+148.9
N_r at $\varphi = 0$ or $\varphi = \pi$ (K)	0	0	0	0
N_r at $\varphi = \pi/2$ (K)	- 2.25	- 3.10	- 3.18	- 3.44
Stress at "a" or "c" (K/sq.in.)	- 4.08	- 2.96	- 2.78	- 2.10
Stress at "b" (K/sq.in.)	+ 3.88	+ 2.73	+ 2.57	+ 1.89
Stress at "d" or "f" (K/sq.in)	+13.90	+ 8.40	+ 6.91	+ 4.76
Stress at "e" (K/sq.in.)	-14.10	- 8.63	- 7.12	- 4.97

$\frac{1}{\rho} = 8.8 \times 10^{-6}\ in^{-1}$ $\quad E = 30 \times 10^3$ k/sq.in. $\quad S = 96$ in.

$$K = \frac{1}{\frac{\lambda}{2}[\psi(\lambda s)] + \frac{t^3}{I_r}} \quad \text{-- (19a)} \qquad \lambda = \frac{1.1}{r}$$

$\psi(\lambda s)$ is evaluated in Table 9

$$M_r = -\frac{pr^2}{4} \cos 2\varphi \quad \text{----(8)} \qquad \text{where } p = K\frac{Ert}{\rho^2}$$

$$N_r = -\,pr \sin^2\varphi \quad \text{-------(9)}$$

$+M_r$ designates tension on the outside face

$+N_r$ designates tension

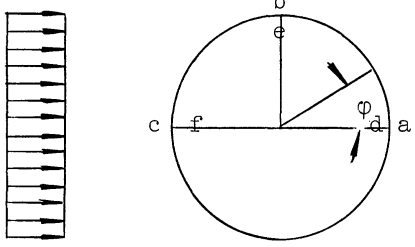

Table 19

STRESSES IN THE STIFFENERS OF A STEEL STACK DUE TO BULGING

Stiffener →	I	II	III	IV
t/A_r (in^{-1})	0.0493	0.0417	0.0376	0.0337
β_1 (in^{-1})	0.0710	0.0710	0.0710	0.0710
ψ ($\beta_1 S$)	1.003	1.003	1.003	1.003
$\mu M/\pi r^2$ (K/in.)	6.54	6.54	6.54	6.54
N_r at $\varphi = 0$ (K)	+77.0	+84.5	+89.3	+94.3
N_r at $\varphi = \pi/2$ (K)	0	0	0	0
N_r at $\varphi = \pi$ (K)	-77.0	-84.5	-89.3	-94.3
Stress at "a" or "d" (K/sq.in.)	+ 6.75	+ 6.26	+ 5.97	+ 5.65
Stress at "b" or "e" (K/sq.in.)	0	0	0	0
Stress at "c" or "f" (K/sq.in.)	- 6.75	- 6.26	- 5.97	- 5.65

$$N_r = \frac{\frac{\mu M}{\pi r^2}\cos\varphi}{\frac{\beta_1}{2}[\psi(\beta_1 S)] + \frac{t}{A_r}} \quad (28a)$$

where $\beta_1 = \frac{0.7}{\sqrt{rt}}$

+ N_r designates tension

$M = 2.05 \times 10^6$ in-K

$\mu = 0.3$

$\psi(\beta_1 S)$ is evaluated in Table 9.

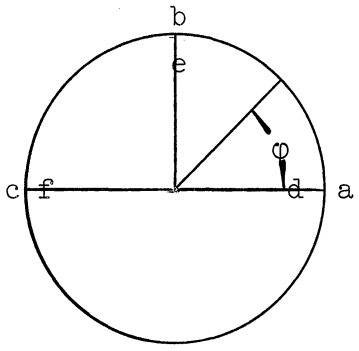

The stresses in the stiffeners due to the separate effect of the transverse local loading on the shell are evaluated and tabulated in Table 20 for three different locations on the stiffeners.

Summary of Stresses in the Stiffeners

The stresses in the stiffeners at the three locations ($\varphi = 0, \pi/2, \pi$) are summarized for the four different size stiffeners and are tabulated in Table 21.

Figure 34 shows the variation of the maximum tension and maximum compression stress on the inside face of the stiffener as a function of the section modulus (I/d_2).

Remarks on the Design of Ring Stiffeners in Steel Stacks

The formulas developed in this thesis for determining the forces acting on ring stiffeners in long thin-walled cylinders of constant wall-thickness and radius, can be applied satisfactorily to the stiffeners of a steel stack. This is illustrated in the previous example where the different size stiffeners analysed were of sizes that fall within the range of current engineering practice.

Although the stiffeners were analysed for the ultimate capacity of the shell, yet, in order to insure more rigidity for the stiffeners, it is recommended that their stresses be kept low (about 16 kips/sq.in.). However, the rigidity of the stiffener, which can be defined as the maximum radial displacement divided by the radius, is not only a function of the stress but it also varies with the depth of the stiffener.

If one ignores the displacements in the stiffener due to the normal forces then a relationship between the $\frac{\Delta}{r}$ ratio (maximum displacement divided by the radius) the maximum stress σ, and the $\frac{r}{d}$ ratio (radius

Table 20

STRESSES IN THE STIFFENERS OF A STEEL STACK DUE TO THE SEPARATE EFFECT OF THE LOCAL LOADING

Stiffener →	I	II	III	IV
$0.21\ t^3/I_r$ (in^{-1})	0.001465	0.000468	0.000380	0.000201
λ' (in^{-1})	0.00260	0.00260	0.00260	0.00260
$\psi(\lambda'S)$	8.00	8.00	8.00	8.00
K' (in)	84.3	92.0	92.7	94.3
Q (K/sq.in.)	0.000194	0.000194	0.000194	0.000194
Q'(K/in.)	0.01635	0.01785	0.01796	0.01830
M_r at $\varphi = 0$ (in-K)	-53.70	-58.63	-58.99	-60.10
M_r at $\varphi = \pi/2$ (in-K)	+61.17	+66.78	+67.19	+68.46
M_r at $\varphi = \pi$ (in-K)	-68.63	-74.93	-75.39	-76.82
N_r at $\varphi = 0$ (K)	+ 1.05	+ 1.15	+ 1.15	+ 1.18
N_r at $\varphi = \pi/2$ (K)	- 1.41	- 1.54	- 1.55	- 1.58
N_r at $\varphi = \pi$ (K)	- 1.05	- 1.15	- 1.15	- 1.18
Stress at "a" (K/sq.in.)	- 2.16	- 1.21	- 1.11	- 0.78
Stress at "b" (K/sq.in.)	+ 2.45	+ 1.36	+ 1.26	+ 0.87
Stress at "c" (K/sq.in.)	- 2.97	- 1.74	- 1.44	- 1.16
Stress at "d" (K/sq.in.)	+ 7.77	+ 3.77	+ 3.14	+ 2.00
Stress at "e" (K/sq.in.)	- 8.87	- 4.30	- 3.47	- 2.28
Stress at "f" (K/sq.in.)	+ 9.73	+ 4.62	+ 3.84	+ 2.39

$$K' = \frac{1}{\frac{\lambda'}{2}\,[\psi(\lambda'S)] + 0.21\,\frac{t^3}{I_r}} \qquad \text{---(33a)}$$

$\lambda' = \frac{0.45}{r}$ S = 96 in.

$\psi(\lambda'S)$ is evaluated in Table 9

$+M_r$ designates tension on the outside face

$+N_r$ designates tension

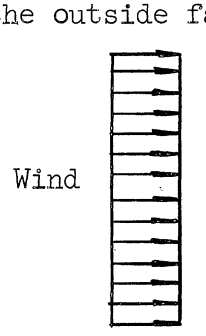

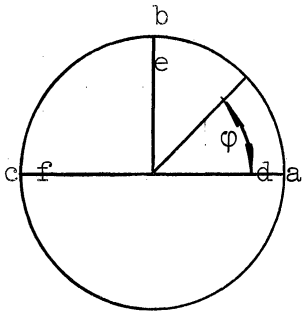

Table 21

SUMMARY OF THE STRESSES IN THE STIFFENERS OF A STEEL STACK

Stiffener	Stress at:	Stress Due to: (K/sq.in.)				Total Stress K/sq.in.
		N	Flattening	Bulging	Local* Loading	
I	a	+0.16	- 4.08	+6.75	-2.16	+ 0.67
	b	+0.16	+ 3.88	0	+2.45	+ 6.49
4	c	+0.16	- 4.08	-6.75	-2.97	-13.64
WF	d	+0.16	+13.90	+6.75	+7.77	+28.58
13	e	+0.16	-14.10	0	-8.87	-22.81
	f	+0.16	+13.90	-6.75	+9.73	+17.04
II	a	+0.14	- 2.96	+6.26	-1.21	+ 2.23
	b	+0.14	+ 2.73	0	+1.36	+ 4.23
6	c	+0.14	- 2.96	-6.26	-1.74	-10.82
WF	d	+0.14	+ 8.40	+6.26	+3.77	+18.57
20	e	+0.14	- 8.63	0	-4.30	-12.79
	f	+0.14	+ 8.40	-6.26	+4.62	+ 6.90
III	a	+0.13	- 2.78	+5.97	-1.11	+ 2.21
	b	+0.13	+ 2.57	0	+1.26	+ 3.96
6	c	+0.13	- 2.78	-5.97	-1.44	-10.06
WF	d	+0.13	+ 6.91	+5.97	+3.14	+16.15
25	e	+0.13	- 7.12	0	-3.47	-10.46
	f	+0.13	+ 6.91	-5.97	+3.84	+ 4.91
IV	a	+0.12	- 2.10	+5.65	-0.78	+ 2.89
	b	+0.12	+ 1.89	0	+0.87	+ 2.88
8	c	+0.12	- 2.10	-5.65	-1.16	- 8.79
WF	d	+0.12	+ 4.76	+5.65	+2.00	+12.53
31	e	+0.12	- 4.97	0	-2.28	- 7.13
	f	+0.12	+ 4.76	-5.65	+2.39	+ 1.62

* Separate effect of the local loading

\+ Stress means tension

\- Stress means compression

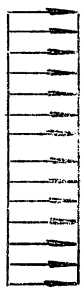

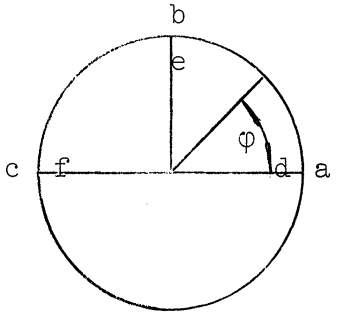

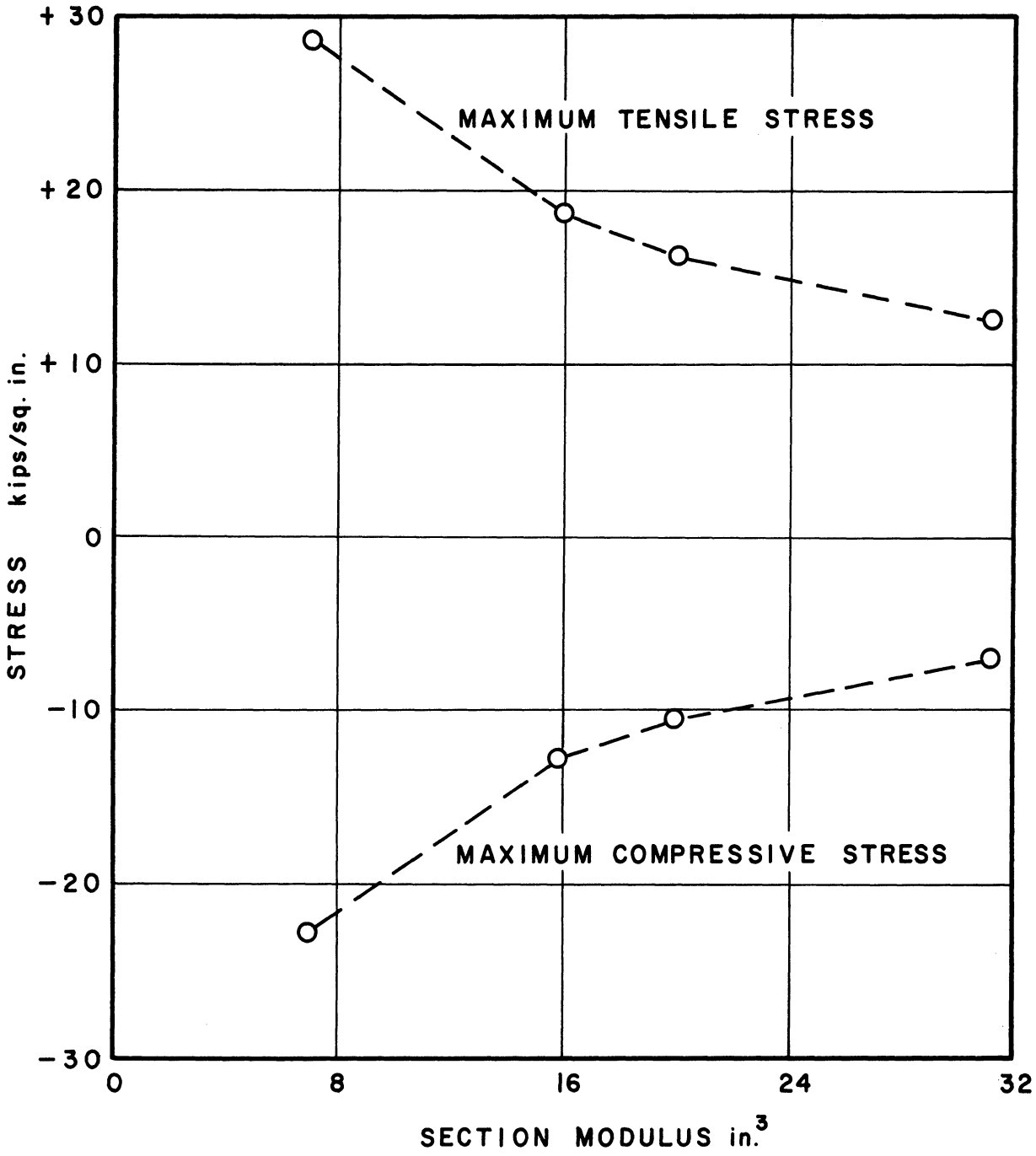

Figure 34. Stress on the Inside Face of the Stiffener Vs. Section Modulus.

to depth of stiffener) can be established. Assuming that the bending moment stresses in the stiffener are limited to 12 k/sq.in., one can find an approximate solution if this stress is assumed to be entirely contributed by the flattening of the cylinder.

Due to the flattening of a ring subjected to the forces shown in Figure 35, both the maximum stress and the maximum radial displacement can be expressed in terms of p, where:

$$M_{max.} = \frac{pr^2}{4}$$

$$\sigma_{max.} = \frac{pr^2}{4} \frac{d2}{I} \quad \ldots\ldots \text{(a)}$$

$$\Delta_{max.} = \frac{pr^2}{12EI} \quad \ldots\ldots \text{(b)}$$

Eliminating p from both Equations (a) and (b), one obtains:

$$\frac{\Delta}{r} = \frac{1}{3E} \left(\frac{r}{d_2}\right) \sigma \qquad (42)$$

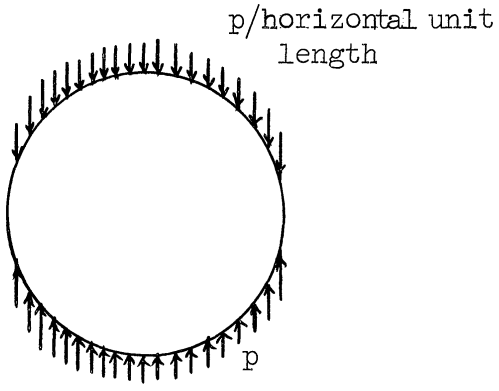

Figure 35. Ring Subjected to Flattening Forces.

It is important to note that the constant "3" in Equation (42) varies with the type of loading on the ring producing the bending moments. This variation, however, is very small especially if the loading on the ring is of a uniformly distributed nature.

Using 12 k/sq. in. for σ and limiting $\frac{\Delta}{r}$ to $\frac{1}{200}$ one obtains $\frac{r}{d_2} = 37.5$ (for steel where $E = 30 \times 10^3$ k/sq.in.). If d_2 as shown in Figure 32 is taken to be approximately equal to 0.8d (where d = depth of the wide flange section), then $\frac{r}{d} = 30$.

It is therefore recommended that the radius/depth ratio of the wide flange used as a ring stiffener in steel stacks does not exceed 30, and that the maximum stress in the stiffeners does not exceed 16 k/sq.in.

SUMMARY AND CONCLUSIONS

The forces acting on ring stiffeners in long thin-walled cylinders subjected to bending, have been studied for cylinders with uniform radius and wall thickness. Both an analytical and an experimental study were used to establish approximate formulas governing the magnitude and distribution of the forces acting on the stiffeners. The forces on the stiffeners were classified under three types of action:

(1) Flattening of the cylinder

(2) Bulging of the cylinder

(3) Separate effect of the local loading.

In one part of the experimental study the cylinder was subjected to pure bending resulting in both the flattening and the bulging actions, and in a second part of the investigation the cylinder was loaded by transverse local loading which resulted in all three types of action listed above.

The analytical investigation was essentially used to establish the major parameters upon which the magnitude of the forces in the stiffeners due to the three types of action depend. In the case of the flattening and the separate effect of the local loading, these major parameters were established by comparison with the analogous problem of beams on elastic foundations. In the case of the bulging the parameters were obtained by making use of the analogous problem of an infintely long cylinder subjected to uniformly distributed radial loads acting around equally spaced circular sections. The constants that were obtained during the analytical investigation were then evaluated by the use of the experimemtal results,

thus obtaining the approximate equations governing the magnitude and distribution of the forces acting on the stiffeners due to the three types of action. These equations will apply to any material whose Poisson's ratio is about 1/3 which is the Poisson's ratio of aluminum.

The separate effect of the local loading was studied by eliminating the effects of the flattening and the bulging actions which are known from the pure bending moment tests on the cylinder. The effects of the shearing forces were ignored for two reasons: (1) The shearing forces in the vicinity of the center stiffener are very small (see Figure 1b), (2) preliminary tests on the cylinder have shown that the shearing forces on the cylinder had no appreciable effect on the stresses in the stiffener and that the bending moments were the primary contributing factor to the stresses. It should be mentioned, however, that further tests should be undertaken to determine quantitatively the effects of the shearing forces on ring stiffeners.

It should be emphasized that the equations developed for determining the forces acting on the ring stiffeners due to the three types of action, are approximate insofar as they only involve what is believed to be the major parameters of the problem. Further tests are desirable to establish more accurately the parameters of the problem as well as the constants involved in the equations.

Although the forces on the stiffeners due to any of the three types of action increase with the increase of the size of the stiffeners, yet the stresses in the stiffeners will decrease as has been illustrated by the example of the steel stack. The results have also shown that the

forces on the stiffeners will increase with the increase of the spacing of the stiffeners until $\frac{s}{r} = \frac{3.5}{\sqrt{\frac{r}{t}}}$ in case of the bulging action, $\frac{s}{r} = 2.2$ in case of the flattening action and $\frac{s}{r} = 5.5$ in case of the separate effect of the local loading. Any further increase in the spacing will actually decrease the forces on the stiffeners slightly until the above three constants reach the values of about 7, 4.5 and 11 respectively, after which the forces on the stiffeners will not change with any increase in the spacing.

Although this investigation was concerned with the stresses and not with the rigidity of the stiffeners, yet, it is believed that rigidity can be controlled by limiting both the stresses as well as the radius/depth ratio of the stiffener. Expressing rigidity as the maximum radial displacement divided by the radius of the stiffener and ignoring the displacements due to the normal forces in the stiffeners, one can write rigidity, $\frac{\Delta}{r}$, in the following form:

$$\frac{\Delta}{r} = \frac{1}{CE} \left(\frac{r}{d_2}\right) \sigma \qquad (43)$$

where C = constant which depends upon the type of loading on the stiffener

Δ = maximum radial displacement

d_2 = distance of fiber of maximum bending stress on the stiffener

σ = maximum bending stress in the stiffener.

It should be mentioned that the constant C is equal to 3 in case of the flattening effect and that for any other type of loading the variation from 3 is very small.

By the use of the above equation the engineer is able to control rigidity by limiting both the stress, σ, on the stiffener and the r/d_2 ratio.

The use of the formulas developed in this thesis have been illustrated by computing the stresses in the ring stiffeners in a steel stack. These stresses were computed on the basis of developing the full capacity of the shell, a condition which is recommended by the writer in the design of ring stiffeners.

APPENDIX A

BENDING MOMENTS AND NORMAL FORCES IN THE STIFFENER DUE TO THE SEPARATE EFFECT OF THE LOCAL LOADING

The bending moments and normal forces in the stiffener due to the separate effect of the two types of local loading considered in this thesis will be computed at different sections around the stiffener. The loading diagrams which have already been given in Figures 19 and 20 as well as the equations expressing the values of the moments and normal forces (Equations 29, 30, 31 and 32) will be repeated here for easy reference. The two types of loading are:

(a) Rings Subjected to Uniform Radial Pressure on the Top Half (Figure 19).

Radial Loading =

w'/circumferential unit

Tangential Loading =

$\frac{2}{\pi}$ w' sin φ/circumferential unit

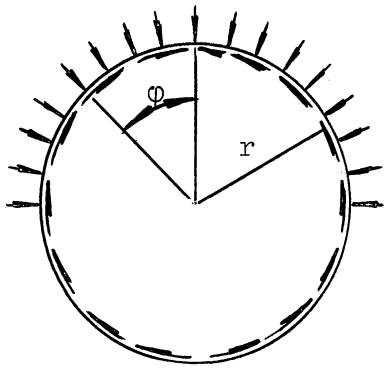

Fig. 19

The bending moments and normal forces in the ring of Figure 19 are given by the following equations:

$$\left.\begin{aligned} M_r &= \left(\frac{1}{2} - \frac{3}{2\pi}\cos\varphi - \frac{1}{\pi}\varphi\sin\varphi\right) w'r^2 \\ &\left[\text{For } 0 \leq \varphi \leq \frac{\pi}{2}\right] \\ M_r &= \left(\sin\varphi - \frac{1}{2} - \frac{3}{2\pi}\cos\varphi - \frac{1}{\pi}\varphi\sin\varphi\right) w'r^2 \\ &\left[\text{For } \frac{\pi}{2} \leq \varphi \leq \pi\right] \end{aligned}\right\} \quad (29)$$

$$N_r = \left(-\frac{1}{2\pi}\cos\varphi - 1 + \frac{1}{\pi}\varphi\sin\varphi\right) w'r \qquad \left[\text{For } 0 \leq \varphi \leq \frac{\pi}{2}\right]$$

$$N_r = \left(-\frac{1}{2\pi}\cos\varphi - \sin\varphi + \frac{1}{\pi}\varphi\sin\varphi\right) w'r \qquad \left[\text{For } \frac{\pi}{2} \leq \varphi \leq \pi\right] \qquad (30)$$

Table 22 gives the values of M_r and N_r of Equations (29) and (30) for different values of φ.

Table 22

VALUES OF M_r AND N_r OF EQUATIONS (29) AND (30)

φ (Degrees)	M_r	N_r
0	+ 0.02254 $w'r^2$	- 1.15915 $w'r$
22.5	+ 0.01104 $w'r^2$	- 1.09920 $w'r$
45	- 0.01440 $w'r^2$	- 0.93576 $w'r$
67.5	- 0.02917 $w'r^2$	- 0.71446 $w'r$
90	0	- 0.50000 $w'r$
112.5	+ 0.02917 $w'r^2$	- 0.28554 $w'r$
135	+ 0.01440 $w'r^2$	- 0.06424 $w'r$
157.5	- 0.01104 $w'r^2$	+ 0.09921 $w'r$
180	- 0.02254 $w'r^2$	+ 0.15915 $w'r$
+ M_r designates tension on the outside + N_r designates tension		

(b) Rings Subjected to Uniform Vertical Pressure on the Top Half (Figure 20).

Vertical Loading =

Q'/horizontal unit

Tangential Loading =

$\frac{2}{\pi}$ Q' sin φ/circumferential unit

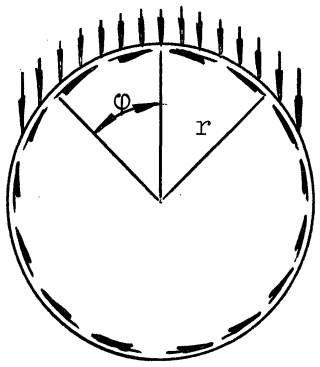

Fig. 20

The bending moments and normal forces in the ring of Figure 20 are given by the following equations:

$$M_r = \left(\frac{1}{8} - \frac{5}{6\pi}\cos\varphi + \frac{1}{2}\sin^2\varphi - \frac{1}{\pi}\varphi\sin\varphi\right) Q'r^2 \quad \left[\text{For } 0 \leq \varphi \leq \frac{\pi}{2}\right]$$

$$M_r = \left(-\frac{3}{8} - \frac{5}{6\pi}\cos\varphi + \sin\varphi - \frac{1}{\pi}\varphi\sin\varphi\right) Q'r^2 \quad \left[\text{For } \frac{\pi}{2} \leq \varphi \leq \pi\right] \qquad (31)$$

$$N_r = \left(\frac{7}{6\pi}\cos\varphi - \sin^2\varphi + \frac{1}{\pi}\varphi\sin\varphi\right) Q'r \quad \left[\text{For } 0 \leq \varphi \leq \frac{\pi}{2}\right]$$

$$N_r = \left(-\frac{7}{6\pi}\cos\varphi - \sin\varphi + \frac{1}{\pi}\varphi\sin\varphi\right) Q'r \quad \left[\text{For } \frac{\pi}{2} \leq \varphi \leq \pi\right] \qquad (32)$$

Table 23 gives the values of M_r and N_r of Equations (30) and (31) for different values of φ .

Table 23

VALUES OF M_r AND N_r OF EQUATIONS (31) AND (32)

φ (Degrees)	M_r	N_r
0	$- 0.14026\ Q'r^2$	$- 0.37136\ Q'r$
22.5	$- 0.09469\ Q'r^2$	$- 0.44169\ Q'r$
45	$+ 0.01065\ Q'r^2$	$- 0.58581\ Q'r$
67.5	$+ 0.10382\ Q'r^2$	$- 0.64921\ Q'r$
90	$+ 0.12500\ Q'r^2$	$- 0.50000\ Q'r$
112.5	$+ 0.07296\ Q'r^2$	$- 0.20434\ Q'r$
135	$- 0.01065\ Q'r^2$	$+ 0.08581\ Q'r$
157.5	$- 0.08210\ Q'r^2$	$+ 0.29526\ Q'r$
180	$- 0.10974\ Q'r^2$	$+ 0.37136\ Q'r$

$+ M_r$ designates tension on the outside

$+ N_r$ designates tension

APPENDIX B

ULTIMATE STRENGTH OF UNSTIFFENED CYLINDERS SUBJECTED TO PURE BENDING

The results of the pure bending moment tests of Lundquist[8] which were made on unstiffened thin-walled duralumin cylinders are given in Figure 36. Lundquist's tests were made on 58 cylinders of 7.5 and 15 inches in radius and with nominal thicknesses of 0.011, 0.016 and 0.022 inches. The length/radius ratio of the cylinders tested ranged from 0.25 to 5.0.

Also included in Figure 36 are the results of tests made by Mossman and Robinson[9] and by Imperial and Bergstrom (reported by Younger[15]). All of these test results are taken directly from Figure 5 of Reference 8.

Added to Figure 36 is the graph of $\frac{\sigma_{cr}}{E}$ as obtained from Equation (3) which was derived by Brazier[2] where $\frac{\sigma_{cr}}{E}$ is taken to be equal to $\frac{M_{cr} \cdot r}{E\pi r^3 t} = \frac{M_{cr}}{E\pi r^2 t}$. Substituting the value of M_{cr} from Equation (3) one obtains:

$$\frac{\sigma_{cr}}{E} = \frac{2\sqrt{2}}{9\sqrt{1 - \mu^2}} \left(\frac{l}{r}\right) \frac{r}{t}$$

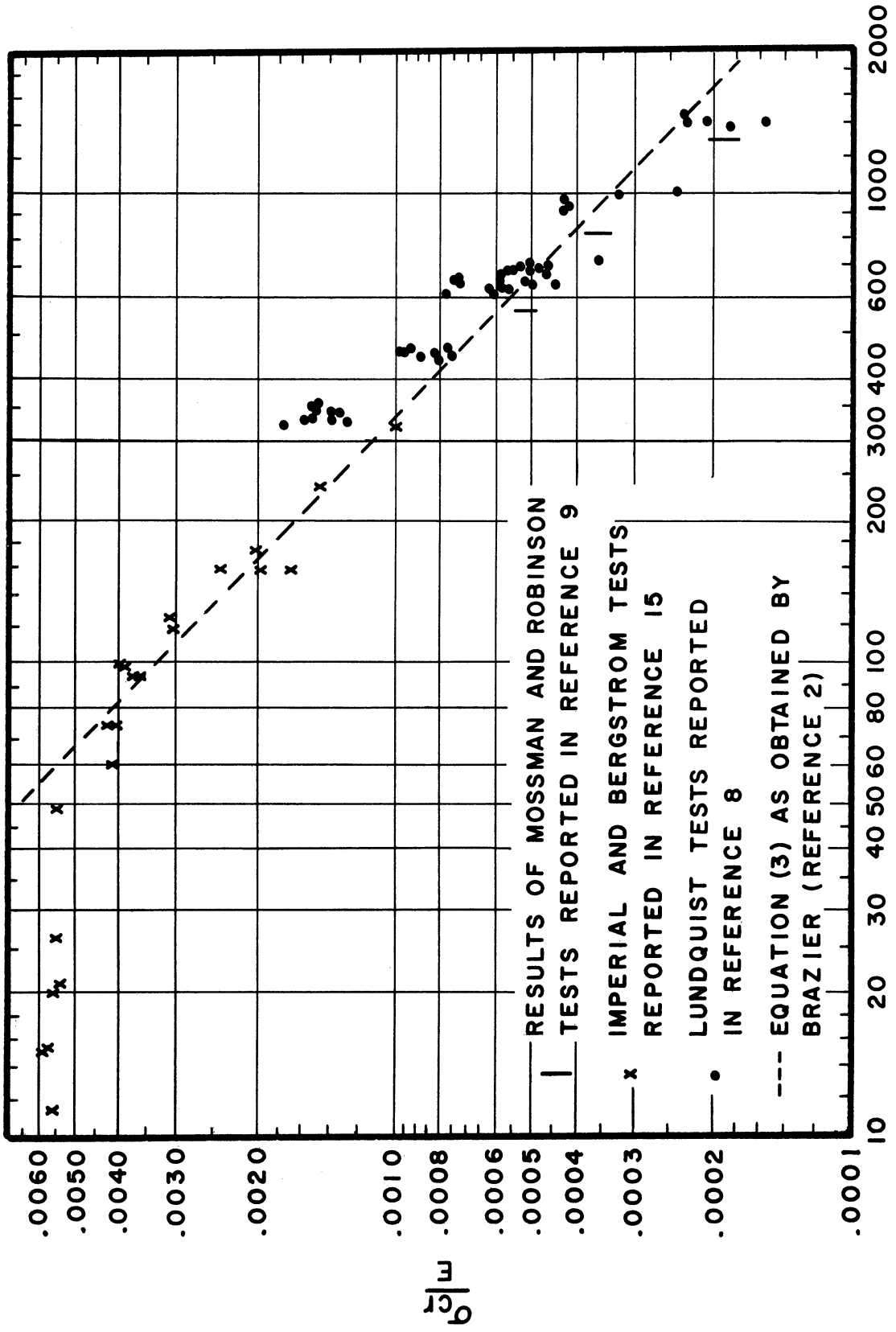

Figure 36. Critical Stress Vs. Radius/Thickness Ratio (Unstiffened Cylinders - Pure Bending).

APPENDIX C

ULTIMATE STRENGTH OF RING-STIFFENED CYLINDERS SUBJECTED TO PURE BENDING

The results of the experimental tests made by Peterson[11] on ring - stiffened cylinders are given in Figure 37 for those cylinders with ring - spacing/radius ratio (S/r) greater than about 1/2. Peterson's tests were made on ring - stiffened cylinders with r/t ranging from 120 - 750 and S/r of 1/4, 1/2 and 1 for most cylinders. For r/t = 180 additional cylinders were tested with S/r of 2 and 4.

Figure 37 which is taken directly from Figure 6 of Reference 11 gives the critical stress in the cylinder as a function of only the r/t ratio of the cylinder, for S/r ranging approximately from 1/2 to 4, where the spacing of the rings (as was found by Peterson) had no appreciable effect on the strength of the cylinder. It should be mentioned that the rings used in the above tests were heavy to eliminate the general - instability type failure, and that the material used was aluminum alloy 7075-T6.

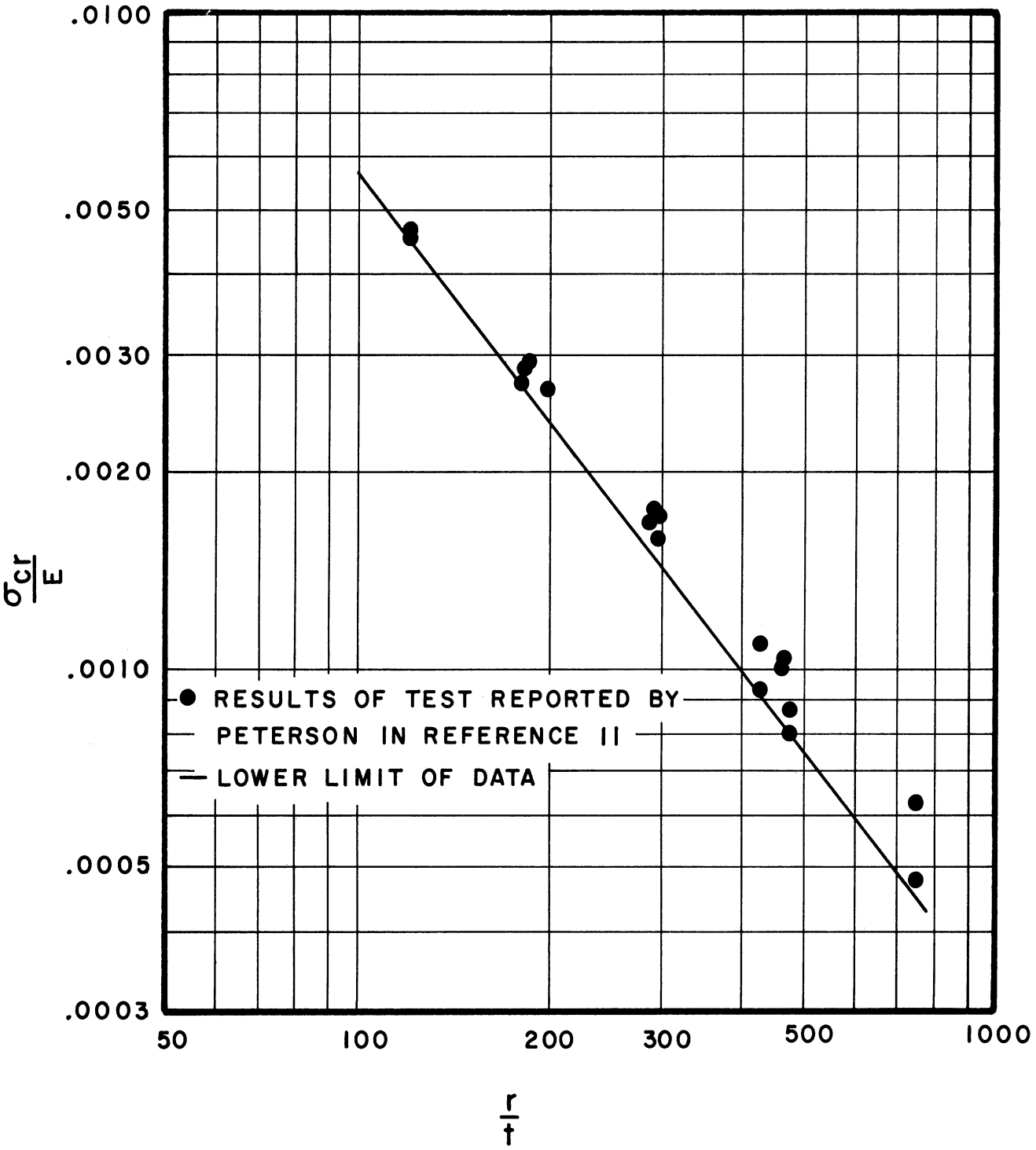

Figure 37. Critical Stress Vs. Radius/Thickness Ratio (Ring Stiffened Cylinders with S/r ratio greater than about 1/2 - Pure bending - Heavy rings).

APPENDIX D

PHOTOGRAPHS OF THE MODEL

Four photographs of the model are given in this appendix. Some explanations regarding the photographs follow:

Photograph 1: This photograph shows the method that was used to place the gages on the inside of the shell. As can be seen from the photograph, a longitudinal opening was maintained by bracing the shell with four wooden braces. The photograph was taken after the gages were in place and all the necessary wiring was completed. It is important to mention that the strains introduced in the gages, as a result of folding the cylinder back to its circular shape, were relatively small, and that no injury to any of the gages was caused. The gages functioned very well during the test.

Photograph 2: This photograph shows part of the center segment of the model with the stiffeners spaced at 2-5/8 inches center to center. The rectangular rosette gages as well as the single gages are clearly shown.

Photograph 3: This photograph shows the three segments of the model connected together and ready to be attached to the wooden end blocks.

Photograph 4: This photograph shows the model completely assembled and placed in the testing frame.

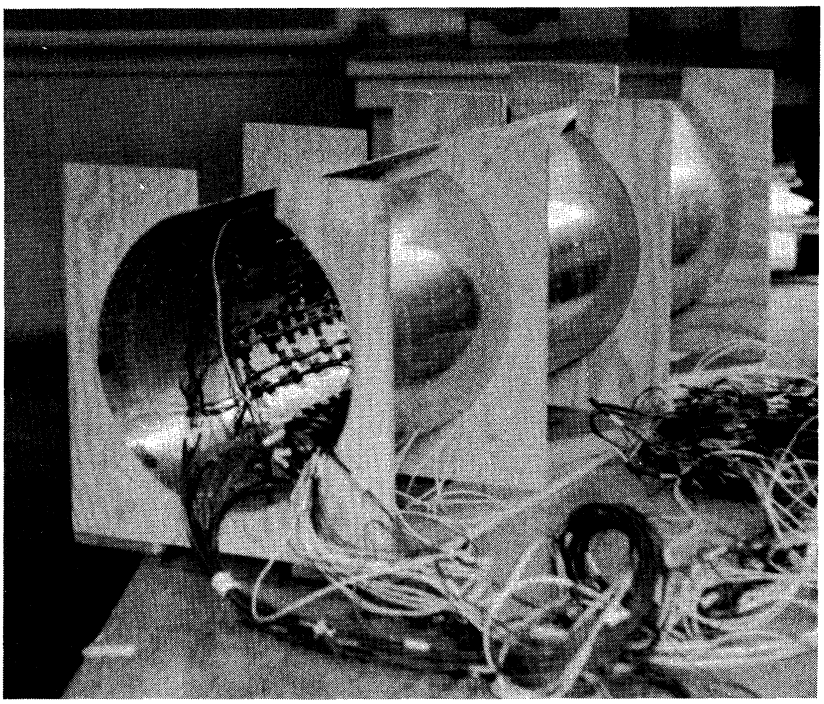

PHOTOGRAPH 1

Method of Applying Gages to the
Inside of the Shell

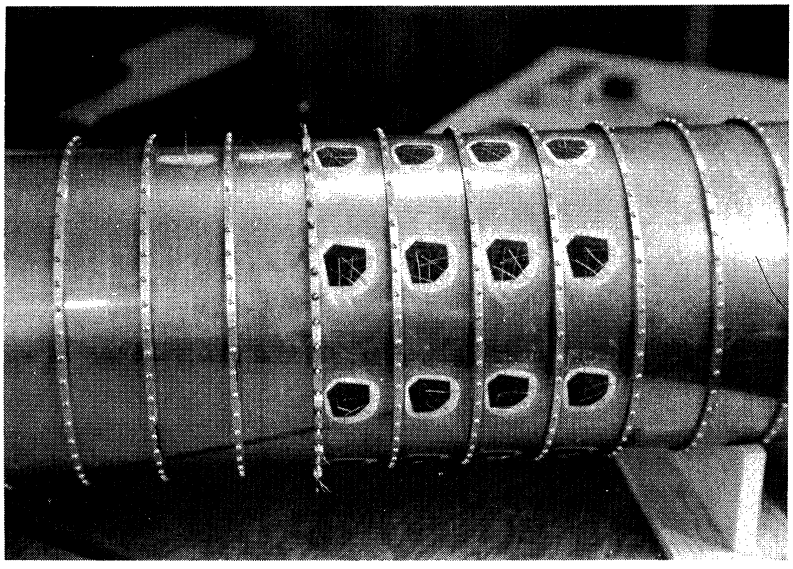

PHOTOGRAPH 2

Stiffeners and Gages on the Center
Segment of the Model

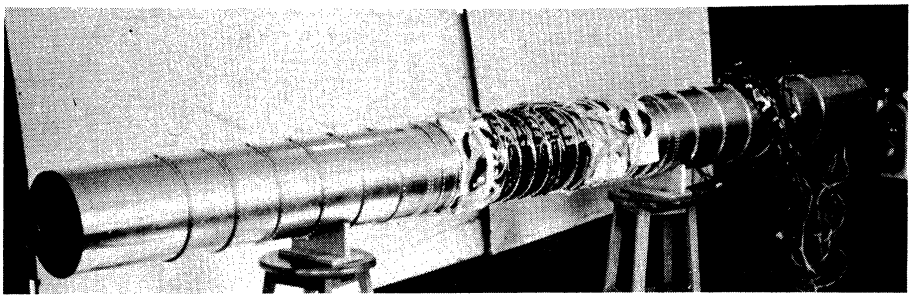

PHOTOGRAPH 3

The Three Aluminum Segments of the Model

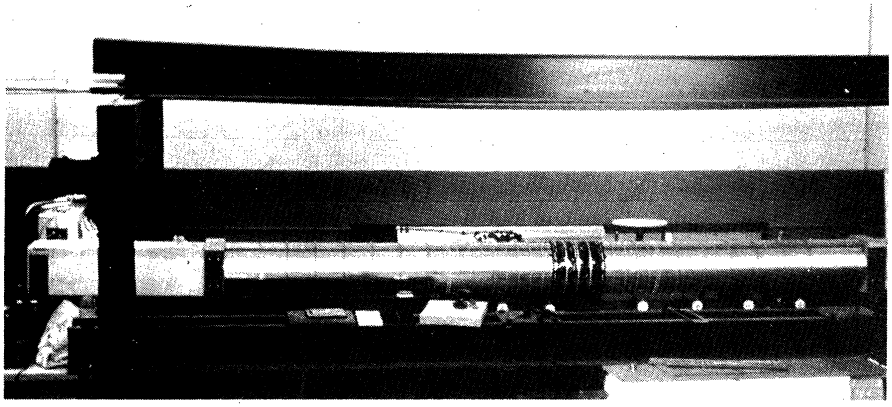

PHOTOGRAPH 4

The Model in the Testing Frame

BIBLIOGRAPHY

1. Biezeno, C. B. and Koch, J. J. "The Effective Width of Cylinders Periodically Stiffened by Circular Rings," Proc. Ned. Akad. Wet. 48, (1945) 147.

   Also to be found in:
   Biezeno, C. B. and Grommel, R. Engineering Dynamics, 2 . Blackie and Sons, Ltd., London, England, 348-357.

2. Brazier, L. G. "The Flexure of Thin Cylindrical Shells and Other 'Thin' Sections." Reports and Memoranda No. 1081, London: Aeronautical Research Committee, 1926.

3. California Institute of Technology, "Some Investigations of the General Instability of Stiffened Metal Cylinders," I Review of Theory and Bibliography, T. N. No. 905, NACA, July, 1943.

4. Dunn, Louis G. "Some Investigations of the General Instability of Stiffened Metal Cylinders," T. N. No. 1198, NACA, 1947.

5. Hetenyi, M. "Beams on Elastic Foundation," The University of Michigan Press, Ann Arbor, Mich., 1946.

6. Hoff, N. J. "Instability of Monocoque Structures in Pure Bending," Journ. Roy. Aero. Soc., 42, (April, 1938) 291-346.

7. Hoff, N. J., Buley, Bruno A., and Nardo, S. V. "Experimental Investigation of Cylinders Subjected to Pure Bending," T. N. No. 1499, NACA, Sept. 1948.

8. Lundquist, Eugene E. "Strength Tests of Thin-Walled Duralumin Cylinders in Pure Bending," T. N. No. 479, NACA, 1933.

9. Mossman, Ralph W. and Robinson, Russell G. "Bending Tests of Metal Monocoque Fuselage Construction," T. N. No. 357, NACA, 1930.

10. Perry, C. E. and Lissner, H. R. The Strain Gage Primer, McGraw-Hill Book Co., Inc., New York, Toronto, London, 1955.

11. Peterson, James P. "Bending Tests of Ring-Stiffened Circular Cylinders," T. N. No. 3735, NACA, 1956.

12. Pippard, A. J. Sutton "Distortion of Thin Tubes Under Flexure," Reports and Memoranda No. 1465, London: Aeronautical Research Committee, 1932.

13. Thurliman, Bruno - Bereuter, Rudolf O. and Johnston, Bruce G. "The Effective Width of a Circular Cylindrical Shell Adjacent to a Circumferential Reinforcing Rib," Proceedings of the First U. S. National Congress of Applied Mechanics, 1951.

14. Timoshenko, S. Theory of Plates and Shells, McGraw-Hill Book Co., Inc., New York and London, 1940.

15. Younger, John E. "Principle of Similitude as Applied to Research on Thin-Sheet Structures," Aero. Eng., ASME, (Oct. - Dec., 1933) 163-169.

16. Yuan, S. W. "Thin Cylindrical Shells Subjected to Concentrated Loads," Quarterly of Applied Mathematics, 4, No. 1, (1946) 13-26.

17. Yuan, S. W. and Ting, L. "On Radial Deflections of a Cylinder Subjected to Equal and Opposite Concentrated Radial Loads," Journal of Applied Mechanics, 24, No. 2, June, 1957.